PROTEOLYTIC PROCESSING OF THE CELL ADHESION MOLECULE COXSACKIEVIRUS AND ADENOVIRUS RECEPTOR (CAR)

Nadia Houri

Integrated Program in Neuroscience

McGill University

Montreal, Quebec, Canada

August 2013

A thesis submitted to McGill University in partial fulfillment of the requirements of the degree of Doctorate of Philosophy

© Nadia Houri 2013

Table of Contents

Abstract	4
Resume	6
Acknowledgements	8
List of Figures and Tables	9
Abbreviations	13
Author Contributions	15
Original Claims to Knowledge	16
Chapter 1: Literature Review and Study Rationale	17
1. Preamble	18
2. Ectodomain shedding of proteins	18
2.1. The ADAM family of metalloproteases	19
2.1.1. Domain organization of ADAMs	20
2.1.2. Regulation of ADAMs	21
2.1.3. ADAMs play a wide variety of physiological roles	24
2.2. Substrates of ADAMs	27
2.2.1. Notch	27
2.2.2. Amyloid Precursor Protein (APP)	28
2.2.3. Cytokines and growth factors	30
2.2.4. Cell adhesion molecules (CAMs)	31
3. Regulated Intramembrane Proteolysis (RIP)	32
3.1. The y-secretase complex	32

3.2. The γ-secretase complex and downstream signaling events	33
4. The Coxsackievirus and Adenovirus Receptor (CAR), a cell adhesion mol	ecule
and virus attachment site	35
4.1. CAR structure and domains	36
4.2. CAR expression patterns and isoforms	39
4.3. CAR in epithelial cell tight junctions	40
4.4. CAR in skeletal and cardiac muscle development	43
4.5. CAR in the developing brain	44
4.6. CAR in the immune system	45
4.7. Other roles for CAR in normal physiology	46
4.8. CAR's role in cancer	47
4.9. CAR interacts with the cytoskeleton	52
5. Study rationale and objectives	53
Chapter 2: Materials and Methods	65
Chapter 3: ADAM10 Mediates CAR Ectodomain Shedding	89
Chapter 4: Modulation of Shedding Does Not Affect CAR's	
Inhibitory Function in Glioma	135
Chapter 5: Ectodomain Shedding of CAR From Developing Neurons	153
Chapter 6: Studies on the Intracellular Domain of CAR, a Product of Regula	ted
Intramembrane Proteolysis (RIP)	165
Chapter 7: Discussion	202
References	226

Abstract

The Coxsackievirus and Adenovirus Receptor (CAR) is a cell adhesion molecule involved in various functions including neuronal and heart development, contribution to epithelial cell tight junction integrity, and suppression of glioma migration and invasion. Proteolysis of cell adhesion molecules, and a wide variety of other proteins, serves as a mechanism for protein turnover and may also have consequences on cellular signaling. Proteolysis by metalloproteases such A Disintegrin and Metalloprotease (ADAM) family members results in ectodomain shedding of substrates, while the presenilin/gamma-secretase complex mediates regulated intramembrane proteolysis (RIP), releasing from the plasma membrane intracellular domain fragments which may enter the nucleus after RIP and affect gene expression. Preliminary data from our laboratory suggested that CAR ectodomain is shed and that the remnant fragment is RIPped. In this study, we identified ADAM10 as a sheddase of CAR using assays involving shRNA knockdown and rescue, overexpression of wild-type ADAM10 and inhibition of ADAM10 activity by addition of its prodomain. *In vitro* peptide cleavage and mass spectrometry analyses suggested the involvement of CAR amino acids 224-227 in its ectodomain shedding. Ectodomain shedding is a prerequisite for RIP of CAR, and free CAR intracellular domain enters the nucleus. Modulation of ectodomain shedding did not affect CAR's inhibitory function in glioma migration. Furthermore, free CAR intracellular domain cannot inhibit glioma cell migration, suggesting that proteolysis of CAR ultimately abolishes this function

and promotes tumorigenesis. On the other hand, in developing neurons, metalloprotease activity is required for CAR-mediated neurite outgrowth. Thus, CAR belongs to an increasing list of cell surface molecules that undergo ectodomain shedding and gamma-secretase-mediated RIP, and these proteolytic events can have a consequence on CAR function.

Résumé

Le récepteur de Coxsackievirus et d'Adenovirus (CAR) est une molécule d'adhésion qui est impliquée en plusieurs fonctions telles que le développement neuronal et cardiaque, la formation des jonctions serrées, ainsi que la suppression de l'invasion et de la migration de certaines cellules tumorales. La protéolyse des molécules d'adhésion cellulaire, ainsi que d'autres protéines de la membrane plasmique peut servir comme mécanisme de renouvellement et aussi peut avoir des conséquences sur la signalisation cellulaire. La protéolyse effectuée par les métallo-protéases, par exemple les membres de la famille « A Disintegrin and Metalloprotease » (ADAM), génère un fragment soluble du domaine extracellulaire du substrat, tandis que le complexe préséniline/gamma-sécrétase libère un fragment intracellulaire du domaine cytoplasmique (par un processus nommé RIP) qui peux être transporté au noyau et qui peux ainsi affecter l'expression génique. Les données préliminaires de notre laboratoire suggèrent que le domaine extracellulaire de CAR est clivé, et le fragment qui en provient subit le processus RIP. Durant ces travaux, nous avons identifié ADAM10 comme étant la protéine qui clivait CAR, basé sur plusieurs approaches expérimentales dont l'utilisation des shRNA contre ADAM10, l'inhibition de son activité enzymatique et son surexpression. Le clivage peptidique in vitro et l'analyse spectrométrique de masse suggèrent que les acides aminés 224-227 de CAR sont impliqués dans le clivage du domaine extracellulaire. Ce clivage est obligatoire pour que CAR subisse le processus RIP, afin que le domaine intracellulaire de CAR puisse entrer dans le noyau. Le clivage du domaine extracellulaire de CAR

n'a pas de conséquence sur l'effet inhibiteur de CAR sur la migration des cellules de gliome. En plus, le domaine intracellulaire de CAR libéré à la suite du processus RIP, n'inhibe non plus la migration des cellules de gliome, ce qui suggère que la protéolyse de CAR bloque cette fonction anti-tumorale de la protéine. Par contre, durant le développement neuronal, l'activité des métalloprotéases est nécessaire pour l'effet de CAR sur l'extension des neurites. En conclusion, CAR appartient au groupe de protéines membranaires qui sont clivés par les métallo-protéases ainsi que la préséniline/gamma sécrétase. Ce phénomène a des conséquences sur la fonction de CAR.

Acknowledgements

I wish to express my deep gratitude and thanks to my supervisor, **Dr. Josephine**Nalbantoglu, for her teaching, mentorship and patience, and for believing in me.

She is an exemplary scientist and I have learned a great deal from her during my time as a student in her laboratory.

Thank you to my advisory committee members, **Dr. Alyson Fournier** and **Dr. Paul Holland**, for their support and constructive comments during my doctoral studies. I also thank my graduate program mentor, **Dr. Don van Meyel**, for his encouragement.

Lab life wouldn't have been the same without the following people: Nancy Larochelle, Luyu Zheng, Songsong Geng, Zak Orfi, David Huang, Patrick Fok, Arjuna Rajakumar, Christine Fagotto-Kaufmann and Carol Allen. Thank you for your friendship and support. Special thanks to Nancy for her help with experiments, to Luyu for teaching me dissections, and to Pat and David for their help when I first joined the lab. Thank you to Linda Gilbert and Liliana Cetola for administrative support.

I had the privilege of receiving studentships and travel awards during my doctoral studies. I am grateful to the CIHR Neuroinflammation Training Program and McGill University's Integrated Program in Neuroscience (IPN) for enriching my graduate student experience.

Last but definitely not least, a big thank you to my parents, my brother and my sister for their encouragement and their faith in me. I love you!

List of Figures and Tables

Figure 1.1: Domain organization of ADAM metalloproteases	. 55
Figure 1.2: The 21 members of the ADAM family in humans	. 57
Figure 1.3: Ectodomain shedding of an Igsf family member CAM	. 59
Figure 1.4: Notch receptor proteolysis	. 61
Figure 1.5: A model of CAR proteolysis	. 63
Figure 3.1: Human glioma U87-MG cells stably expressing CAR shed CAR E0	CD
constitutively or with 4 hours of treatment with 1 µM PMA	101
Figure 3.2: Ectodomain shedding results in a decrease in amount of CAR at the)
cell surface	103
Figure 3.3: PMA-stimulated CAR shedding is inhibited by the PKC inhibitor	
Gö6983	105
Figure 3.4: The Ca ²⁺ ionophore ionomycin stimulates CAR ECD shedding	107
Figure 3.5: PMA treatment of U87 CAR cells is accompanied by phosphorylation	ion
of CAR's cytoplasmic domain	109
Figure 3.6: CAR ECD shedding is not stimulated by treatment of U87 CAR cel	lls
with EGF, IGF-1 or pervanadate	111
Figure 3.7: CAR shedding is inhibited by the broad-spectrum metalloprotease	
inhibitor GM6001	113
Figure 3.8: Treatment of U87 CAR cells with PMA under conditions known to	
trigger ADAM17-mediated shedding of proteins does not induce CAR ECD	
shedding	115
Figure 3.9: ADAM10 is involved in CAR ectodomain shedding	117

Figure 3.10: Confirmation of shRNA knockdown of ADAM10	119
Figure 3.11: shRNA knockdown of ADAM10 decreases constitutive, PMA-	
mediated and ionomycin-mediated CAR ECD shedding	121
Figure 3.12: Partial rescue of shRNA-mediated loss of CAR shedding using ar	1
shRNA-resistant mutant of ADAM10	123
Figure 3.13: Mapping the sites of ectodomain cleavage on CAR	125
Figure 3.14: Expression of CAR ECD mutants in	
human glioma U251N cells	128
Figure 3.15: Mutations in CAR's juxtamembrane region of the ECD greatly	
diminish receptor levels on the surface of human glioma cells	130
Figure 3.16: The mutants MLRL \rightarrow AAAA and Δ 221-232 are expressed at	
similar levels on the surface of HEK 293 cells as wild-type CAR	133
Figure 4.1: The modified Boyden chamber cell migration assay	139
Figure 4.2: Inhibition of CAR ECD shedding does not affect migration of CAI	R-
expressing glioma cells	141
Figure 4.3: Stimulation of CAR ECD shedding with PMA does not change CA	AR's
effect on glioma migration	143
Figure 4.4: Glioma cells expressing a shedding-defective CAR mutant or a CA	ιR
mutant that sheds its ectodomain migrate similarly	145
Figure 4.5: The BioFlux cell migration assay	147
Figure 4.6: BioFlux migration of U87 cells expressing the Δ 221-232 mutant or	r the
MLRL → AAAA mutant	149

Figure 4.7: Tailless CAR, a mutant lacking CAR cytoplasmic domain and which
does not inhibit glioma migration, sheds its ectodomain
Figure 5.1: CAR ECD is shed from developing cortical neurons
Figure 5.2: CAR ECD shedding from developing cortical neurons is stimulated by
the phorbol ester PMA, by the calcium ionophore ionomycin and by KCl 159
Figure 5.3: The ECD of CAR promotes neurite outgrowth from cerebellar
microexplants, an effect abolished by inhibition of metalloprotease activity 163
Figure 5.4: ADAM10 activity is required for basal ECD shedding of CAR from
developing cortical neurons
Figure 6.1: RIP of CAR is mediated by the presentiin/γ-secretase complex 175
Figure 6.2: Generation of CAR CTF1 precedes CTF2 production
Figure 6.3: Detection of V5 tag immunoreactive speckles in nuclei of 293 cells
transiently transfected with full-length CAR-V5
Figure 6.4: CAR intracellular domain (ICD) enters the nucleus
Figure 6.5: Confocal microscopy Z stack images of a U87 cell transiently
expressing V5-tagged CAR ICD
Figure 6.6: CAR ICD binds the nuclear import protein importin alpha
Figure 6.7: CAR ICD is subject to proteasomal degradation
Figure 6.8: CAR ICD fused to GAL4 DNA-binding domain (DBD) does not
induce expression of a GAL4-dependent luciferase reporter
Figure 6.9: CAR ICD inhibits luciferase expression induction by full-length
GAL4

Figure 6.10: Lentiviral-mediated expression of V5-tagged full-length CAR and	
CAR ICD	96
Figure 6.11: BioFlux migration assays comparing U87 cells expressing full-leng	th
CAR, CAR ICD or control	98
Figure 6.12: XTT cell proliferation assays on U87 cells expressing control pWPI	[,
pWPI-CAR-V5 or pWPI-ICD-V5 constructs	00
Table 7.1: Molecular weight of the ICDs of some proteins known to undergo γ-	
secretase-mediated RIP	24

Abbreviations

ADAM- A Disintegrin and Metalloprotease

APH-1- Anterior Pharynx-defective 1

CAM- Cell Adhesion Molecule

CAR- Coxsackievirus and Adenovirus Receptor

ECD- ectodomain

CTF- <u>C</u>-terminal fragment

ICD- intracellular domain

CIP- Calf intestinal alkaline phosphatase

CTX- Cortical Thymocyte marker in *Xenopus*

DAF- Decay Accelerating Factor

DAG- Diacylglycerol

DBD- DNA-Binding Domain

DCC- Deleted in Colorectal Carcinoma

ECD- Ectodomain

ECM- extracellular matrix

GBM- Glioblastoma multiforme

GFP- Green Fluorescent Protein

GST- Glutathione S-transferase

HEK293- Human Embryonic Kidney 293 cells

ICD- Intracellular domain

Ig- Immunoglobulin

Igsf- Immunoglobulin super family

IM- Ionomycin

IRES- Internal Ribosomal Entry Site

JAM- Junctional Adhesion Molecule

JAML- Junctional Adhesion Molecule-Like

KCl- potassium chloride

LNX- Ligand-of-Numb protein-X

MAGI-1b- Membrane associated guanylate kinase 1b

MALDI-MS- Matrix-assisted laser desorption/ionization mass spectrometry

MEF- Mouse Embryonic Fibroblast

MMP- Matrix Metalloprotease

MS/MS- Tandem mass spectrometry

MUPP1- Multi-PDZ domain protein 1

NCAM- neural cell adhesion molecule

NECD- Notch extracellular domain

NEXT- Notch extracellular truncation

NICD- Notch intracellular domain

PDL- Poly-d-lysine

PDZ- Post-synaptic density protein 95/Drosophila discs large tumor suppressor/Zonula occludens-1

PEN-2- Presenilin Enhancer-2

PKC- Protein Kinase C

PICK1- Protein interacting with protein C kinase 1

PMA- phorbol-12-myristate-13-acetate

PMS- N-methyl dibenzopyrazine methyl sulfate

PPC- Proprotein Convertase

PS- Presenilin

PSD-95- Post-Synaptic Density protein 95

RIP- Regulated Intramembrane Proteolysis

SIV- serine/isoleucine/valine

TVV- threonine/valine/valine

XTT- sodium 2,3,-bis(2-methoxy-4-nitro-5-sulfophenyl)-5-[(phenylamino) carbonyl]-2H- tetrazolium) inner salt

ZO-1- Zonula Occludens-1

Author Contributions

The majority of the experimental work presented in this thesis was performed by the candidate, Nadia Houri. The thesis was written by Nadia Houri and edited by the candidate's supervisor, Dr. Josephine Nalbantoglu.

<u>Chapter 3</u>: Ms. Zivart Yasruel, a former research assistant in Dr. Nalbantoglu's laboratory, performed the experiments for figure 3.2B. Dr. Nancy Larochelle, a research associate in Dr. Nalbantoglu's laboratory, performed the adenovirus infections and luminescence experiments for figure 3.15D.

<u>Chapter 4</u>: Dr. Nancy Larochelle performed the BioFlux migration assays shown in figures 4.6 and 4.7, and analyzed the data.

<u>Chapter 6</u>: Dr. Nancy Larochelle performed the BioFlux migration assays shown in figure 6.11. The candidate prepared the samples and analyzed the data for these experiments.

All other experiments were performed by the candidate.

Data from Chapters 3 and 6 contributed to the following manuscript:

"The Coxsackievirus and Adenovirus Receptor (CAR) Undergoes Ectodomain Shedding and Regulated Intramembrane Proteolysis (RIP)". Nadia Houri*, Kuo-Cheng Huang, Josephine Nalbantoglu. PLoS One. 2013 Aug 28;8(8):e73296.

^{*}First author

Original Claims to Knowledge

The following are the main novel findings on the proteolysis of CAR discovered during my doctoral research and presented in this thesis:

- 1- ADAM10 is a major sheddase of CAR, mediating constitutive shedding of CAR as well as its regulated shedding (via the Ca²⁺ and PKC pathways).
- 2- The presence of amino acids 224-227 of CAR are important for its shedding.
- 3- CAR undergoes RIP mediated by presenilin/γ-secretase, and RIP follows shedding of CAR.
- 4- The intracellular domain fragment of CAR generated upon RIP is capable of nuclear entry.
- 5- Proteolytic processing of CAR plays a role in regulating its functions as a virus receptor and a cell adhesion molecule that mediates neurite outgrowth and inhibits glioma tumorigenesis.

Chapter 1: Literature Review and Study Rationale

1. Preamble

Proteolysis, or protein cleavage by enzymes, is a term that refers to a wide variety of cleavage events including post-translational protein maturation, degradation of abnormal or damaged proteins, and protein cleavage during signal transduction. This thesis focuses on two specific types of proteolysis, ectodomain shedding and regulated intramembrane proteolysis (RIP). The introduction section describes the players involved and examples of substrates. Next, literature on a cell adhesion molecule of interest in our laboratory, the Coxsackievirus and Adenovirus Receptor (CAR), is reviewed, followed by the rationale for studying the proteolysis of CAR.

2. Ectodomain shedding of proteins

Ectodomain shedding is the detachment of the extracellular domain of a protein by proteolytic cleavage within its juxtamembrane region (Arribas and Borroto, 2002). This process is employed by cells to turn over the inventory of proteins at the surface and is an alternative to the down-regulation of receptors via ligand binding, endocytosis and lysosomal degradation (Dello Sbarba and Rovida, 2002). Enzymes that mediate ectodomain shedding are referred to as "sheddases", and their substrates include a wide diversity of cell surface proteins such as cell adhesion molecules (CAMs), ligands, growth factors, cytokines and receptors (Werb and Yan, 1998). Ectodomain shedding occurs at basal (constitutive) levels

in non-stimulated cells, and it can also be enhanced by treating cells with chemicals such as phorbol esters (Arribas and Borroto, 2002).

With over 600 genes, proteases comprise the largest family of enzymes in vertebrates (Sterchi et al., 2008). Two families of proteases mediate ectodomain shedding: Matrix Metalloproteinases (MMPs) and A Disintegrin and Metalloproteases (ADAMs), with ADAMs contributing to the majority of known ectodomain shedding events (Huovila et al., 2005). MMPs and ADAMs fall within the metzincin sub-family, with metzincins containing the conserved zinc-binding amino acid motif HEXXHXXG/NXXH/D, where X is any amino acid (Sterchi et al., 2008).

2.1. The ADAM family of metalloproteases

ADAMs are expressed in a wide variety of organisms including *C. elegans*, *S. pombe*, and mammals. There are 25 *ADAM* genes in humans, 21 of which are functional and 4 are pseudogenes. Not all functional ADAMs are catalytically active; 13 ADAMs in humans have catalytic activity and 8 ADAMs lack it (Edwards et al., 2008).

2.1.1. Domain organization of ADAMs

Figure 1.1 illustrates the domains found in a typical ADAM protein. Moving from the N-terminus to the C-terminus, the first domain is the prodomain. Removal of the prodomain is required for maturation and activation of the enzyme (Huovila et al., 2005, Edwards et al., 2008). The prodomain has also been proposed to contribute to the proper folding of ADAMs (Tousseyn et al., 2006). The metalloproteinase domain binds a zinc atom and mediates the catalytic cleavage of substrates. The disintegrin domain is the site of interaction of some ADAMs with integrins, a process that promotes cell-cell adhesion (Edwards et al., 2008). The cysteine-rich domain has been proposed to play a role in substrate specificity, in improving the binding capacity of the disintegrin domain and in binding to proteoglycans (Reiss and Saftig, 2009). The epidermal growth factor-like domain is not very well understood. It has been proposed to play a role in the function of ADAM17 via the formation of multimers (Lorenzen et al., 2011). The transmembrane domain has been proposed to play a role in substrate specificity, at least for ADAM17 (Li et al., 2007b). Finally, the cytoplasmic domain interacts with a wide variety of cytoplasmic proteins that are involved in signal transduction, trafficking and cell architecture (Edwards et al., 2008).

2.1.2. Regulation of ADAMs

The pre-mRNAs of some ADAMs (ADAM9, ADAM11, ADAM12, ADAM15, ADAM19, ADAM22, and ADAM28) are alternatively spliced (Edwards et al., 2008), which is one form of regulation by the cell. Alternative splicing can also result in secreted isoforms. ADAM12-S, a short, secreted isoform of ADAM12, is catalytically active and can cleave extracellular matrix proteins (gelatin, type IV collagen and fibronectin) and insulin-like growth factor binding proteins IGFBP-3 and IGFBP-5 (Loechel et al., 2000, Shi et al., 2000, Roy et al., 2004).

Alternative splicing can also affect whether or not isoforms of an ADAM protease bind to certain cytoplasmic partners. Some ADAM15 isoforms bind nephrocystin while others bind sorting nexin-33 (Kleino et al., 2009). Since ADAM15 promotes prostate and breast tumorigenesis (Najy et al., 2008b, a), and it exists in several isoforms in tumorigenic, but not normal, breast cancer cell lines (Ortiz et al., 2004), it is possible that the different protein-protein interactions arising from alternative splicing are involved in ADAM15-mediated pathology.

As previously mentioned, prodomain removal is required for maturation of ADAMs. When the prodomain is intact, a cysteine binds to a zinc atom in the metalloproteinase domain and keeps this catalytic domain inactive, a mechanism referred to as a cysteine switch (figure 1.1). Cleavage of ADAMs in the trans-Golgi network by proprotein convertases (PPCs) (or autocatalysis of ADAM8 and

ADAM28) removes the prodomain and results in a mature protease (Huovila et al., 2005, Edwards et al., 2008, Murphy, 2009). Thus, synthesis of ADAMs as immature zymogens that require cleavage for maturation is one way for cells to control ADAM activity.

The activity and cellular location of ADAMs can be regulated via their interaction with a wide variety of cellular partners. A proline-rich Src homology 3 (SH3) binding domain in ADAM10's cytoplasmic tail is required for ADAM10 localization to adherens junctions in polarized epithelial cells, where it plays a role in processing the cell adhesion molecule E-cadherin and in regulating cell migration (Wild-Bode et al., 2006). The SH3 domain in synapse-associated protein-97 (SAP-97) mediates localization of ADAM10 to post-synaptic membranes in neurons (Marcello et al., 2007). The endocytosis protein dynamin regulates ADAM10, as overexpression of a dominant negative dynamin mutant results in increased levels of ADAM10 at the cell surface (Carey et al., 2011); it remains to be determined what proteins directly interact with ADAM10 in this process. Extracellular signal-regulated kinase (ERK) phosphorylates a threonine residue in ADAM17's cytoplasmic domain, a step involved in ADAM17-mediated cleavage of TrkA receptor following phorbol ester treatment (Diaz-Rodriguez et al., 2002). ADAMs in turn can also regulate the activity of other cellular proteins; for example, ADAM12 binds to and activates Src tyrosine kinase and phosphatidylinositol 3-kinase (PI3K) (Kang et al., 2000, 2001).

ADAM-mediated shedding can be triggered by signaling events such as ligand binding, calcium influx, cholesterol depletion and activation of the diacylglycerol (DAG)- protein kinase C (PKC) pathway (Murphy, 2009). Studies using mouse embryonic fibroblast (MEF) knockout cells and specific pharmacological inhibitors have shown that, in general, ADAM10 mediates constitutive (basal shedding) as well as shedding stimulated by calcium influx, while ADAM17 mediates shedding stimulated by phorbol esters that activate the PKC pathway (Ludwig et al., 2005, Horiuchi et al., 2007).

Cross-talk signaling between two receptor families, the G protein-coupled receptors (GPCRs) and the epidermal growth factor receptors (EGFRs), is a well-studied phenomenon and plays a role in mitogenesis of normal and cancerous cells (Fischer et al., 2003). ADAMs have emerged as mediators of GPCR activation of EGFRs. In this model, a GPCR is stimulated by an agonist, triggering signaling pathways that activate ADAMs, which in turn cleave pro-EGF ligands into their mature forms. The released EGF ligands then activate their cognate receptors, leading to downstream signaling pathways such as cell proliferation (Fischer et al., 2003, Ohtsu et al., 2006). GPCRs can also activate non-EGFR targets via ADAMs, for example, activation of the muscarinic M1 receptor increases processing of amyloid precursor protein (APP) via ADAM17 activation (Caccamo et al., 2006).

Yet another mechanism of regulation of ADAM activity is via endogenous tissue inhibitors of metalloproteases (TIMPs). TIMPs, of which there are 4 in vertebrates, are proteins that inhibit the activities of ADAMs, ADAMs with thrombospondin domains (ADAMTSs) and MMPs via enzyme-TIMP complex formation (Brew and Nagase, 2010). Figure 1.1 shows the ADAM inhibition profile of TIMPs 1-4 (parentheses indicate minor inhibition).

2.1.3. ADAMs play a wide variety of physiological roles

Studies using knockout mice have provided valuable information about the functions of ADAM family members. Knocking out ADAM10 (Kuzbanian) from mice results in lethality at embryonic day 9.5, defects in development of the heart, central nervous system and somites, and defects in the Notch receptor pathway (Hartmann et al., 2002). A conditional knockout model (peri- and post-natal) in the skin revealed an essential role for ADAM10 in epidermal integrity, with a phenotype reminiscent of Notch loss-of-function (Weber et al., 2011). Conditional deletion of ADAM10 from the brain (specifically targeting neural precursor cells (NPCs), NPC-derived neurons and glial cells) resulted in perinatal death and abnormal cortical layer organization (Jorissen et al., 2010).

ADAM17 also has an essential role in development, as the majority of transgenic mice with catalytically inactive ADAM17 ($tace^{\Delta Zn/\Delta Zn}$ mice) die between embryonic day 17.5 and post-natal day 1, and have eye, skin and hair defects

(Peschon et al., 1998). ADAM17 inactivation also results in pulmonary hypoplasia, impaired lung branching (Zhao et al., 2001), cardiac enlargement, increased cardiomyocyte cell size and number (Shi et al., 2003), aberrant migration of osteoclasts in developing bone (Boissy et al., 2003), and abnormal lymphocyte (T cell and B cell) development (Li et al., 2007a). Conditional ADAM17 deletion in adult mice led to an osteoporosis-like phenotype and abnormal hematopoiesis (Horiuchi et al., 2009). ADAM17-inactive mice have a phenotype resembling EGFR family and EGFR ligand knockout phenotypes (reviewed in (Blobel, 2005)).

Most ADAM19 knockout mice die perinatally and display defects in the cardiac ventricular septum, aortic and pulmonic valves and endocardial cushion (Kurohara et al., 2004, Zhou et al., 2004). Loss of the catalytically inactive ADAM22, which is abundantly expressed in the nervous system, results in hypomyelination of peripheral nerves, severe ataxia (lack of self-support on hindlimbs), and death before weaning, although the brain is normal (Sagane et al., 2005).

While loss of ADAM10, ADAM17, ADAM19 or ADAM22 causes dramatic developmental defects, loss of ADAM8, ADAM9, ADAM12, ADAM15 or ADAM33 leads to viable mice without severe phenotypes (Blobel, 2005, Reiss and Saftig, 2009). The ADAM15 knockout phenotype is a decrease in neovascularization and smaller melanoma tumor sizes, suggesting that this

protease may be a therapeutic target in inhibition of neovascularization in cancer (Horiuchi et al., 2003).

As previously mentioned, some ADAMs are catalytically inactive but physiologically functional. Several catalytic and non-catalytic ADAMs are restricted in expression to the testis (see figure 1.2) (Edwards et al., 2008). It is thought that some ADAMs play a role in sperm maturation and sperm-egg interactions (Edwards et al., 2008, Cho, 2012). However, rodents have more *ADAM* genes (37 genes in mice and 34 genes in rats compared to 21 in humans), and many of the family members that have been studied in the context of male rodent fertility are not found in humans, so it is unclear what role ADAMs play in human male fertility (Edwards et al., 2008).

While ADAMs influence adhesion via cleavage of cell adhesion molecules, they can also participate directly in cell-cell adhesion, often via interactions with integrins. $\alpha4\beta1$ integrin-expressing cells adhere to ADAM12, and this interaction (likely via ADAM12's disintegrin domain) inhibits cell migration on fibronectin substrate (Huang et al., 2005a). ADAM17 inhibits $\alpha5\beta1$ integrin-mediated migration, while ADAM19 and ADAM33 inhibit both $\alpha4\beta1$ - and $\alpha5\beta1$ -mediated migration (Huang et al., 2005a). ADAM23, which is expressed in the brain, promotes attachment of neuroblastoma and astrocytoma cells, and interacts with $\alpha\nu\beta3$ integrin to promote attachment of HeLa cells (Cal et al., 2000). Active $\beta1$ integrins promote attachment of mouse F9 carcinoma cells to a substrate of

ADAM13 disintegrin and cysteine-rich domains (Gaultier et al., 2002). Purified disintegrin and cysteine-rich domains of ADAM12 promote adhesion of C2C12 myoblasts and NIH 3T3 fibroblasts (Zolkiewska, 1999). Cellular adhesion and spreading on a substrate of ADAM12 cysteine-rich domain is mediated by syndecan-4 and β1 integrin, and involves active PKCα and RhoA (Iba et al., 2000, Thodeti et al., 2003). ADAM15 is the only family member that contains an RGD (Arg-Gly-Asp) tripeptide motif in its disintegrin domain, through which it binds ανβ3 and α5β1 integrins (Nath et al., 1999).

2.2. Substrates of ADAMs

The following pages highlight some well-known substrates of ADAM metalloproteases.

2.2.1. Notch

The Notch receptor signaling pathway is widely conserved and regulates cell proliferation, apoptosis, fate determination and differentiation (Kopan, 2012). The Notch receptor is activated by transmembrane ligands, named Jagged and Deltalike in humans, expressed on neighboring (signal-transmitting) cells (Kopan, 2012). Notch is cleaved by furin in a step referred to as site 1 (S1) cleavage, resulting in a heterodimeric receptor that is transported to the plasma membrane (Logeat et al., 1998). Site 2 (S2) cleavage is the ligand-triggered, ADAM-

mediated ectodomain shedding of the receptor. (Groot and Vooijs, 2012, Kopan, 2012).

In the absence of a ligand, Notch is kept in an inactive conformation by a negative regulatory region (NRR) (Sanchez-Irizarry et al., 2004). Ligand activation opens up the extracellular domain of the receptor for S2 cleavage by metalloproteases. ADAM10 (Kuzbanian) was initially characterized as the sheddase of Notch in Drosophila and Xenopus (Pan and Rubin, 1997, Sotillos et al., 1997), and later confirmed to mediate ligand-dependent Notch S2 cleavage in mammals (van Tetering et al., 2009, Groot and Vooijs, 2012). Both ADAM10 and ADAM17, and possibly other proteases, cleave Notch ectodomain independently of ligand activation in situations where Notch has gain-of-function mutations, for example in cancer (Bozkulak and Weinmaster, 2009, van Tetering et al., 2009). The stub that remains after Notch extracellular domain (NECD) shedding is referred to as NEXT (Notch extracellular truncation) and is prone to rapid degradation. S2 cleavage is required for the subsequent site 3 (S3) cleavage of Notch, with downstream effects on gene expression (Groot and Vooijs, 2012) (S3 cleavage is discussed in a later section of this chapter).

2.2.2. Amyloid Precursor Protein (APP)

APP-derived amyloid beta $(A\beta)$ peptides are thought to contribute to the pathology of Alzheimer's disease, a progressive, neurodegenerative disease and

the most common type of dementia (Selkoe, 2001, Vingtdeux and Marambaud, 2012). APP undergoes ectodomain shedding and RIP via two pathways: the amyloidogenic pathway (producing A β peptides) and the non-amyloidogenic, neuroprotective pathway. β -secretase cleavage by the β -site amyloid precursor protein converting enzyme (BACE) results in a shed fragment, sAPP β , and a remnant, C99. As will be further discussed later on in this chapter, cleavage of C99 produces A β peptides of varying length (Vassar et al., 1999, Vingtdeux and Marambaud, 2012). While there is strong evidence supporting a role for A β peptides in Alzheimer's disease, the exact nature of their role remains to be clarified. Currently, it is thought that changes in A β peptide clearance and oligomerization are involved (Benilova et al., 2012) .

The non-amyloidogenic pathway mediated by ADAMs (α -secretases) produces a shed fragment, sAPP α , and a remnant, C83, that does not lead to A β production as the α -secretase cleavage site is within the A β region (Esch et al., 1990, Vingtdeux and Marambaud, 2012). ADAMs 9, 10 and 17 have all been reported to act as α -secretases for APP, indicating that there may be functional redundancy (Vingtdeux and Marambaud, 2012). However, there is strong evidence that the α -secretase responsible for constitutive APP ectodomain shedding in the brain (i.e. the physiologically relevant α -secretase) is ADAM10 (Postina et al., 2004, Jorissen et al., 2010, Kuhn et al., 2010).

2.2.3. Cytokines and growth factors

ADAM17, also known as tumor necrosis factor alpha converting enzyme (TACE), is a major sheddase of cytokines and cytokine receptors in the immune system (Scheller et al., 2011). TACE/ADAM17 cleaves the cytokine tumor necrosis factor alpha (TNFα) from its membrane-bound precursor, releasing active TNFα during inflammation (Black et al., 1997, Moss et al., 1997). As TNFα is involved in inflammatory diseases such as rheumatoid arthritis and Crohn's disease, investigating anti-TACE therapies is a worthwhile endeavour, although earlier clinical trials have so far not been successful due to hepatic toxicity (Moss et al., 2008). Antibodies targeting TACE may be a viable alternative (Tape et al., 2011). Other cytokines that are substrates of TACE include the interleukins IL-1, IL-6 and IL-15, as well as the cytokine receptors TNFRI, TNFRII, IL-6R and IL-15R (Saftig and Reiss, 2011).

A role for TACE in the shedding of the transforming growth factor alpha (TGFα) was discovered in studies on TACE knockout mice. These mice had defects in the eyes, skin and hair similarly to the TGFα knockout phenotype as well as reduced TGFα shedding (Peschon et al., 1998). Other growth factor ligands cleaved by TACE/ADAM17 are the heparin-binding epidermal growth factor (EGF)-like growth factor (HB-EGF), amphiregulin and epiregulin, while ADAM10 cleaves EGF and betacellulin (Sahin et al., 2004). The consequence of the proteolysis of these growth factors is their activation of EGF receptors. As EGFR pathways are

often involved in tumorigenesis, ADAM10 and ADAM17 are possible therapeutic targets in cancer (Saftig and Reiss, 2011).

2.2.4. Cell adhesion molecules (CAMs)

Cell-cell adhesion is mediated by *cis* and *trans* interactions of CAMs at the cell surface. These CAMs include members of the Immunoglobulin superfamily (Igsf), cadherins and claudins (Cavallaro and Dejana, 2011). Ectodomain shedding of CAMs via ADAMs regulates the paracrine, autocrine and juxtracrine signaling by these proteins (Saftig and Reiss, 2011).

ADAM10 and ADAM17 mediate constitutive and phorbol ester-stimulated shedding, respectively, of the neuronal Igsf member L1, and these shedding activities promote L1-mediated neurite outgrowth (Maretzky et al., 2005b). Shedding of the close homolog of L1 (CHL1) by ADAM8 also stimulates neurite outgrowth (Naus et al., 2004). ADAM10 cleaves the γ-protocadherins Pcdhγ C3 and B4, and inhibition of metalloprotease activity increases Pcdhγ C3-mediated cell-cell adhesion (Reiss et al., 2006b). ADAM10 proteolysis of vascular endothelial (VE)-cadherin is associated with increased permeability of endothelial cells, likely due to disruptions of adherens junctions (Schulz et al., 2008). ADAM10 regulates cell-cell adhesion via cleavage of N-cadherin and E-cadherin, and loss of ADAM10 leads to cell surface sequestration of β-catenin and reduced β-catenin activity (Maretzky et al., 2005a, Reiss et al., 2005).

The classic view of CAMs is their role in cell-cell adhesion, but their ectodomain shedding can result in signaling pathways that are independent of cell-cell adhesion, such as activation of integrins and growth factors and the nuclear translocation of CAM intracellular domain (figure 1.3) (Cavallaro and Dejana, 2011).

3. Regulated Intramembrane Proteolysis (RIP)

3.1. The y-secretase complex

RIP is the proteolysis of a substrate within a lipid bilayer. It is carried out by several classes of intramembrane cleaving proteases (I-CLiPs): Site 2 proteases (S2Ps), signal peptide peptidase (SPP), rhomboids and the presentilin/γ-secretase complex (Beel and Sanders, 2008).

Over 60 substrates that shed their ectodomains have been discovered to also undergo RIP via the γ-secretase complex. The γ-secretase complex is composed of 4 proteins, all of which are required for proper activity: Presenilin (PS), Aph-1, Nicastrin and Pen-2 (Jorissen and De Strooper, 2010). PS is an aspartyl protease, the catalytic component of the complex (De Strooper et al., 1998, Esler et al., 2000, Li et al., 2000). Nicastrin is involved in substrate recognition (Shah et al., 2005), Pen-2 is required for the endoproteolysis and subsequent activation of PS

(Luo et al., 2003), and Aph-1 promotes complex assembly and trafficking as well as aiding Pen-2 in PS endoproteolysis (Luo et al., 2003, Niimura et al., 2005).

3.2. The y-secretase complex and downstream signaling events

The γ -secretase complex is thought to act as a proteasome in the sense that it is a way for cells to turn over proteins. However, in some cases, RIP of a substrate by the γ -secretase complex may generate intracellular fragments that actively participate in cell signaling (Beel and Sanders, 2008).

As previously mentioned, ADAM-mediated S2 cleavage results in Notch shedding an NECD fragment, leaving a transmembrane stub, NEXT. Sequential S3 cleavage and S4 cleavage of NEXT are mediated by the γ-secretase complex, generating a Notch intracellular fragment (NICD) and Nβ fragments. NICD enters the nucleus and participates in downstream signaling (Struhl and Adachi, 1998, De Strooper et al., 1999, Struhl and Greenwald, 1999, Mumm et al., 2000). NICD in the nucleus interacts with the DNA-binding protein CSL, disrupting CSL interaction with co-repressors. Interaction of NICD and CSL with Mastermind and transcriptional co-activators turns on expression of target genes such as *hes* (Schroeter et al., 1998, Kopan and Ilagan, 2009). Figure 1.4 illustrates Notch proteolysis and nuclear translocation of NICD.

RIP of N-cadherin via γ-secretase frees an intracellular domain that sequesters the transcriptional coactivator CREB binding protein (CBP) in the cytoplasm, leading to CBP proteasomal degradation and repression of cyclic AMP responsive element (CRE) genes (Marambaud et al., 2003). L1 is another CAM that has effects on gene expression following proteolysis. A 28 kDa fragment generated from RIP of L1 translocates to the nucleus, and overexpression of L1 ICD increases expression of beta 3 integrin and decreases expression of cellular retinoic acid-binding protein II (CRABPII), similar to full-length L1 (Riedle et al., 2009).

APP is processed by the γ -secretase complex following α - or β -secretase cleavage. After β -secretase-mediated cleavage, the remnant (C99) is sequentially processed by the γ -secretase complex: first at the ϵ cleavage site, freeing the APP intracellular domain (AICD) and producing the longest $A\beta$ peptide, then at the ζ and γ cleavage sites generating progressively shorter $A\beta$ peptides (Zhao et al., 2005, Beel and Sanders, 2008). The AICD enters the nucleus and induces changes in the expression of a wide variety of genes such as BACE, the histone acetylase Tip60, the tumor suppressor p53, glycogen synthase kinase-3 β (GSK-3 β) and EGFR, and also induces apoptosis (reviewed in (Pardossi-Piquard and Checler, 2012)).

The next section describes the biology of the Coxsackievirus and Adenovirus Receptor (CAR), a new substrate for metalloprotease –mediated ectodomain shedding and RIP.

4. The Coxsackievirus and Adenovirus Receptor (CAR), a cell adhesion molecule and virus attachment site

In the 1990s, there was great interest in isolating an elusive receptor that was believed to be a common attachment site for group B coxsackieviruses and several groups of adenoviruses (Lonberg-Holm et al., 1976, Carson, 2001). It was unusual that these types of viruses would share, and compete for, a common receptor on host cells due to differences in these viruses' structures and infection profiles. Coxsackieviruses are non-enveloped RNA viruses that cause acute pancreatitis, acute myocarditis and meningoencephalitis (Woodruff, 1980). Adenoviruses are non-enveloped DNA viruses that mainly cause gastrointestinal, respiratory and heart infections (Lynch et al., 2011). Some serotypes of adenoviruses are employed as vectors in gene therapy (Ginsberg, 1996). Although the attachment site is common, coxsackieviruses and adenoviruses infect cells via different mechanisms. Adenoviruses infect cells using an antennae-like fiber attached to a knob protein (Philipson et al., 1968) and use integrins as secondary receptors for internalization (Wickham et al., 1993), while coxsackievirus infection occurs via a structural canyon or groove into which the receptor on host cells is inserted (Muckelbauer et al., 1995).

Because of the severity of diseases caused by coxsackieviruses, and the use of adenoviruses in gene therapy, uncovering the identity of the common binding site was an attractive challenge. A 46 kDa protein, highly expressed in fetal and newborn mice (particularly in the brain) was reported to bind coxsackieviruses (Xu and Crowell, 1996). A common receptor for adenoviruses and coxsackieviruses was finally isolated by 3 independent groups in 1997 and subsequently named CAR. Different methods were used by these groups of researchers in identifying the same protein: immunoaffinity purification using an antibody (Rmcb) that interferes with Coxsackie B virus infection of HeLa cells (Bergelson et al., 1997), expression cloning and detection with RmcB antibody (Tomko et al., 1997), and chromatography using radiolabeled Coxsackie B virus (Carson et al., 1997). Subgroup C adenoviruses 2 and 5 were initially reported to attach to CAR (Bergelson et al., 1997, Tomko et al., 1997), and a later study showed that adenovirus subgroups A, D, E and F also employ CAR as a virus fiber receptor (Roelvink et al., 1998). All 6 serotypes of Coxsackie B viruses, as well as the swine vesicular disease virus, employ CAR as a receptor on host cells (Martino et al., 2000).

4.1. CAR structure and domains

CAR is a type 1 transmembrane protein and has one variable and one constanttype Immunoglobulin superfamily (Igsf) domains, one transmembrane domain and one cytoplasmic domain, classifying it as a member of the Immunoglobulin (Ig) superfamily and Cortical Thymocyte marker in Xenopus (CTX) sub-family (Chretien et al., 1998). Two cysteines at positions 259 and 260, near the inner plasma membrane face, are required to be palmitoylated for proper cell surface targeting of the protein (van't Hof and Crystal, 2002).

The extracellular domain of CAR contains 2 sites of N-glycosylation, one in each Ig-like domain, each of which can be independently glycosylated (Excoffon et al., 2007). De-glycosylation of CAR changes its molecular weight from 46 kDa to 40 kDa, the latter being the expected molecular weight from the total number of amino acids (Honda et al., 2000, Excoffon et al., 2007).

The transmembrane and cytoplasmic domains are not required for virus attachment and entry (Leon et al., 1998, Nalbantoglu et al., 1999, Wang and Bergelson, 1999, Tallone et al., 2001, van't Hof and Crystal, 2001, Walters et al., 2001). With regards to the extracellular portion of CAR, the most N-terminal Ig domain (D1 or IgV) is necessary and sufficient for binding to adenovirus, with one side of CAR D1 participating in the interaction with adenovirus fiber knob (Bewley et al., 1999, Freimuth et al., 1999, Kirby et al., 2000). Although the most N-terminal domain, D1, is required for adenovirus infection, the D2 domain also seems to play a role in adenovirus binding (Excoffon et al., 2005). Site-directed mutagenesis in the D1 domain inhibits adenovirus, but not coxsackievirus, binding (Tomko et al., 2000). Three CAR molecules bind to one adenovirus fiber

head (Lortat-Jacob et al., 2001). Coxackieviruses bind the most distal end of CAR D1 domain (He et al., 2001).

Like many members of the Ig superfamily, CAR participates in homophilic cell adhesion. This was first reported using aggregation assays of rat glioma C6 cells overexpressing CAR, which formed larger aggregates compared to non-expressing cells (Honda et al., 2000). Further evidence for a role in cell adhesion came from the observation that CAR expression is high at cell-cell contacts in Chinese Hamster Ovary (CHO) cells (Cohen et al., 2001b). The first (most N-terminal) Ig domain is capable of homodimerization, with a dissociation constant (16 μ M) in a similar range as those of other cell adhesion molecules (van Raaij et al., 2000). More recent research has revealed that both D1 and D2 domains participate in CAR homophilic interactions, including D1-D2 and D2-D2 binding (Patzke et al., 2010). Deletion of all or part of the ectodomain, as well as total elimination of glycosylation, disrupts CAR-mediated cell-cell adhesion (Excoffon et al., 2005, Excoffon et al., 2007).

CAR extracellular domain has also been reported to participate in heterophilic binding to the following extracellular matrix proteins: fibronectin, laminin-1, agrin and tenascin-r; these interactions have higher affinity than homophilic CAR binding (Patzke et al., 2010). It also binds to the cell adhesion molecule junctional adhesion molecule-like (JAML) protein (Zen et al., 2005, Verdino et al., 2010).

4.2. CAR expression patterns and isoforms

CAR is expressed in various species including humans, rodents, pigs, dogs and zebrafish (Tomko et al., 1997, Bergelson et al., 1998, Fechner et al., 1999, van Raaij et al., 2000, Petrella et al., 2002). It is highly conserved, especially in the cytoplasmic domain where there is 95% homology between mouse and human CAR (Bergelson et al., 1997, Tomko et al., 1997, Bergelson et al., 1998). It is most expressed in the pancreas, brain, heart, small intestine, testis and prostate in humans, and in kidney, heart, lung, brain and liver in mice (Tomko et al., 1997, Bergelson et al., 1998). In addition to spatial regulation, it is temporally regulated, with the greatest adenoviral gene transduction (and thus, CAR expression) occurring in mouse embryos at 15 days post-conception (Schachtner et al., 1999). Negative CAR expression in tissue presents an obstacle to the use of adenovirus-mediated gene therapy (Bergelson, 1999); as a result, researchers have engineered viruses that do not require CAR as a receptor (Tanaka et al., 2007).

The functional CAR gene is located on chromosome 21q11.2 in humans (Bowles et al., 1999), and is alternatively spliced. The pre-mRNA has 8 exons which give rise to 5 different transcripts, 3 of which are truncated soluble forms (Bergelson et al., 1998, Fechner et al., 1999, Thoelen et al., 2001, Excoffon et al., 2010). The membranous isoforms are referred to as mCAR isoforms 1 and 2 (mouse) or hCAR^{Ex7} and hCAR^{Ex8} (human). The soluble isoforms can compete with the

longer, membranous ones for binding to virus, conferring protection from viral infection (Bernal et al., 2002, Dorner et al., 2004, Goodfellow et al., 2005).

Although initially characterized as a virus receptor, interest has grown in elucidating the native cellular functions of CAR. The main findings are summarized in the following pages.

4.3. CAR in epithelial cell tight junctions

Human airway epithelial cells are resistant to adenovirus infection (Zabner et al., 1997), due to localization of CAR expression to the basolateral surface rather than the apical surface that is in contact with the lumen (Walters et al., 1999, Pickles et al., 2000). Treatment of the apical surface with H₂O or ethylene glycol tetraacetic acid (EGTA) disrupts cell-cell tight junctions, increases cellular permeability and enhances infection by apically-applied adenovirus (Walters et al., 1999). CAR mutant constructs that lack the cytoplasmic domain or that are anchored to the plasma membrane via a glycosylphosphatidylinositol (GPI) anchor are targeted to both the apical and basolateral surfaces (Pickles et al., 2000), suggesting that proper sorting of CAR in epithelial cells is dependent on its cytoplasmic domain. Indeed, basolateral sorting information is contained between amino acids 315-349 in the cytoplasmic domain (tyrosine 318 being especially important), and to a lesser extent between amino acid residues 261-315 (Cohen et al., 2001a, Carvajal-Gonzalez et al., 2012). The extracellular domain of CAR also plays a role in

proper cellular distribution of the receptor, as deletion of part or all of the ectodomain results in diffuse expression in polarized human airway epithelial cells (Excoffon et al., 2005).

CAR participates in the formation of tight junctions (Cohen et al., 2001b), protein complexes that control inter-epithelial cell permeability and establish apical/basolateral cell polarization (Stevenson and Keon, 1998, Fanning et al., 1999). CAR expression correlates with increased transepithelial electrical resistance (and thus, lower cell permeability) (Raschperger et al., 2006). Adenoviruses from the airway lumen take advantage of breaks in epithelial cell integrity and bind to CAR, disrupting the integrity of tight junctions and allowing viruses to travel and replicate between host epithelial cells (Walters et al., 2002). Some coxsackievirus isolates, on the other hand, bind to decay accelerating factor (DAF) on the apical surface where CAR is unavailable (Shieh and Bergelson, 2002, Coyne and Bergelson, 2006).

CAR has a PSD-95/DlgA/ZO-1 (PDZ) domain-binding motif in its C-terminus, allowing it to interact with the tight junction protein Zonula Occludens-1 (ZO-1). It recruits ZO-1 to cell-cell contacts in non-polarized cells and colocalizes with it in tight junctions of polarized epithelial cells (Cohen et al., 2001b). CAR also colocalizes with occludin, another tight junction protein (Raschperger et al., 2006). CAR's PDZ domain-binding motif at its C-terminus is required for optimal CAR-mediated transepithelial cell resistance (Excoffon et al., 2004).

Other PDZ domain-containing proteins that bind to CAR include: (1) Ligand-of-Numb protein-X (LNX1) and LNX2 (Sollerbrant et al., 2003, Mirza et al., 2005), which regulate the expression of Numb, a protein involved in cell fate determination (Dho et al., 1998); (2) Multi-PDZ domain protein 1 (MUPP1), with loss of CAR expression disrupting proper MUPP1 localization to tight junctions (Coyne et al., 2004); (3) Membrane associated guanylate kinase 1b (MAGI-1b) (Excoffon et al., 2004); (4) Protein interacting with protein C kinase 1 (PICK1) (Excoffon et al., 2004); and (5) Post-synaptic density 95 (PSD-95) (Excoffon et al., 2004). CAR complexes with the acid-sensing ion channel ASIC3 via PSD-95, brings both ASIC3 and PSD-95 to cell-cell junctions, and relieves PSD-95-mediated inhibition of ASIC3 channel activity (Excoffon et al., 2012).

In human airway epithelia, there are isoform-specific differences in CAR localization and protein interaction. CAR^{Ex8} (with amino acids TVV at the C-terminus), in contrast to CAR^{Ex7} (C-terminal amino acids SIV), is found in small amounts on the apical surface, does not bind PICK1 and is degraded by MAGI-1b (Excoffon et al., 2010, Kolawole et al., 2012). This discrepancy between the two CAR isoforms possibly results in different intracellular signaling pathways (Excoffon et al., 2010). Interestingly, second-hand tobacco smoke increases amounts of CAR^{Ex8} on the apical surface of airway epithelia (and subsequently, greater susceptibility of these cells to adenoviral infection), possibly explaining

the link between second-hand tobacco smoke exposure and increased incidence of lower respiratory tract viral infection (Sharma et al., 2012).

4.4. CAR in skeletal and cardiac muscle development

CAR expression is barely detectable in skeletal muscle (Nalbantoglu et al., 1999), with isoform 1 (SIV) specifically expressed (Shaw et al., 2004) and limited to the neuromuscular junction (Sinnreich et al., 2005). An exception is a mouse model of muscular dystrophy (mdx), in which muscle fibers are continuously regenerating and CAR levels are elevated compared to normal muscle (Nalbantoglu et al., 1999).

In the heart, CAR expression is abundant during development and becomes barely detectable by adulthood (Ito et al., 2000), localizing to intercalated discs (Kashimura et al., 2004, Selinka et al., 2004, Shaw et al., 2004). Dissociated cardiomyocytes from newborn rats lose CAR expression in culture but regain it when cells cluster and start beating (Ito et al., 2000), suggesting a role for CAR in cardiomyocyte cell-cell adhesion. Knockout of CAR expression before embryonic day 11 in mice results in cardiac defects and embryonic lethality (Asher et al., 2005, Dorner et al., 2005, Chen et al., 2006), indicating that it is necessary for early heart development. CAR complexes with ZO-1, the gap junction protein connexin 45 and the adherens junction protein β-catenin, and promotes their correct localization to cell-cell junctions in the atrioventricular node and in

intercalated discs, thereby contributing to maintenance of cellular integrity and proper cardiac conduction (Lim et al., 2008, Lisewski et al., 2008).

Results from experiments using *in vitro* and *in vivo* rat models of giant cell myocarditis revealed induction of CAR expression during inflammation, an effect possibly mediated by cytokines (Ito et al., 2000). These results were confirmed in human donor cardiomyopathic hearts, which had higher levels of CAR compared to normal hearts or hearts with other diseases, suggesting that cardiomyopathy increases patients' susceptibility to viral infection via increased CAR expression (Noutsias et al., 2001, Poller et al., 2002).

4.5. CAR in the developing brain

The central nervous system is another example of strict spatio-temporal regulation of CAR. CAR is highly expressed in most brain structures during development, with levels peaking at birth and rapidly diminishing to undetectable levels by adulthood (Honda et al., 2000). It is expressed throughout developing hippocampal neurons including in the growth cones, structures that are involved in neuronal pathfinding (Honda et al., 2000, Huang et al., 2007). In the adult brain, on the other hand, CAR expression is limited to choroid plexus (Persson et al., 2006) and regions of neurogenesis (the hippocampal dentate gyrus, the subventricular zone of the lateral ventricles and the rostral migratory stream) (Hotta et al., 2003). CAR is also present in the peripheral nervous system; it is

highly expressed in dorsal root ganglia and peripheral nerves during embryogenesis (Tomko et al., 2000, Hotta et al., 2003).

As CAR is a cell adhesion molecule that participates in homophilic and heterophilic adhesion, and its expression is under tight control in the brain, this raised the possibility that it plays an important role in the brain during development. Indeed, results from our laboratory indicate that CAR promotes outgrowth of developing hippocampal and cortical neurons. Plating dissociated neurons on a substrate of soluble CAR extracellular domain increases neurite length, an effect that is dependent on the expression of endogenous CAR in neurons, suggesting the involvement of homophilic interactions (Huang K-C. et al, in preparation). Furthermore, endogenous CAR promotes outgrowth of developing neurons on fibronectin or laminin-1 substrates (Patzke et al., 2010).

4.6. CAR in the immune system

One role for CAR in the immune system involves the recruitment of neutrophils (polymorphonuclear leukocytes) to mucosal surfaces in response to bacterial infection. CAR on epithelial cells directly binds to junctional adhesion molecule-like protein (JAML) on neutrophils, allowing for neutrophil migration across colon epithelial cell tight junctions during inflammation (Zen et al., 2005). Similarly, CAR in endothelial cells has been proposed to facilitate migration of

monocytes across the endothelial cell monolayer during inflammation via interaction of endothelial CAR with JAML on monocytes (Guo et al., 2009).

Dendritic epidermal T cells (DETCs) residing in the skin provide a first line of defense against environmental insults such as infection, wounds and tumors (Macleod and Havran, 2011). DETCs express JAML, allowing them to bind to epithelial cells via binding of JAML to CAR-expressing epithelial cells, a step that promotes DETC proliferation and cytokine and growth factor production in response to wounds (Witherden et al., 2010).

4.7. Other roles for CAR in normal physiology

CAR has been proposed to play a role in the development of male gonads. It is highly expressed in Sertoli and germ cells during development, and associates with junctional adhesion molecule-C (JAM-C), LNX1 and LNX2 (Mirza et al., 2006, Mirza et al., 2007). It also contributes to the integrity of the blood-testis barrier (Lie et al., 2010, Su et al., 2012).

CAR is highly expressed in skin-derived lymphatic endothelial cells compared to blood vascular endothelial cells (Vigl et al., 2009). It promotes cell adhesion and lymph vascular tube formation, and lowers permeability of inter-lymphatic endothelial cell junctions (Vigl et al., 2009). A conditional embryonic mouse knockout model, in which CAR is knocked out between embryonic days 12.5-

15.5, revealed a requirement for CAR in the proper development of lymphatic vessel structures and the complete separation of the blood and lymphatic systems (Mirza et al., 2012). It is also involved in the proper development of the intestine and pancreas as well as control of thymocyte number (Pazirandeh et al., 2011).

4.8. CAR's role in cancer

Many cancer cell lines are resistant to adenoviral-mediated gene therapy due to low levels of endogenous CAR, and levels of CAR often negatively correlate with degree of cancer aggressiveness. CAR has been reported to inhibit growth, migration and invasion of several types of cancer (Okegawa et al., 2002, Sharma et al., 2009).

One mechanism of downregulation of CAR expression is via the Raf-MEK-ERK pathway, which is often activated in cancer (Anders et al., 2003). Another negative regulator of CAR expression in cancer cells is transforming growth factor beta (TGF β) pathway (Bruning and Runnebaum, 2003, Vincent et al., 2009). Hypoxia, a feature of many tumors, reduces CAR promoter activity and gene expression, possibly via hypoxia-inducible factor-1 α (HIF-1 α) (Kuster et al., 2010).

On the one hand, CAR plays an inhibitory role in several cancer types:

<u>Prostate cancer</u>: The prostate cancer cell line PC3 has lower endogenous CAR expression relative to other prostate cancer cell lines (Okegawa et al., 2000). Stable overexpression of CAR in PC3 cells inhibits *in vitro* growth in a dosedependent manner, and also suppresses *in vivo* tumor incidence and volume in nude mice (Okegawa et al., 2000).

Gliomas: CAR expression is downregulated in several glioma cell lines, with consequences on the efficacy of adenovirus-mediated gene therapy (Mori et al., 1999, Asaoka et al., 2000). Downregulation of CAR expression correlates with increasing tumor grade (Fuxe et al., 2003), suggesting that loss of CAR is advantageous in highly malignant gliomas. Re-expression of full-length CAR in the human glioma cell line U87MG inhibited *in vitro* glioma cell invasion in collagen as well as *in vivo* tumor growth in brains of nude mice; these effects required the presence of CAR's cytoplasmic domain and did not involve changes in cell proliferation (Huang et al., 2005b).

Bladder cancer: CAR expression in bladder cancer is variable, with some bladder cancer cell lines displaying little to no CAR expression, whereas others are unaffected (Li et al., 1999). Similar to glioma, there is a positive correlation between loss of CAR and increased grade of human bladder cancer (Okegawa et al., 2001, Sachs et al., 2002, Matsumoto et al., 2005). One CAR-deficient bladder cancer cell line is T24 (Li et al., 1999). Introducing CAR in T24 cells increased *in vitro* cell adhesion and decreased cell proliferation, and conversely, knockdown of

endogenous CAR expression in the bladder cancer cell line 253J decreased adhesion and increased proliferation (Okegawa et al., 2001). CAR overexpression increased p21 protein levels and decreased phosphorylation of the retinoblastoma (Rb) protein (events that promote cell cycle arrest or apoptosis), illustrating a role for CAR in cell cycle regulation (Okegawa et al., 2001). Decreased CAR expression in bladder cancer was accompanied by decreased expression of the cell adhesion molecule E-cadherin and increased nuclear immunoreactivity of the tumor suppressor protein p53, and was associated with increased lymph node metastasis and higher mortality (Matsumoto et al., 2005).

Gastrointestinal cancers: Low CAR expression is associated with poorly differentiated (anaplastic) primary and metastatic gastrointestinal tumors (Korn et al., 2006) and lower patient survival (Anders et al., 2009). CAR knockdown in gastric cancer cells resulted in increased proliferation, migration and invasion; the opposite effects were obtained with CAR overexpression (Anders et al., 2009, Stecker et al., 2011). Knockdown of CAR in the human colon cancer cell line DLD1 decreased expression of α -catenin, a protein often lost in cancer, and increased cell proliferation, migration and invasion (Stecker et al., 2009). Overexpression of α -catenin reversed these effects, and CAR was found to colocalize with, but not directly bind to, α -catenin (Stecker et al., 2009). CAR is highly expressed at the plasma membrane of normal colon mucosa, colon adenomas and metastases, while it is expressed at lower levels in colon cancer cells, suggesting that it may be both pro- and anti-tumorigenic depending on the

stage of colon carcinogenesis (cytoplasmic distribution had an opposite pattern in these tissues, suggesting that it is cellular distribution that differs rather than overall levels of CAR expression) (Stecker et al., 2011).

On the other hand, CAR acts as a tumor promoter in other cancers:

Breast cancer: CAR is elevated in primary breast cancer tissue samples, especially in metastatic breast cancer, and it is expressed in 21 out of 28 breast cancer cell lines that were tested (Martin et al., 2005); these data suggest that CAR may be involved in cell detachment from primary breast tumors early in the metastatic process. CAR expression strongly associated with presence of estrogen receptor, but not progesterone receptor, in breast cancer tissue samples, but its expression was not associated with a poorer outcome (Auer et al., 2009) in contrast with an earlier study (Martin et al., 2005). Estradiol treatment of the estrogen receptor-positive breast cancer cell line MCF-7 increased levels of CAR protein via an estrogen-responsive element in *CAR*'s gene promoter region (Vindrieux et al., 2011); thus, hormonal regulation of CAR levels occurs at the transcriptional level. CAR promoted proliferation of MCF-7 cells (in an estrogen-dependent manner) and the estrogen receptor-negative breast cancer cell line MDA-MB-231 (Vindrieux et al., 2011).

<u>Lung cancer</u>: CAR promoted lung cancer tumor formation in mice and decreased their survival (Qin et al., 2004). It was found to be expressed in lung cancer cells

of mesenchymal, but not epithelial, origin, and its expression was associated with loss of E-cadherin, decreased α -catenin and γ -catenin, and increased Vimentin, Snail, Twist and Zeb-1; these events are characteristic of epithelial-to-mesenchymal transition (EMT) (Veena et al., 2009). CAR expression was elevated in cancer stem cell populations of non-small lung cancer (NSLC) resistant to paclitaxel or radiation; CAR expression was associated with self-renewal, tumorigenesis and EMT in these cells (Zhang et al., 2012). However, when CAR was overexpressed in cell lines of melanoma or colon adenocarcinoma origin, metastasis of these cancer cells to lung was reduced in mice (Yamashita et al., 2007).

Ovarian cancer: Overexpression of CAR increased adhesion and decreased migration of A2780 ovarian cancer cells (Bruning and Runnebaum, 2004). However, these cells displayed enhanced resistance to apoptosis and had increased levels of the apoptosis regulator bcl-2, suggesting that the presence of CAR may promote cell survival early in tumorigenesis (Bruning et al., 2005).

Oral squamous cell carcinoma: *In vitro*, knockdown of CAR expression results in cell lifting, suppression of cell proliferation, cell death, movement of E-cadherin and β-catenin away from the plasma membrane, and inhibition of colony formation (Saito et al., 2013). *In vivo*, knockdown of CAR expression results in inhibition of tumor colony formation in mice (Saito et al., 2013). CAR binds to Rho-associated protein kinases (ROCKs) in oral squamous cell carcinomas and

inhibits ROCK-mediated apoptosis (Saito et al., 2013). CAR expression is relatively low in basal epithelial cells of normal squamous layer of tongue tissue, whereas it is upregulated in well-differentiated and poorly-differentiated squamous cell carcinomas from patients (Saito et al., 2013).

Clearly, CAR's role in cancer is complex and context-dependent, but at least in glioma, a topic of interest to our research group, it acts as a tumor suppressor.

4.9. CAR interacts with the cytoskeleton

CAR interacts with the cytoskeleton via direct binding to actin and tubulin. These interactions were initially discovered in a proteomics screen performed in our laboratory to identify proteins that bind to CAR's intracellular domain, and were confirmed *in vitro* and *in vivo* (Fok et al., 2007, Huang et al., 2007).

CAR promotes bundling of actin *in vitro*, and colocalizes with actin in growth cones of developing hippocampal neurons. Disruption of F-actin polymerization greatly reduced CAR immunoreactivity in dendrites and growth cones (Huang et al., 2007). CAR also promotes microtubule bundling *in vitro* and stabilizes the microtubule network in cells, as CAR-expressing glioma cells were more resistant to disruption of microtubules with nocodazole (Fok et al., 2007). The microtubule stabilizing agent paclitaxel reduced chemotactic migration of control, but not CAR-expressing, glioma cells, suggesting that one mechanism by which CAR inhibits glioma migration is via its stabilization of the microtubule network (Fok

et al., 2007). Thus, within this context it would be advantageous for a cancer cell to downregulate CAR expression. The last 26 amino acids in CAR's intracellular domain are required for CAR binding to actin and tubulin (Fok et al., 2007, Huang et al., 2007).

5. Study rationale and objectives

Since a wide variety of proteins including cell adhesion molecules undergo ectodomain shedding and RIP, we wondered if that is the case for CAR.

Preliminary results from our laboratory indicated that U87MG human glioma cells exogenously expressing CAR (U87 CAR cell line) release a 32 kDa N-terminal CAR fragment into conditioned media. This was found to occur constitutively as well as by phorbol ester treatment. Generation of the 32 kDa shed fragment (named CAR ECD) decreased when cells were treated with the broad spectrum metalloprotease inhibitors TAPI-1 and O-phenanthroline, indicating the involvement of metalloproteases in this event. The TIMP inhibition profiles suggested that ADAM10 may be a sheddase of CAR in the U87 CAR cell line.

Western blots analyses of cell lysates with an anti-CAR C-term antibody revealed that ectodomain shedding events were associated with the appearance of two fragments that were 20 kDa and 14 kDa in size. Generation of the 14 kDa

fragment was inhibited when cells were treated with the γ-secretase inhibitors MG132 and DAPT. Thus, the 20 kDa fragment (CAR CTF1) is the transmembrane/cytoplasmic domain remnant from ectodomain shedding, and the 14 kDa fragment (CAR CTF2) is the product of RIP of CAR CTF1. Figure 1.5 illustrates a model of CAR proteolysis based on these preliminary data, indicating the molecular weights of CAR ECD, CTF1 and CTF2.

As previously mentioned, CAR acts as a tumor suppressor in several cancers, including glioma (Huang et al., 2005b), a subject of interest in our laboratory. Furthermore, data from our group shows that CAR promotes outgrowth of developing neurons (Huang et al., in preparation). It is possible that ectodomain shedding and RIP would affect CAR's roles in gliomas and neuronal outgrowth.

Thus, the main aims of this study were:

- 1) To further characterize CAR ectodomain shedding and RIP, including the players involved;
- 2) To investigate what the consequences of these proteolytic cleavages are on CAR function within the contexts of glioma inhibition and neuronal outgrowth.

Figure 1.1: Domain organization of ADAM metalloproteases and sites of ADAM interactions with proteins such as integrins, tissue inhibitors of metalloproteases (TIMPs) and intracellular proteins containing interaction motifs such as SH2, SH3 and PDZ. Abbreviations of domains: PRO = pro-domain, MP = metalloproteinase, DI = disintegin, ACR = ADAM cysteine-rich, E = epidermal growth factor-like, TM = transmembrane region, CT = cytoplasmic tail. Adapted from (Huovila et al., 2005).

Figure 1.1

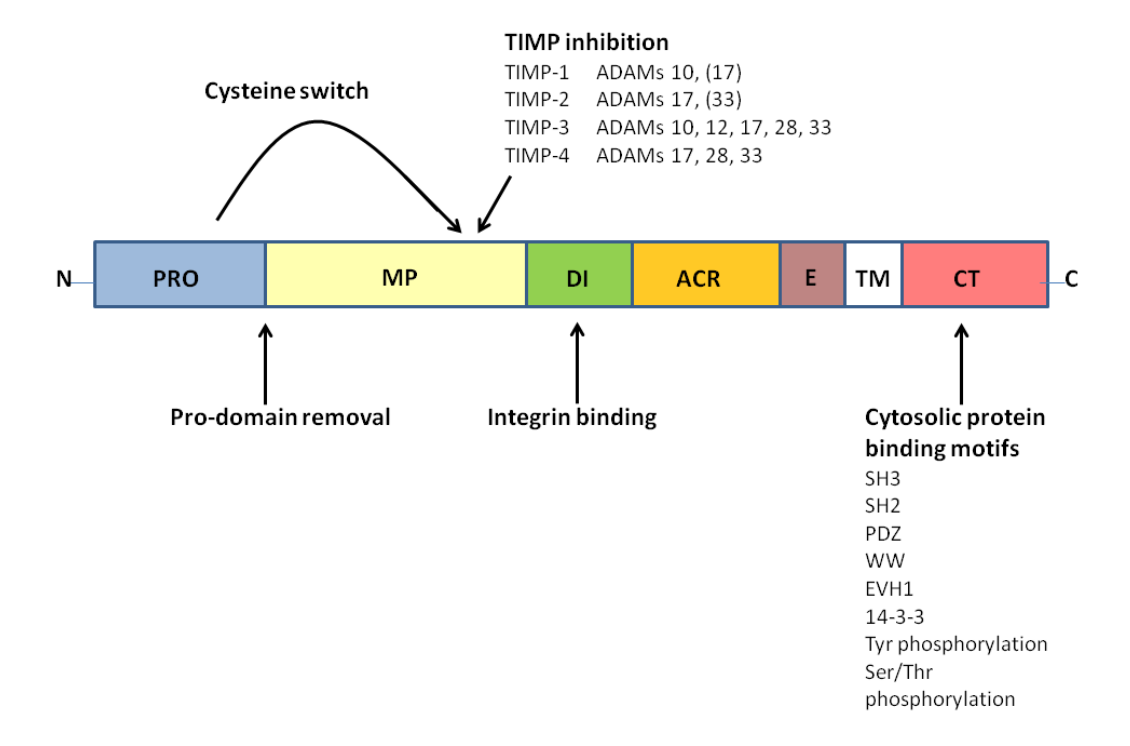


Figure 1.2: The 21 members of the ADAM family in humans. The presence or absence of catalytic activity is indicated, as well as which members are restricted to the testis. Adapted from (Edwards et al., 2008).

Figure 1.2

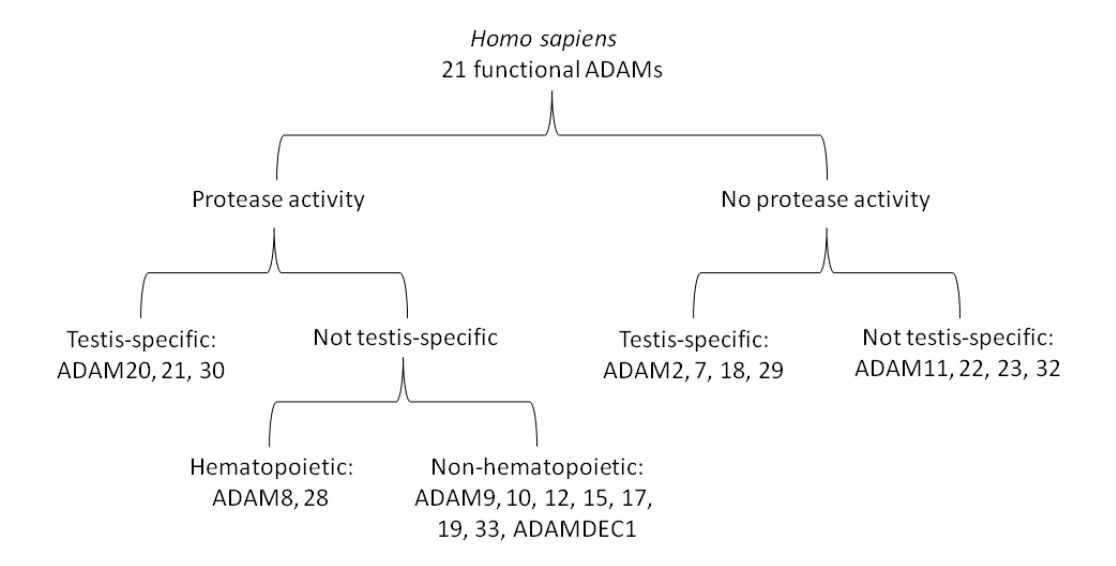


Figure 1.3: Ectodomain shedding of an Igsf family member CAM (a) results in a shed fragment capable of triggering a signaling pathway via homophilic interactions (b), binding and activating growth factor receptors (c), promoting integrin-mediated signal transduction (d) and integrin-mediated cell adhesion (e). In some cases, ectodomain shedding is a prerequisite for regulated intramembrane proteolysis (RIP), which results in a freed cytoplasmic domain that participates in downstream signaling (f) and/or regulation of gene expression (g). Adapted from (Cavallaro and Dejana, 2011).

Figure 1.3

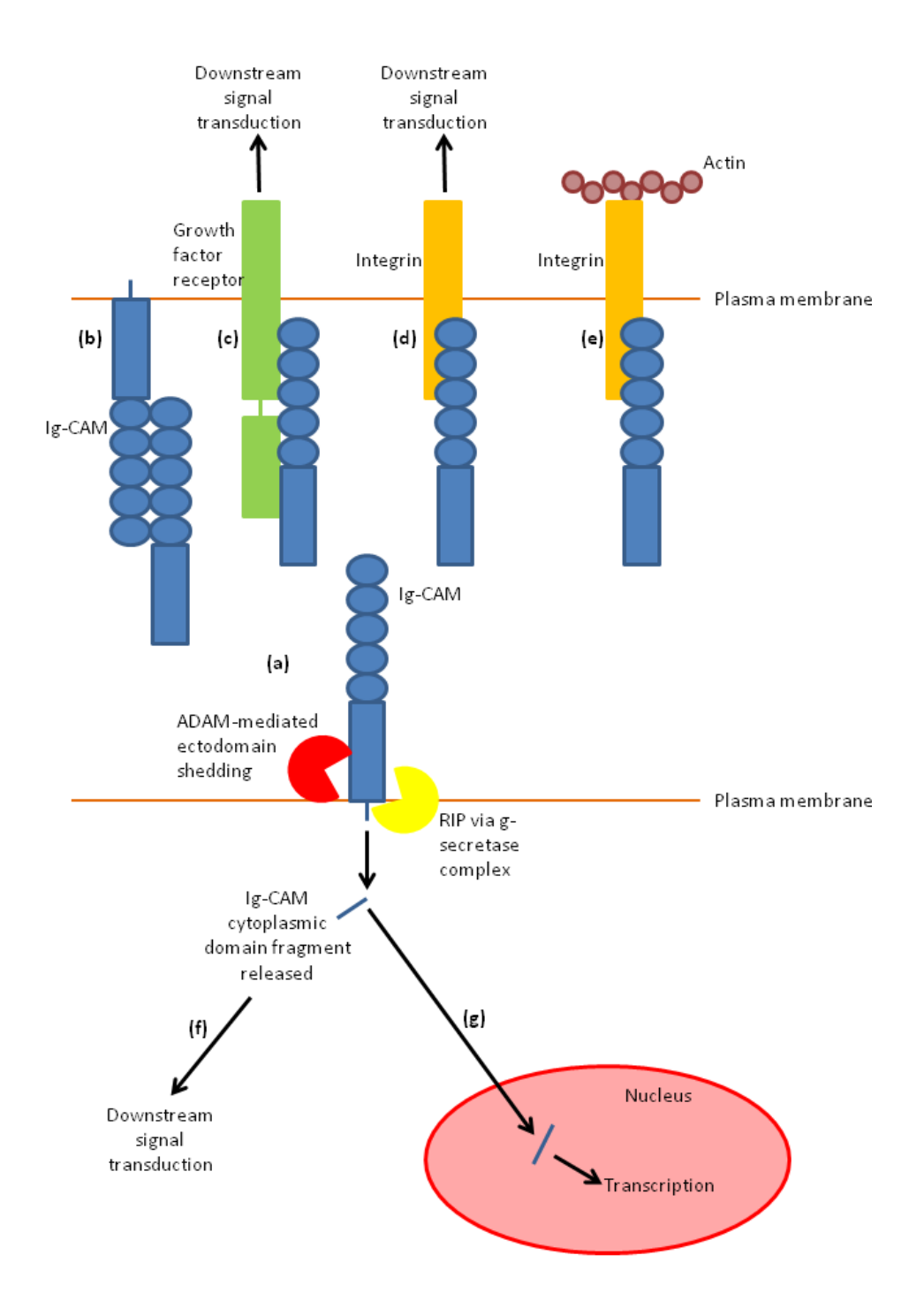


Figure 1.4: Notch receptor proteolysis. Site 1 (S1) Furin cleavage of Notch in the Golgi results in heterodimerization of the receptor. At the cell surface, a transmembrane ligand (Jagged or Delta) from a signal-transmitting cell interacts with Notch on the signal-transmitting cell, triggering proteolysis by ADAM 10 (S2) and the γ-secretase complex (S3/S4). The Notch intracellular domain (NICD) that is generated enters the nucleus, interacts with CSL and transcriptional activators, and activates expression of target genes such as *hes* (Hairy/Enhancer of Split). Adapted from (Kopan and Ilagan, 2009).

Figure 1.4

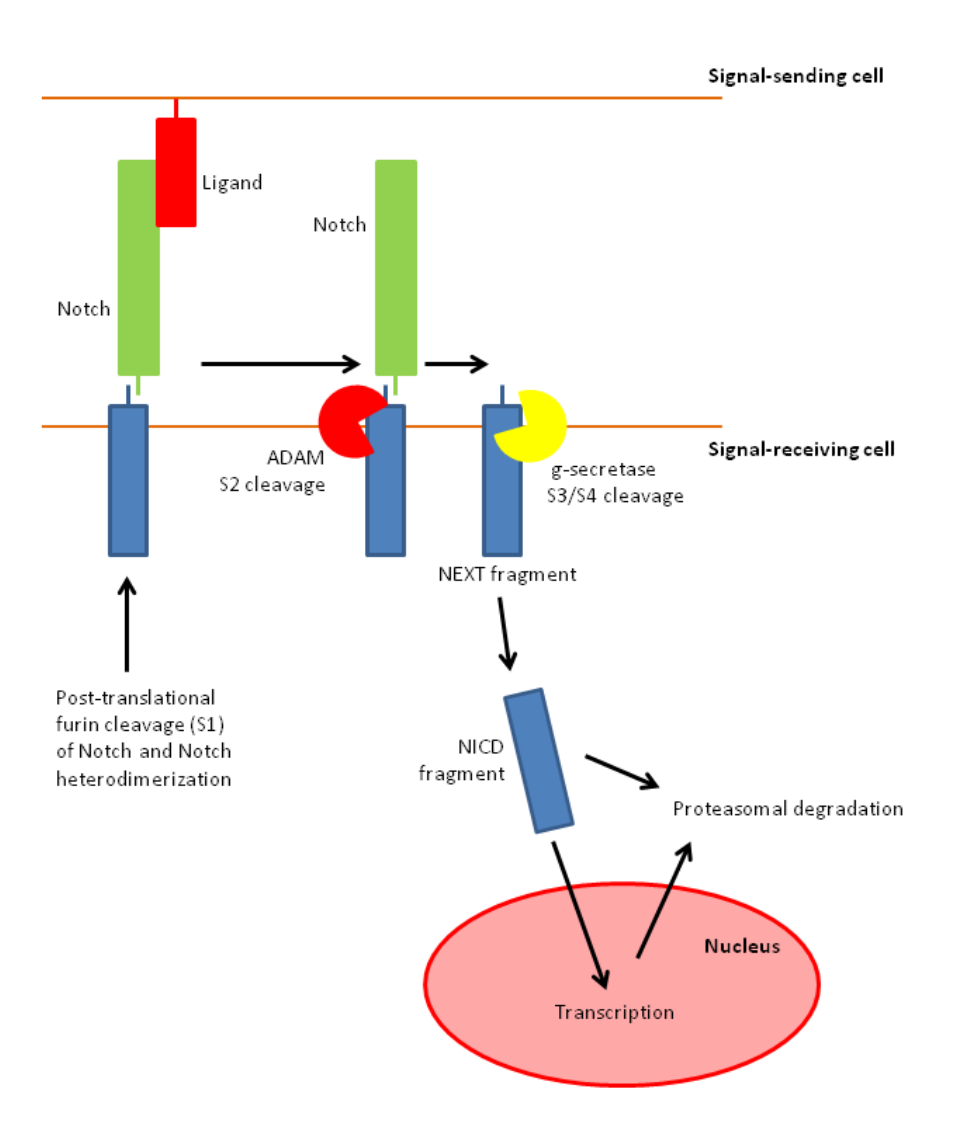
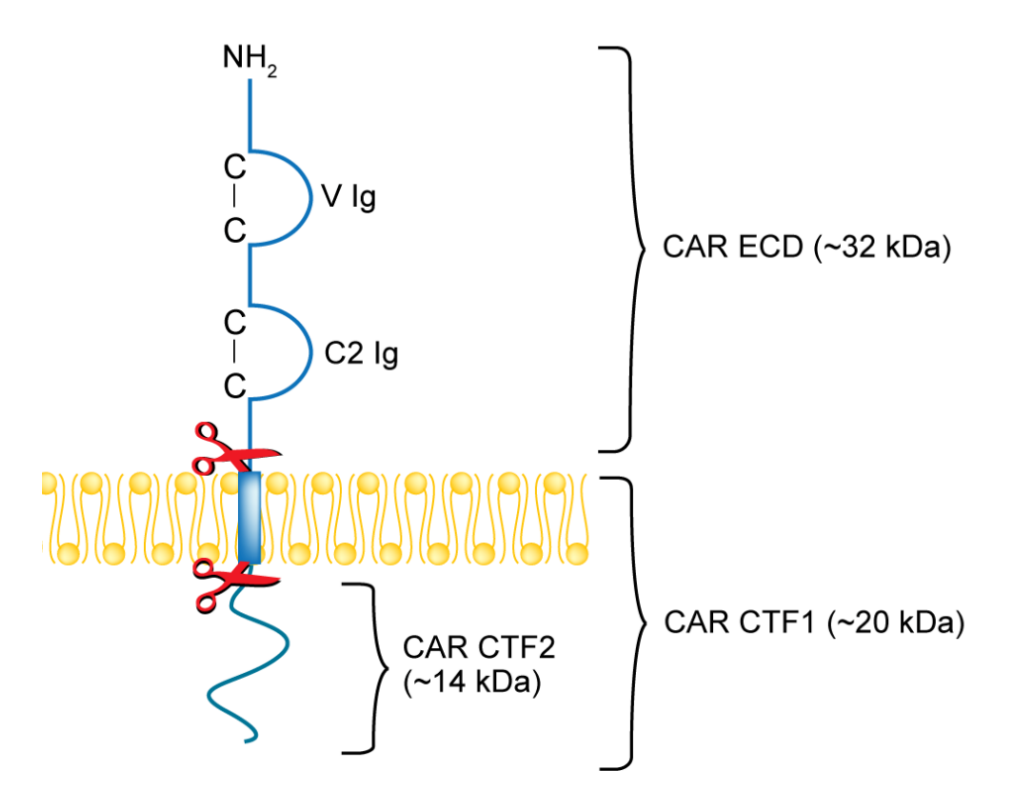


Figure 1.5: A model of CAR proteolysis. The top pair of scissors represents ectodomain shedding of CAR, releasing a fragment of 32 kDa (CAR ECD) and leaving behind a 20 kDa transmembrane/cytosolic stub (CTF1). RIP of CTF1, represented by the lower pair of scissors, generates a 14 kDa fragment (CTF2) that is freed from the lipid bilayer. V Ig and C2 Ig are the variable and constant immunoglobulin-like domains, respectively.

Figure 1.5



Chapter 2: Materials and Methods

Chemicals

Phorbol 12-myristate 13-acetate (PMA), ionomycin and tricholoracetic acid (TCA) were from Sigma. GM6001, GM6001 negative control, Compound E (gamma-Secretase Inhibitor XXI), Gö 6983, and MG132 were from Calbiochem. Epoxomicin was from Biovision (Cedarlane). EGF and IGF-1 were from Peprotech. Purified prodomain of ADAM10 was a kind gift from Dr. Marcia Moss (Biozyme, Inc.).

Antibodies

The production, purification and characterization of the rabbit polyclonal antibodies 2239 and 2240 raised against CAR N-terminal extracellular domain have been previously described (Nalbantoglu et al., 1999). The rabbit polyclonal antibody RP291 raised against the C-terminal intracellular domain of human CAR (46 kDa isoform) cross-reacts with the murine homolog mCAR1 (Sollerbrant et al., 2003, Shaw et al., 2004), and was a kind gift from Dr. Kerstin Sollerbrant (Karolinska Institute and University Hospital, Stockholm, Sweden). Rabbit polyclonal antibody raised against ADAM10 was from AnaSpec, Inc. Mouse monoclonal antibody raised against GAL4 DNA-binding domain (RK5C1) was from Santa Cruz Biotechnology, Inc. Rabbit polyclonal antibody raised against Green Fluorescent Protein (GFP) was a kind gift from Dr. Rénald Gilbert

(Biotechnology Research Institute, National Research Council Canada, Montreal, Canada). Mouse monoclonal antibody raised against importin alpha was from Sigma. Horseradish peroxidase (HRP)-conjugated anti-glyceraldehyde -3-phosphate dehydrogenase (GAPDH) antibody was from Abcam. Goat or swine anti-mouse and anti-rabbit HRP-conjugated secondary antibodies were from Pierce and Dako. Goat anti-mouse Alexa Fluor 555 secondary antibody was from Molecular Probes.

Lentivirus production and shRNA knockdown

Five different small hairpin ribonucleic acid (shRNA) sequences (TRC library) in a lentiviral vector (pLKO.1) targeting human ADAM10 and a control shRNA targeting enhanced green fluorescent protein (eGFP) were purchased from Open Biosystems. Production of lentiviruses, infection and stable selection of cells with 2 μg/ml puromycin were performed according to the RNAi Consortium (TRC) guidelines for second generation lentiviruses. Cell lines were maintained with 2 μg/ml puromycin. The level of knockdown in cells was initially assayed by real-time polymerase chain reaction (PCR) of reverse-transcribed RNA, normalizing over GAPDH. Only shRNA sequences that sufficiently knocked down *adam10* expression without affecting *adam17* levels were considered specific. Experiments were subsequently performed using the anti-ADAM10 hairpin sequence

CCGGGCAGTATTACTTATGGGAATTCTCGAGAATTCCCATAAGTAATA

CTGCTTTTT (thereafter referred to as "6676") or a second hairpin shRNA, CCGGGCTGTGCAGATCATTCAGTATCTCGAGATACTGAATGATCTGCA CAGCTTTTT (referred to as "6675").

For the bicistronic IRES-GFP plasmid (pWPI) (pWPI, CAR-V5 in pWPI and ICD-V5 in pWPI), production of lentiviruses was carried out per RNAi Consortium (TRC) guidelines for second generation lentiviruses. Prior to each experiment, human glioma U87-MG cells were infected with lentivirus with titers that resulted in similar GFP expression per equal quantities of proteins for each sample (pWPI only, CAR-V5, ICD-V5). Experiments were performed 3 or 5 days post-infection.

Plasmids

Murine CAR (isoform 1) cloned in pcDNA3 plasmid has been previously described (Nalbantoglu et al., 1999). All point-mutations or deletions were performed with the QuikChange II XL site-directed mutagenesis kit (Strategene), per manufacturer's directions. Four mutants of CAR were generated using pcDNA3-mCAR1 as template: ML→AA (in which amino acids M224 and L225 were mutated to alanine residues), RL→AA (in which amino acids R226 and L227 were mutated to alanine residues), MLRL→AAAA (in which M224, L225, R226 and L227 were mutated to alanine residues) and Δ221-232 (in which amino acids 221-232 were deleted).

The plasmid pcDNA 3.1/V5-His6x B (Invitrogen) was a kind gift from Dr. Alyson Fournier (McGill University, Montreal, Canada). To generate the CAR-V5 construct (full-length murine CAR isoform 1 with a V5/His6x tag at the C-terminus), CAR insert in pcDNA3 plasmid was amplified with Phusion High Fidelity DNA polymerase (Finnzymes Inc.), including the Kozak sequence and excluding the stop codon. Blunt-end cloning of the PCR product was performed with EcoRV-digested pcDNA 3.1/V5-His. To obtain a construct of the intracellular domain of CAR with C-terminal V5-His6x tags (herein referred to as CAR ICD-V5), full-length CAR in pcDNA3.1 V5-His plasmid was used as template with the QuikChange II XL site-directed mutagenesis kit (Stratagene). Amino acids 2-260 inclusive were deleted from CAR-V5 to generate ICD-V5.

Human ADAM10 cDNA in pCR4-TOPO plasmid (clone ID 8991969) was purchased from Open Biosystems and cloned into pcDNA3.1 plasmid using the NotI and PmeI sites. The shRNA-resistant mutant was generated from this construct by deleting nucleotides 2319-2325 using the QuikChange II XL site-directed mutagenesis kit (Strategene), per manufacturer's directions.

The plasmids pUAS-luc2 (Addgene ID # 24343) and pCMV-GAL4 (Addgene ID # 24345) were kind gifts of Dr. Liqun Luo (Stanford University) (Potter et al., 2010). PCR was performed Phusion High Fidelity DNA polymerase (Finnzymes Inc.), with pCMV-GAL4 as template and primers that introduced a 5' BamHI site

and a 3' NheI site in GAL4 (no stop codon), and with CAR ICD (pcDNA3.1) as template using primers that introduced a 5'NheI site and a 3' NotI site (with a stop codon) in CAR ICD. The GAL4 PCR product was digested with BamHI and NheI, and the CAR ICD PCR product was digested with NheI and NotI. The plasmid pCMV-GAL4 was digested with the restriction enzymes BamHI and NotI. The digested plasmid and PCR products were then ligated to generate the pCMV-Gal4-CAR ICD plasmid.

The pCMV-GAL4 DNA-binding domain (DBD) vector was generated by amplifying the DBD sequence of GAL4 by PCR using pCMV-GAL4 plasmid as template and primers that introduced a 5' BamHI site and a 3' NotI site with a stop codon. The insert was digested with BamHI and NotI, and cloned into pCMV-GAL4 vector cut with BamHI and NotI. To generate the pCMV-GAL4 DBD-CAR ICD vector, the GAL4 DBD sequence was amplified by PCR using pCMV-GAL4 plasmid as template and primers that introduced a 5' BamHI site and a 3' NheI site, and CAR ICD was amplified as mentioned above (with 5' NheI and 3' NotI sites). The amplified products and pCMV-GAL4 vector were digested with the appropriate enzymes and ligated.

The plasmid pWPI with IRES-GFP (Addgene ID # 12254) was a kind gift of Dr. Didier Trono. Full-length CAR or CAR intracellular domain, with C-terminal V5/6xHis tag and stop codon, were amplified by PCR using the corresponding

pcDNA3.1 plasmids as template. The PCR products were cloned into the PmeI site in the pWPI vector.

All constructs were verified by sequencing at the Plateforme de séquençage et de génotypage des génomes, Centre de recherche du CHUL, Québec, Canada.

Cell lines and culture conditions

The human embryonic kidney (HEK) 293 cell line and the human glioma cell lines U87-MG and U251N were obtained from the American Type Culture Collection (ATCC) (Rockville, MD). The murine embryonic fibroblast (MEF) cell line knock-out for presenilin 1 and 2 (herein referred to as "MEF PS 1/2 KO") and wild-type MEF cell line were kind gifts from Dr. Bart de Strooper, K.U. Leuven, Belgium (Herreman et al., 1999, Herreman et al., 2003). Cells were maintained in an incubator at 37°C with 5% CO₂ using Dulbecco's Modified Eagle Medium (DMEM) supplemented with 10% heat-inactivated fetal bovine serum (FBS) and antibiotic cocktail (100 units of penicillin/ml, 100 μg of streptomycin/ml).

The generation of U87-MG polyclonal cell populations over-expressing CAR or CAR lacking the cytoplasmic domain (tailless CAR) via a retroviral vector has been previously described (Nalbantoglu et al., 1999, Huang et al., 2005b). Briefly, retroviruses carrying the sequence for full-length or tailless murine CAR (isoform

1) were produced. Retroviruses carrying empty vector with the neomycin resistance gene were used as control. The supernatants from the producer cell lines were used for infection of U87-MG cells, which were then selected for 10 days with G418 (600 μ g/ml). Clones were pooled together to generate bulk populations stably expressing full-length CAR (U87 CAR), tailless CAR (U87 CAR tailless) or control cells (U87 LNCX).

U87-MG and U251N cells were transfected with wild-type or mutant CAR constructs using FuGENE 6 (Roche) or TransIT-2020 (Mirus), as per manufacturers' guidelines. Cells were selected for 7-10 days with 600 μ g/ml G418 and then maintained with 200 μ g/ml G418. Clones were pooled together during generation of stable cell lines in order to minimize clonal-specific effects. For some experiments that involved transient transfection of U87-MG and U251N cells with DNA, the aforementioned transfection reagents were also used.

Wild-type or presenilin 1 and 2 double knockout MEF (PS 1/2 KO) cells were infected with adenovirus carrying the gene for the full-length coding sequence of CAR in opti-MEM at MOI between 100-200. A few hours later, the media were replaced with DMEM containing 10% FBS and antibiotic cocktail, and experiments were performed 48 hours post-infection. For other experiments, MEF cells were infected with lentivirus for expression of V5-tagged CAR (in pWPI vector) per RNAi Consortium (TRC library) guidelines. Cells were lysed 3 days post-infection for analysis via SDS-PAGE and Western blot.

6-well plates were coated with 33 µg/ml poly-d-lysine (Millipore) for 1 hour at room temperature, then rinsed with sterile water and left to dry for 1 hour at room temperature. Timed pregnant mice (Charles River Laboratories) at 17 days gestation were sacrificed by CO₂ and cervical dislocation, and embryos were sacrificed by decapitation. Cortices were dissected from brains of embryos and collected into 3 ml of cold Hank's Balanced Salt Solution (HBSS) (Wisent) surgical buffer (HBSS, 1M HEPES pH 7.4, 1 M D-glucose, 100 mM CaCl₂, 100 mM MgSO₄, 1M NaHCO₃). The cortices were homogenized using a fire-polished pipette (20-25 strokes), and dissociated individual cells were separated out from undissociated tissue debris by filtering the sample through a 70µm cell strainer and pelleted by centrifugation for 3 minutes at 200 x g. The cell pellet was then gently resuspended in Neurobasal medium (Invitrogen) supplemented with B-27 (1X) (Invitrogen), N2 (1X) (Invitrogen), 0.5mM L-glutamine (Gibco), penicillin (100 U/ml), and streptomycin sulfate (100 µg/ml). Cells were counted, and dead cells were identified using Trypan blue. Between 1 x 10⁶ - 2 x 10⁶ cells were seeded per well of a 6-well plate. Half the volume of medium was replaced for each well every 4 days, and experiments were performed between 7 - 9 days in vitro.

The plasmid for dimeric Fc-CAR ectodomain was a generous gift from Dr. Brad Spiller (Cardiff University, UK) (Goodfellow et al., 2005) and it contains the sequence for V and C2 immunoglobulin domains ligated to the hinge and Fc portion of human IgG antibody (Yanagawa et al., 2004). Human embryonic kidney (HEK) 293A cells were transfected with the Fc-CAR plasmid using Lipofectamine 2000 (Invitrogen) per manufacturer's directions, and stable transfectants were selected with hygromycin B (Roche) at 400 µg/ml. For production of purified Fc-CAR, the stable HEK 293A cell line was grown in opti-MEM for 48 hours, and secreted Fc-CAR was purified from the conditioned media by protein A affinity chromatography. The beads were washed twice with each of 100 mM Tris-HCl (pH 8) and 10 mM Tris-HCl (pH 8). Fc-CAR was eluted with 100 mM glycine buffer (pH 3). The pH of eluted Fc-CAR was neutralized to pH 8 with 1 M Tris buffer, and purity was confirmed by Western blot analysis. Fractions containing Fc-CAR were pooled. Protein yield was determined using a bovine serum albumin (BSA) standard curve, SDS-PAGE, Coomassie blue staining of the gel and densitometry quantification.

Cerebellar microexplant cultures

24-well plates were coated with poly-d-lysine (PDL) overnight at 4°C, followed by an additional coating of half of the number of wells with 0.125 µg Fc-CAR

overnight at 4°C. Cerebella from brains of post-natal day 2 mice were dissected in surgical buffer (Hank's balanced salt solution (HBSS) with 1mM sodium pyruvate, penicillin/streptomycin cocktail (1X) and 0.5 ml of 10 mM HEPES pH 7.4). Cerebella were strained through a Nitex mesh with 100 µm-sized pores, allowed to settle and then rinsed before resuspending in Neurobasal media containing B27 (1X), N2 (1X), penicillin (100 U/ml), streptomycin sulfate (100 μg/ml), Glutamax (1X), 6 mM glucose, and 10% horse serum. Microexplants were seeded on the coated wells, and cultured at 37°C and 5% CO₂ overnight (16-18 hours). Explants were then treated with GM6001 or its negative control at a final concentration of 25 µM at 37°C and 5% CO₂, and the experiment was stopped 24 hours later by fixing the microexplants with 4% paraformaldehyde, followed by Coomassie blue staining and 2-3 washes with PBS. Pictures were taken with a 100X objective using a wide-field light microscope (Leica). The 5 longest neurites were measured from each explant using the NeuronJ plugin from ImageJ software. Neurite lengths were summed up for each explant, the mean and the standard error of the mean (SEM) were calculated for each group, and pixels were converted to µm.

Preparation and collection of conditioned media

For PMA (phorbol 12-myristate 13-acetate)-induced, ionomycin-induced or constitutive shedding of CAR, 2.5×10^5 - 5.0×10^5 cells were seeded per well of a 6-well plate. The following day, cells were washed and incubated in 1 ml of opti-

MEM, either for 3-4 hours in the presence of PMA (10^{-6} M final concentration; dimethyl sulfoxide (DMSO) vehicle as control) for PMA-induced shedding or for 30 minutes with ionomycin ($1.5~\mu M$ final concentration; DMSO vehicle as control). For constitutive shedding, cells were incubated for 16-24 hours in opti-MEM. In the case of experiments with pervanadate, 500~mM of Na_3VO_4 was prepared. $25~\mu l$ of this solution was added to $565~\mu l$ PBS and $10~\mu l$ of $3\%~H_2O_2$ and left at room temperature for 5~minutes. This solution was used as 100X stock to treat cells for 30~minutes.

At the end of shedding experiments, conditioned media were transferred into chilled microtubes. Cells were lysed with buffer containing 0.06M Tris-HCl pH 6.8, 4% sodium dodecyl sulfate (SDS), 10% glycerol and protease inhibitors (complete EDTA-free protease inhibitor cocktail from Roche), and heated at 95°C. The collected conditioned media were cleared of cell debris. The tricholoracetic acid (TCA) protein precipitation method was adapted with minor modifications from the protocol developed by the Bjorkman group (Howard Hughes Medical Institute, California Institute of Technology). Per 1 ml of conditioned media, 5 µg of BSA was added, followed by 250 µl of chilled 100% TCA (drop-wise). Samples were incubated overnight at 4°C and then pelleted at high speed in a microcentrifuge at 4°C, followed by two washes with ice-cold acetone. The acetone was evaporated by heating the samples briefly in a 60°C heating block. Protein pellets were solubilized in Laemmli/2-mercaptoethanol buffer.

For collection of conditioned media from neuronal cultures, protease inhibitor cocktail (Roche, complete EDTA-free) was added to samples followed with clearance of debris at high speed in a microcentrifuge at 4°C. Media were transferred to centrifugation columns (Millipore, Amicon Ultra-4 10,000 MWCO) and centrifuged at 3800 rcm, 4°C for 45-60 minutes. Concentrated media in the column were then resuspended in Laemmli/2-mercaptoethanol.

SDS-PAGE and Western blots

Protein concentrations of cell lysates were determined using the bicinchoninic acid (BCA) assay kit from Pierce Biotechnology, Inc. Samples were loaded on 13% SDS-PAGE gel, and electrophoresis was performed under reducing conditions. Precision Plus Protein Dual Color Standards (BioRad) and MagicMark XP (Invitrogen) were used to visualize band sizes on SDS-PAGE gel and Western blot, respectively. Proteins were transferred to polyvinylidene fluoride (PVDF) membranes (Immobilon P, Thermo Scientific) at 0.3 amps for 1 hour in a mini-transblot apparatus (BioRad). Transfer efficiency was verified with Ponceau staining, and membranes were then blocked in 10% (w/v) skim milk in Tris-buffered saline (TBS) containing 0.1% Tween-20 (TBS-T). Primary antibodies were diluted with 5% skim milk in TBS-T and applied to membranes with gentle shaking overnight at 4°C. After extensive washes with TBS-T, HRP-conjugated secondary antibody was applied with gentle shaking to membranes for

1 hour at room temperature. The membranes were extensively washed with TBS-T, and SuperSignal West Femto substrate (Pierce Biotechnology, Inc.) was used as per manufacturer's instructions. Chemiluminescence signal was detected with a cooled charge-coupled device (CCD) camera attached to an imaging capturing system (Gene-Gnome, Syngene) or on film (Denville HyBlot CL). Quantification of band intensities was performed using Syngene software. Western blots shown are representative of at least 3 independent experiments each, unless otherwise indicated

Reverse transcription of total RNA and real-time PCR

Total RNA was harvested from cells using the RNeasy Mini kit and QiaShredder (both from Qiagen), followed by reverse transcription with M-MLV reverse transcriptase (Invitrogen) according to the manufacturers' instructions. cDNA samples were diluted to fall within the standard curves, and samples were run in triplicates using an ABI Prism 7000 Sequence Detection System and SYBR Green PCR Core reagents (Applied Biosystems, Inc.) per manufacturer's recommendations. Analyses were performed using the 7000 System software (Applied Biosystems, Inc.) and data were normalized over GAPDH transcript levels. Primers were designed using Primer Express 2.0 software (Applied Biosystems, Inc.) and the sequences used were as follows: human GAPDH-forward: 5'-CATCAATGACCCCTTCATTGAC -3'; human GAPDH-reverse: 5'-CGCCCCACTTGATTTTGGA-3'; human ADAM10-forward: 5'-

GCGGCCCCGAGAGAGTTA-3'; human ADAM10-reverse: 5'AGGAAGAACCAAGGCAAAAGC-3'; human ADAM17-forward: 5'GGATACATGCTCTTAGAAAATTCACTATTG-3'; and human ADAM17reverse: 5'-GCAACCTCAGCCTCTCCAAGT-3'. Different concentrations were
tested for each pair of primers, and the optimal concentration for each pair was
found to be 900 nM. Primers were synthesized by Alpha DNA, Montréal, Québec,
Canada.

In vitro enzymatic cleavage and mass spectrometry

A peptide with sequence VGSDQCMLRLDVVPPSNRAG representing amino acids 218-237 of murine CAR isoform 1 (mCAR1) was manufactured by GenScript, Inc. Recombinant human ADAM10 was purchased from R & D Systems, Inc. The buffer used for *in vitro* digestion contained 25 mM Tris, 2.5 μM ZnCl₂ and 0.005% Brij-35 detergent at pH 9.0. 10 μg of peptide was digested with 2 μg recombinant enzyme in 10 μl final volume at 37°C for 4 or 16 hours. The following controls were also included: peptide only or recombinant ADAM10 only (16 hours digestion at 37°C for each), and peptide plus recombinant ADAM10 at 0 hours incubation (prepared on ice and stopped immediately). 20% trifluoroacetic acid (TFA) was used to stop each reaction with a final pH of 3. Samples were analyzed at the Genome Quebec Proteomics Platform (Montreal, Canada) via matrix-assisted laser desorption/ionization mass spectrometry (MS/MS).

Calf intestinal alkaline phosphatase (CIP) was purchased from New England Biolabs. U87 CAR cells were treated with 1 μM PMA (vs. DMSO vehicle) for 4 hours to trigger CAR ectodomain shedding. Cells were lysed with lysis buffer and proteins were quantified using BCA protein assays as previously described. 20 μg of protein per sample were treated with 40 units of CIP (or H₂O as negative control) for 1 hour at 37°C. Samples were analyzed by SDS-PAGE and Western blot using the rabbit polyclonal anti-CAR N-term antibody 2240.

Cell surface biotinylation

Cells were seeded at a density of 10⁶ cells per 10 cm dish. The next day, cells were washed in PBS twice at 4°C and incubated with 7.5 mg of EZ-Link Sulfo NHS-LC-Biotin (Pierce Biotechnology) for 30 minutes at 4°C. The reaction was quenched by washing cells twice with 1 mM glycine, followed by two washes with PBS, all for 10 minutes each at 4°C. Cells were then harvested with modified RIPA buffer (20 mM HEPES pH8, 150 mM NaCl, 0.1% SDS, 1% Triton X-100, 1% sodium deoxycholate and protease inhibitor cocktail (Roche)), incubated on ice for 10 minutes, cleared by high speed centrifugation, and incubated with streptavidin beads (Pierce Biotechnology) for 2 hours at 4°C with gentle rotation. Streptavidin beads were washed three times with modified RIPA buffer, eluted with Laemmli/2-mercaptoethanol buffer, and boiled.

For experiments with PMA-stimulated shedding of CAR, cells were washed with room temperature PBS, and cell surface biotinylation was performed at room temperature for 5 minutes. The reaction was terminated by adding Tris-HCl (pH 7.5, 670 µM final concentration) and incubating for 5 minutes at room temperature. Samples were washed twice with PBS, harvested with buffer A (2% NP40, 0.2% SDS, protease inhibitor cocktail (Roche)) and kept on ice for 30 minutes, followed by incubation with streptavidin beads (2 hours at 4°C with gentle rotation). Beads were washed three times with buffer A and once with buffer B (0.1% NP40, 0.5 M NaCl in PBS), resuspended in Laemmli/2-mercaptoethanol buffer, and boiled.

Adenovirus infection and β -galactosidase luminometry assays

Cells were seeded in 24-well plates at a density of 30,000 cells/well. After attachment, cells were washed and incubated with opti-MEM, and infected with adenovirus carrying the gene for β -galactosidase (AdV lacZ) at multiplicities of infection (MOIs) of 0, 2, 5 or 10. Each group consisted of 3 biological replicates. 24 hours later, cells were washed with PBS and lysed with 100 μ l of lysis buffer (Galacto-Star system, Applied Biosystems). Lysates were cleared from debris by centrifugation. 150 μ l of reaction buffer (Galacto-Star system, Applied Biosystems) was added to 10 μ l of lysate per manufacturer's directions and incubated at room temperature for 30 minutes. Lysate samples were also used to

quantify protein concentration using BCA protein assays. A Bio-Orbit 1250 luminometer was used to measure light emission, expressed in relative light units (RLU) per mg of protein. For each sample, 3 measurements were taken spaced 10 seconds apart and the average calculated.

Boyden cell migration chamber assays

10⁶ cells were seeded per 10 cm dish for each cell line. The next day, cells were extensively washed with serum starvation medium (0.1% BSA in DMEM) and incubated overnight in serum starvation medium. Transwell chambers with 8 µm polycarbonate filter inserts (purchased from Corning) were prepared the following day by coating filter inserts with a thin layer of Matrigel basement membrane matrix (BD Bioscience) at a final concentration of 0.125 µg/µl and left to dry for 4-5 hours under a sterile tissue culture hood. Conditioned media were added to the bottom chamber as chemoattractant for the serum starved cells. The serum starved cells were washed, trypsinized and suspended in Boyden media (0.1% BSA and 1% FBS in DMEM), and seeded (1,500 cells/insert or 5,000 cells/insert). For experiments with glioma cells expressing MLRL to AAAA or del 221-232 mutant CAR, conditioned media used came from the respective cell lines and migration was allowed overnight (16 hours) before stopping the experiment. For experiments on U87 CAR cells using PMA or GM6001, conditioned media used came from U87 LNCX cells, PMA, DMSO, GM6001 or its negative control were added inside the insert and in the lower chamber at the appropriate final

concentrations, and cells were allowed to migrate for 4 hours before stopping the experiment. To stop the experiment, inserts were washed with PBS and fixed with 4% paraformaldehyde for 30 minutes. Cells remaining in the top part of the insert were scraped off gently with a cotton Q-tip so that only migrated cells on the other side of the filter remained. Nuclei were stained with Hoechst (1:10,000 dilution) for 5 minutes followed by two washes with PBS. Using a Leica widefield fluorescence microscope, images for the nuclear staining were acquired for each chamber. Cells were counted using ImageJ, ensuring that they were not counted more than once in overlapping images. Means were obtained for each experimental group, and the appropriate statistical tool (t test or One-way ANOVA) was used.

BioFlux cell migration assays

24-well chambers (0-20 dyne) were purchased from Fluxion Biosciences for use in the BioFlux 200 System (Fluxion Biosciences). Chambers were freshly coated with 100 μg/ml fibronectin at a shear of 5 dyne/cm² prior to every assay. Conditioned medium was used as chemoattractant, and it was prepared from cells that were seeded the day before the assay. In the case of the MLRL to AAAA and del. 221-232 mutant cell lines, conditioned media were used from the respective cell lines. In the case of lentiviral infected cells (pWPI, CAR-V5 (pWPI) and CAR ICD-V5 (pWPI), experiments were performed 3 or 5 days post-infection, and parental U87 cells were used to supply conditioned media. Samples were

prepared at a density of 2 x 10⁶ cells per ml. 50 ul per sample was seeded into the chamber channels at a shear of 2 dyne/cm², and the chambers were incubated at 37°C for 1-2 hours to ensure proper attachment of cells to fibronectin substrate. The media were aspirated, and to one inlet serum starvation medium was added (0.5% BSA in DMEM), and to the other inlet conditioned medium was added, using a shear of 0.5 dyne/cm². Cells were allowed to migrate in the chambers at 37°C under a widefield light miscroscope, and images were acquired using timelapse video capture. For quantification of migration, the image at time 0 as well as one image every hour thereafter for 7 hours were used, for a total of 8 images. For each experimental group, the migration of cells from the serum starvation media to the conditioned media was tracked using the Manual Tracking plugin from ImageJ. Cells that died before 7 hours were excluded from the analysis. For the lentiviral infection experiments, GFP-positive cells were tracked. The data were imported into the Chemotaxis and Migration Tool software (Ibidi) to generate data for accumulated distance, accumulated distance with direction, and Euclidean distance with direction. Data were combined from 7 independent experiments performed in pairs, and statistics were performed using One-Way ANOVA.

Production of GST and GST-CAR fusion proteins and GST pull-downs

GST and GST-CAR intracellular domain fusion protein production and GST pull-down experiments were performed as previously described (Fok et al., 2007).

GST and GST-CAR expression was verified by SDS-PAGE and Coomassie blue

staining, and protein concentration was determined using a BSA standard curve. Equal amounts of protein bound to glutathione Sepharose beads were used in experiments. For each experimental group, U87 CAR cells were seeded at a density of 10⁶ cells per 10 cm plate, and experiments were performed the following day.

XTT cell proliferation assays

Leftover cells from the Bioflux cell migration experiments were used in parallel for XTT cell proliferation assays to determine whether or not there were differences in cell viability between the experimental groups during the BioFlux run. 25,000 cells were seeded per well of a 96-well plate (12 wells per group) and allowed to adhere. 3 blank wells were also included. The final volume of media was 200 μl per well. 1 mg/ml of XTT (BioShop Canada) stock solution dissolved in opti-MEM was activated with 1.53 mg/ml PMS stock solution dissolved in PBS by adding 25 μl of PMS to 5 ml of XTT. 50 μl of the activated XTT solution was dispensed into each well, including blank controls, once the cells had attached and spread out. The 96-well plate was incubated at 37°C for 4 hours. Measurements were taken in a plate reader at 450 nm and 690 nm. Specific absorbance was calculated by taking the difference of the two measurements minus the measurements for the blanks. Results are expressed as means with SEM. Statistics were performed using Student's t test.

Immunofluorescence

Cells were seeded on 22x22 mm square coverslips (glass, grade 1.5) in 6-well plates and transfected the following day. Immunofluorescence experiments were performed 24-48 hours post-transfection. Cells were washed with phosphatebuffered saline (PBS), fixed using 4% paraformaldehyde for 15 minutes at room temperature, and washed again with PBS. Cell permeabilization was done using 0.1% Triton X-100 in PBS for 10 minutes at room temperature, followed by washing the samples with PBS. Samples were incubated for 1 hour at room temperature in blocking buffer (PBS with 10% goat serum). Primary antibody incubation using anti-V5 antibody at 1:500 dilution in blocking buffer was performed for 1 hour at room temperature, followed by a PBS wash and a 30 minute incubation at room temperature with goat anti-mouse Alexa Fluor 555 secondary antibody (1:1000 dilution in blocking buffer). Nuclei were stained for 5 minutes using DRAQ5 (Cell Signaling Technology) diluted 1:3000 in PBS. Coverslips were mounted on slides using ProLong Gold Antifade Reagent (Molecular Probes).

Confocal microscopy

Images of samples were acquired using a Zeiss LSM 510 Meta laser scanning confocal microscope with a Plan-Apochromat 63x/1.4 oil DIC objective (Cell Imaging and Analysis Network, McGill University). Multitrack mode was used

with dual excitation (633 nm for DRAQ5 and 543 nm for Alexa Fluor 555) and emission (LP 650 nm for DRAQ5 and BP 560-615 nm for Alexa Fluor 555) filter sets.

Luciferase reporter assays

U87 cells were seeded in 12-well plates at a density of 100,000 cells per well and transfected the following day using TransIT 20-20 transfection reagent (Mirus). There were 3 experimental groups, each in biological triplicates. The following amounts of DNA were used for transfection (per well): pUAS-luciferase only (1.25 ug DNA), pUAS-luciferase (0.625 ug DNA) with pCMV-GAL4 (0.625 ug DNA), or pUAS-luciferase (0.625 ug DNA) with pCMV-GAL4-CAR ICD (0.625 ug DNA). TransIT 20-20 reagent was used at a ratio of 1:3 (or 3.75 µl per well). Experiments were performed 24-48 hours post-transfection using a luciferase assay system (Promega, catalog no. E4030) according to the manufacturer's instructions. Samples were measured in a Bio-Orbit 1250 luminometer, and equal volumes of lysates were used between samples to measure light produced, expressed in relative light units (RLU). 3 measurements were taken per biological replicate, spaced 10 seconds apart, and the average RLU per replicate was calculated. Results shown are from one experiment with each group performed in biological triplicates. Similar data were obtained from 3 independent experiments. Experiments with full-length GAL4, GAL4 DBD and GAL4 DBD-CAR ICD were performed as above.

Statistical analyses

All values reported are expressed as mean \pm SEM (standard error of the mean). Statistical significance was assessed by Student's t-test or by one-way analysis of variance (ANOVA) as stated in the figure legends using GraphPad Prism software version 3.0. Statistical significance was defined as p<0.05.

Chapter 3: ADAM10 Mediates CAR Ectodomain Shedding

CAR ectodomain is shed, resulting in a decrease in amount of full-length receptor on the cell surface

First, we confirmed the previous observation that CAR ectodomain (CAR ECD) is constitutively shed into the extracellular environment (Huang, 2008).

Populations of human glioma U87-MG cells stably expressing CAR (designated as U87 CAR) or empty LNCX retrovirus vector (designated as U87 LNCX) were assayed for CAR ECD shedding by collecting conditioned media after 16 to 24 hours of incubation. A fragment of 32 kDa in size was detected from conditioned media of U87 CAR cells, but not from U87 LNCX cells, using antibody raised against CAR's N-terminus (extracellular domain) (figure 3.1A). This fragment was not detected using antibody raised against CAR's intracellular domain (RP291 antibody) (Huang, 2008), indicating that it is indeed CAR's ECD. Full-length CAR, migrating close to the 50 kDa molecular weight marker, is also shown (figure 3.1A).

In addition to basal (constitutive) shedding, the shedding of cell surface proteins can be controlled by various cell signaling pathways. Phorbol esters, such as phorbol 12-myristate 13-acetate (PMA), activate the protein kinase C (PKC) pathway (Castagna et al., 1982) and induce shedding of cell surface proteins (Arribas and Borroto, 2002). We confirmed the previous observation that treatment of U87 CAR cells with 1 μ M PMA for 4 hours triggers CAR ECD shedding (Huang, 2008) (figure 3.1B).

To determine whether or not shedding decreases cell surface levels of CAR, U87 CAR cells were treated with PMA (vs. DMSO vehicle) for 4 hours, followed by biotinylation and pull down with streptavidin beads of cell surface proteins. PMA treatment induced shedding of the 32 kDa CAR ECD into conditioned media, as expected (figure 3.2A, 5th and 6th lanes from the left). This was accompanied by a decrease in levels of biotinylated full-length CAR (46 kDa) (figure 3.2A, 3rd and 4th lanes from the left), indicating that CAR ECD shedding results in loss of full-length receptor from the cell surface. As CAR is an adenovirus receptor, we performed a PMA stimulation experiment on U87 CAR cells followed by infection of treated and non-treated cells with adenovirus carrying the lacZ gene. β-galactosidase assays revealed that PMA-treated cells were less susceptible to adenovirus infection (figure 3.2B), further confirming results obtained from cell surface biotinylation experiments.

PMA-mediated stimulation of CAR ECD shedding requires PKC activity

The phorbol ester PMA mimics diacylglycerol (DAG) and activates PKC (Castagna et al., 1982). Co-treatment of cells with Gö6983, a pharmacological inhibitor of PKC isozymes α , β , γ , δ and ζ , decreased PMA-mediated CAR ECD shedding in a dose-dependent manner (figure 3.3).

The Ca²⁺ ionophore ionomycin is known to induce shedding of cell surface proteins (Yee et al., 1993). U87 CAR cells were treated with ionomycin for 30 minutes, resulting in acute induction of CAR ECD shedding (figure 3.4). Thus, in addition to constitutive shedding and shedding via the DAG-PKC pathway, CAR shedding is triggered by changes in intracellular Ca²⁺ levels.

PMA-induced shedding is accompanied by phosphorylation of CAR cytoplasmic domain

During the course of these studies, we noticed that PMA treatment led to the appearance of multiple bands of full-length CAR (see cell lysates in figure 3.1B, figure 3.2A and figure 3.3). These higher molecular weight species did not appear under constitutive or ionomycin-induced shedding conditions (figure 3.1A and figure 3.4, respectively). We wondered if these bands were the result of post-translational modification of CAR in the form of phosphorylation. Indeed, treatment of cell lysates with calf intestinal phosphatase (CIP) abolished these bands (figure 3.5A), indicating that PMA-mediated CAR ECD shedding results in phosphorylation of the receptor. Note that the presence of these bands is also dependent on PKC activity (refer to lysates shown in figure 3.3), indicating phosphorylation of CAR via PMA treatment downstream of PKC activation.

This post-translational modification with PMA treatment occurs within CAR's cytoplasmic domain, as a mutant of CAR lacking the cytoplasmic domain, CAR tailless (Huang et al., 2005b), did not display higher molecular weight bands upon PMA treatment (figure 3.5B).

EGF, IGF-1 and pervanadate do not induce CAR ECD shedding from U87 CAR cells

During the course of these studies, we tested various chemicals or biological factors known to stimulate shedding of other proteins. For example, epidermal growth factor (EGF) stimulates shedding of the heparan sulfate proteoglycans Syndecan-1 and -4 (Subramanian et al., 1997). Insulin-like growth factor-1 (IGF-1) stimulates shedding of APP and APP-like proteins (APLP) 1 and 2 (Adlerz et al., 2007). However, we found that in our system of choice (human glioma U87 stably expressing CAR), treatment with EGF or IGF-1 did not upregulate CAR ECD shedding (figure 3.6A and figure 3.6B).

The phosphatase inhibitor pervanadate triggers shedding of cell surface proteins such as Syndecan-1 (Reiland et al., 1996). However, pervanadate treatment did not stimulate CAR ECD shedding from U87 CAR cells beyond basal levels that accumulated in conditioned media over the course of 30 minutes (figure 3.6C).

Therefore, while 3-4 hours of treatment with PMA and 30 minutes of treatment with ionomycin induce robust CAR ECD shedding, pervanadate, EGF and IGF-1 do not upregulate CAR ECD shedding, at least not from our cell line of choice.

CAR ECD shedding requires metalloprotease activity

Previous results from our lab indicated that the broad-spectrum metalloprotease inhibitors O-phenanthroline and TAPI-1 inhibited CAR ECD shedding from U87 CAR cells, while the aspartyl protease inhibitor pepstatin, the cysteine protease inhibitor E64, and the cysteine/serine protease inhibitor leupeptin did not (Huang, 2008). We used a third broad-spectrum metalloprotease inhibitor, GM6001, to validate results obtained with O-phenanthroline and TAPI-1. Treatment of U87 CAR cells with GM6001 inhibited PMA-stimulated CAR ECD shedding as well as basal levels of shedding seen in the presence of DMSO vehicle (figure 3.7). Thus, metalloproteases, and not other classes of proteases, are required for CAR ECD shedding.

ADAM10 is a major sheddase of CAR in human glioma cells

Previous results from our laboratory showed that TIMP1 and TIMP3, but not TIMP2, blocked CAR ECD shedding (Huang, 2008). TIMP1 inhibits ADAM10, and TIMP3 inhibits ADAM10, ADAM12, ADAM17, ADAM28 and ADAM33 (figure 1.1) (Edwards et al., 2008).

Ectodomain shedding of substrates via treatment with low concentrations of PMA for one hour or less is generally mediated by ADAM17 (Sahin et al., 2004, Horiuchi et al., 2007). In the case of U87 CAR cells treated with 25 ng/ml of PMA, substantial levels of CAR ECD were detected in conditioned media only after 2 hours of treatment (figure 3.8), suggesting that ADAM17 may not be involved in CAR ECD shedding from U87 cells.

Given the TIMP inhibition profile of CAR shedding, the above results with low concentrations of PMA, and that ionomycin-stimulated shedding of proteins is generally mediated via ADAM10 (Horiuchi et al., 2007, Le Gall et al., 2009), we further investigated ADAM10 as a candidate sheddase of CAR from human glioma cells.

When ADAM10 was overexpressed in the glioma cell line U251N stably expressing CAR (U251N CAR), CAR ECD shedding increased (figure 3.9A). As purified recombinant prodomain of ADAM10 inhibits ADAM10 activity when added to cell culture media (Moss et al., 2007), we examined the effect of ADAM10 prodomain on CAR shedding. Addition of ADAM10 prodomain markedly decreased constitutive shedding of CAR (figure 3.9B), further indicating the involvement of ADAM10 in CAR ectodomain shedding.

To further investigate ADAM10's role in CAR shedding, we used shRNA to knock down ADAM10 expression in U87 CAR cells. Stable cell lines were generated for anti-eGFP shRNA (used as control) or anti-ADAM10 shRNA (sequences #6675 or #6676). The shRNA sequences targeting ADAM10 successfully knocked down ADAM10 mRNA levels (figure 3.10A) and, subsequently, ADAM10 protein levels (figure 3.10B).

The shRNA stable cell lines were then used to investigate the role of ADAM10, if any, in constitutive, ionomycin-induced and PMA-induced CAR shedding.

Knockdown of ADAM10 in U87 CAR cells significantly decreased levels of constitutively shed CAR by 40% (figure 3.11A). Similar results were obtained with the ADAM10 shRNA sequence #6675 (data not shown).

PMA-mediated shedding of CAR also significantly decreased (by 41%) with knockdown of ADAM10 (figure 3.11B), although it should be noted that the concentration and length of time used for the PMA treatments is considered to be chronic with a wide range of pleiotropic cellular effects; thus, under these conditions, PMA activation of ADAM10 may be non-specific.

Ionomycin-induced shedding of CAR ECD, following treatment of U87 CAR cells at $1.5~\mu M$ for 30 minutes, was also found to be ADAM10-dependent, with ADAM10 knockdown resulting in a significant decrease of 52% in levels of shed CAR (figure 3.11C).

Thus, data from ADAM10 shRNA studies confirm that ADAM10 mediates constitutive, ionomycin-stimulated, and chronic PMA-stimulated ECD shedding of CAR.

For additional validation of ADAM10's role in CAR ECD shedding, we generated a mutant ADAM10 construct resistant to shRNA #6676 by deleting nucleotides 2319-2325 (the target sequence of shRNA #6676, lying outside the coding sequence of human ADAM10). U251N CAR cells stably expressing control shRNA or ADAM10 shRNA were transiently transfected with either the shRNA-resistant ADAM10 plasmid or empty plasmid. The shRNA-resistant ADAM10 mutant partially rescued the ADAM10 shRNA-mediated decrease in CAR shedding (figure 3.12). Thus, these data provide further evidence for ADAM10's role in CAR ECD shedding.

Mapping the site of ADAM10 cleavage on CAR

As ADAMs do not have consensus cleavage sites, *in vitro* experiments were performed using recombinant human ADAM10 to map the putative cleavage site(s) within CAR's ECD. A peptide consisting of the 20 amino acid residues upstream of the transmembrane domain of murine CAR (isoform 1) having the sequence VGSDQCMLRLDVVPPSNRAG was digested *in vitro* with recombinant ADAM10 at 37°C for 4 or 16 hours. The following controls were

also included: peptide only or enzyme only (16 hours of incubation at 37°C each) and peptide with enzyme for 0 hours. Samples were analyzed by MALDI-MS, and unique peaks at 1008 m/z and 1393 m/z were found that did not appear in the three control samples (figure 3.13). MS/MS fragmentation was performed to deduce the amino acid identity of the fragments. The 1008 m/z peak corresponded to the peptide fragment VGSDQCMLR, whereas the 1393 m/z peak corresponded to the peptide fragment LRLDVVPPSNRAG.

Figure 3.14A illustrates the two putative cleavage sites (indicated by arrows) within CAR's ECD as determined from the mass spectrometry results: between M224 and L225, and between R226 and L227. To verify the cleavage sites *in vivo*, we generated CAR constructs in which these pairs of amino acids were mutated to alanines and the mutants named ML→AA and RL→AA, respectively. A third mutant (Δ221-232) was generated in which 12 amino acids were deleted (amino acids 221-232 inclusive) comprising most of the peptide sequence used for the *in vitro* digestion experiments. Wild-type CAR and the mutants ML→AA, RL→AA, and Δ221-232 were stably expressed in U251N cells. The ML→AA and RL→AA point mutants displayed abrogated ECD shedding, although not completely or consistently over subsequent passages of the stable cell lines (figure 3.14B). Therefore, a third mutant of CAR was generated in which amino acids M224 to L227, inclusive, were changed to alanine residues (MLRL→AAAA).

3.14C), and furthermore this effect was consistent over further passages of these stable cell lines. Similar results were obtained in U87-MG cells (data not shown).

Although we expected the deletion mutant $\Delta 221$ -232 not to shed since it lacked most of the amino acid sequence used in the *in vitro* digestion experiments, this mutant's ECD shed robustly, generating a slightly larger fragment than that of wild-type CAR (figure 3.14B and figure 3.14C). As the deleted region contains one of the cysteines that participate in a disulfide bridge (Jiang and Caffrey, 2007), the structure of $\Delta 221$ -232 is presumably disrupted, possibly exposing additional cleavage sites.

However, these mutations may alter the trafficking of CAR in glioma cells, as cell surface biotinylation experiments revealed that the mutants were expressed at very low levels on the cell surface as compared to wild-type CAR (figure 3.15A and figure 3.15C). Similar results were obtained when the glioma stable cell lines were infected with adenovirus carrying the lacZ gene, followed by β -galactosidase and luminometry assays for reporter activity (figure 3.15B and figure 3.15D).

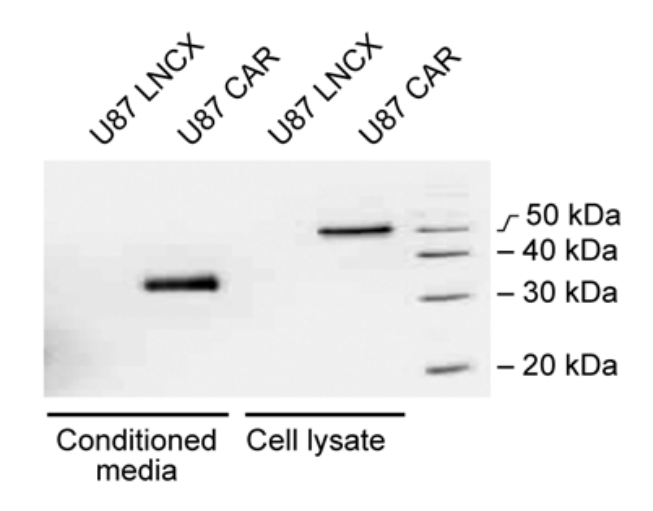
On the other hand, when we performed similar studies in HEK 293 cells, which express low levels of CAR endogenously, stable transfection of wild-type CAR, MLRL \rightarrow AAAA and Δ 221-232 revealed that the two mutants were expressed on the cell surface similarly to wild-type CAR and that the MLRL \rightarrow AAAA mutant is

indeed defective in ECD shedding (figure 3.16). Taken together, these results indicate that amino acids M224-L227 are important for cleavage of CAR ECD.

Figure 3.1: Human glioma U87-MG cells stably expressing CAR shed CAR ECD constitutively or with 4 hours of treatment with 1 μM PMA. (A) U87 LNCX and U87 CAR cells were assayed for shedding by collection of conditioned media (16-24 hours of incubation). Conditioned media and equal amounts of lysates were analyzed via SDS-PAGE and Western blot (anti-CAR N-term. antibody 2240). Full-length CAR from cell lysate migrated at approximately 50 kDa. A fragment of 32 kDa was released from U87 CAR, but not U87 LNCX, cells and was detected using the anti-CAR N-term antibody. The molecular weight of this fragment corresponds to the expected size of CAR ECD. (B) U87 CAR cells were treated with 1 μM PMA (vs. DMSO vehicle control) for 4 hours, followed by collection of cell lysates and conditioned media. SDS-PAGE and Western blotting (using anti-CAR N-term. antibody 2239) revealed that under these conditions of PMA stimulation, CAR ECD was robustly shed into conditioned media of U87 CAR cells.

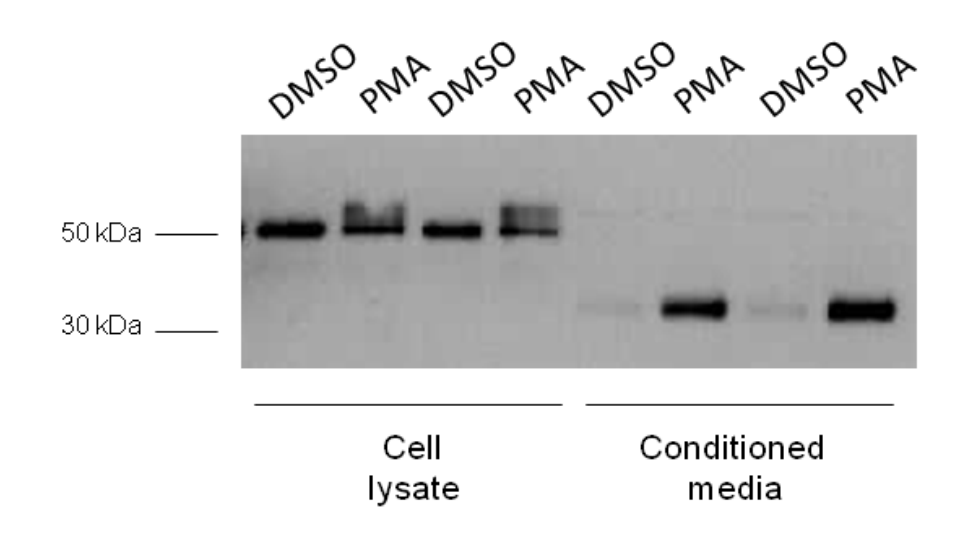
Figure 3.1

Α



α-CAR N-term ab.

В

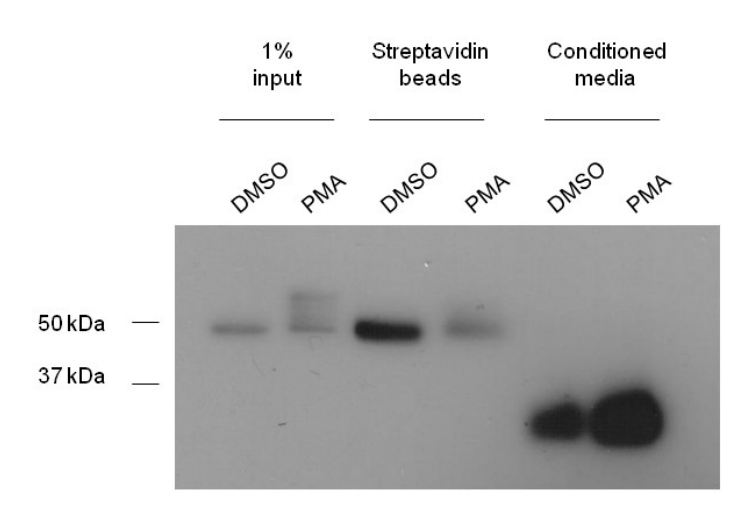


α-CAR N-term ab.

Figure 3.2: Ectodomain shedding results in a decrease in amount of CAR at the cell surface. (A) U87 CAR cells were treated with PMA (1 μM) or DMSO vehicle control for 4 hours to stimulate CAR ectodomain shedding. This was followed by cell surface biotinylation and pull down of biotinylated proteins with streptavidin beads. Conditioned media were also collected and processed (TCA protein precipitation protocol). Samples were analyzed by Western blot using an antibody raised against CAR's extracellular domain (CAR 2240). Less biotinylated CAR was pulled down with streptavidin in the PMA condition, indicating that CAR decreases at the cell surface with PMA treatment. (B) U87 CAR cells were treated with PMA (1 µM) or DMSO vehicle control for 4 hours to stimulate CAR ectodomain shedding, followed by infection of cells with adenovirus carrying the lacZ gene (multiplicites of infection 1 or 2). X-gal and luminometry assays revealed that PMA-treated cells were less susceptible to adenoviral infection, likely due to less CAR ECD available on the cell surface for adenoviruses to bind to. Unpaired t-test, n = 3 per group, p = 0.0047 (**).

Figure 3.2

Α



α-CAR N-term ab.

В

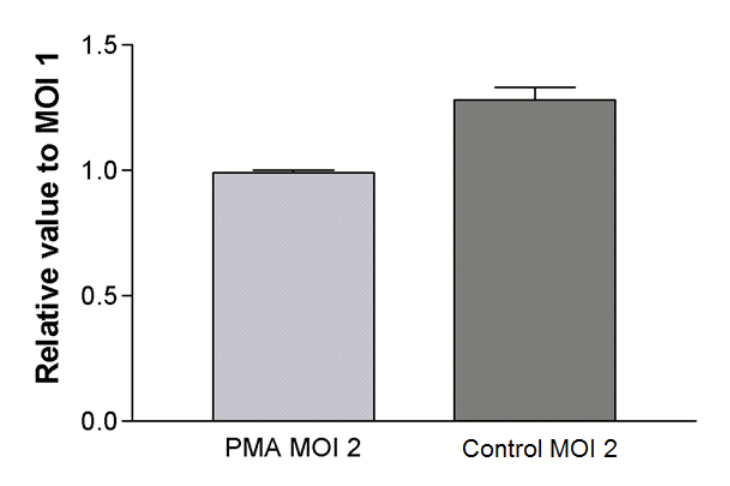


Figure 3.3: PMA-stimulated CAR shedding is inhibited by the PKC inhibitor Gö6983. Gö6983 inhibited PMA-mediated CAR ECD shedding in a dose-dependent manner. Final concentration of PMA used was 1 μ M. Gö6983 was used at the following concentrations: +=1 nM, ++=10 nM, +++=100 nM. Western blots were performed using the anti-CAR N-term. antibody 2239.

Figure 3.3

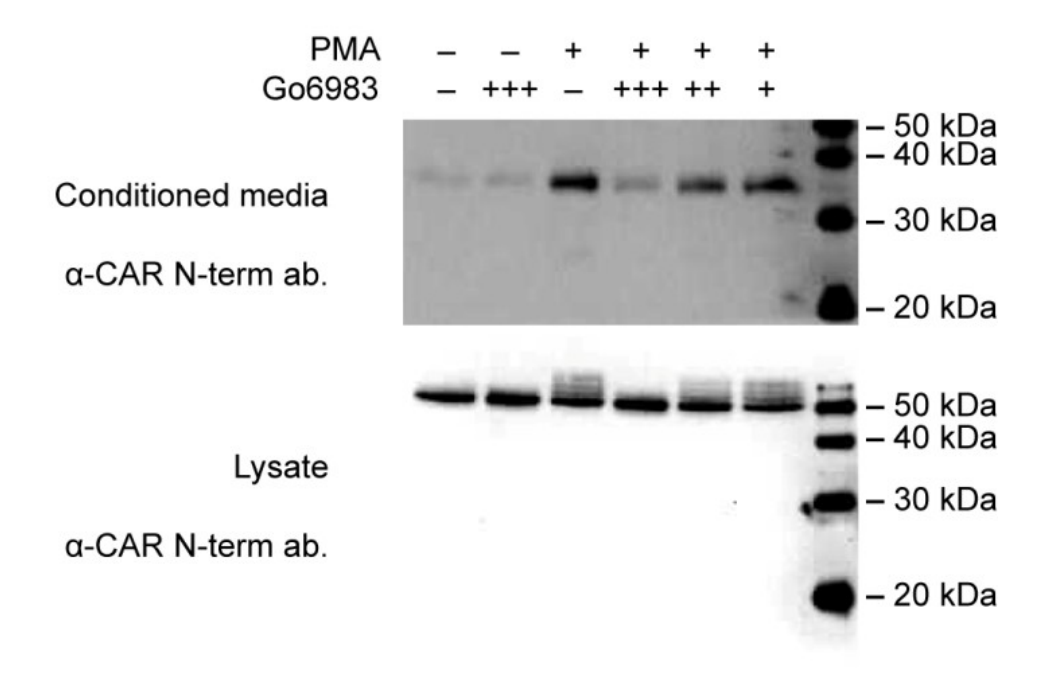


Figure 3.4: The Ca^{2+} ionophore ionomycin stimulates CAR ECD shedding. U87 CAR cells were treated with the indicated concentrations of ionomycin for 30 minutes. Conditioned media and cell lysates were analyzed by SDS-PAGE and Western blot using anti-CAR N-term. antibody 2240. Note that using ionomycin at a final concentration of 2.5 μ M (a concentration commonly reported in the literature) led to robust CAR ECD shedding but degradation of CAR detected in lysate (data not shown).

Figure 3.4

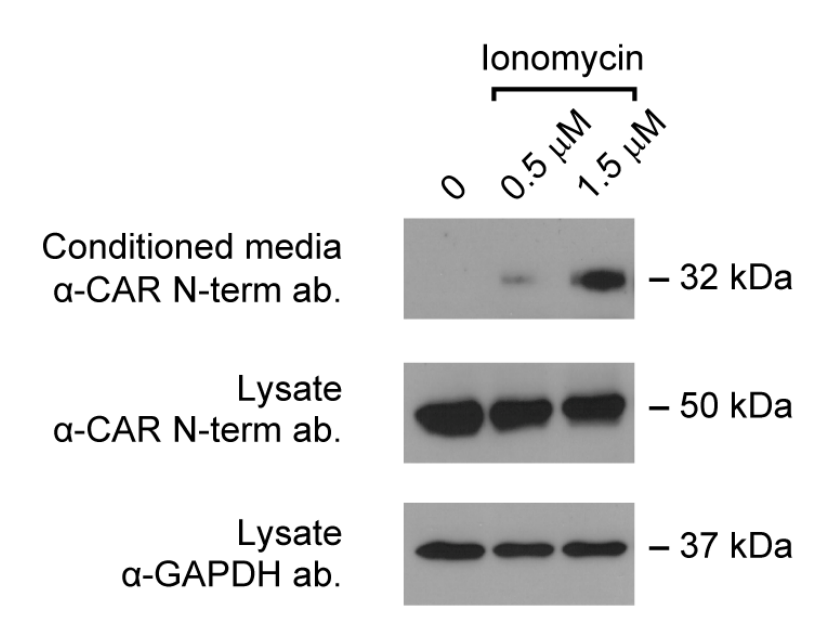
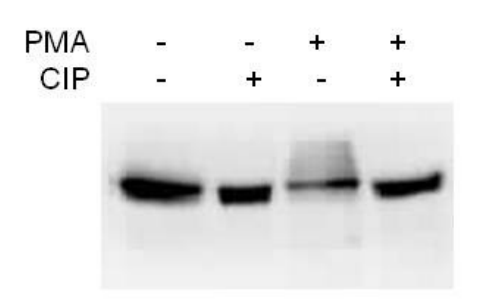


Figure 3.5: PMA treatment of U87 CAR cells is accompanied by phosphorylation of CAR's cytoplasmic domain. (A) PMA treatment results in a post-translational modification of CAR in the form of phosphorylation. Calf intestinal phosphatase (CIP) treatment abolished the appearance of the multiple higher molecular weight species of full-length CAR in lysates of U87 CAR cells treated with PMA. Western blots were performed with anti-CAR N-term.

antibody 2240. (B) This PMA-induced phosphorylation occurs within CAR's cytoplasmic domain, as a mutant of CAR lacking the cytoplasmic domain does not display higher molecular weight species in the cell lysates. Western blots were performed with anti-CAR N-term. antibody 2240.

Figure 3.5

Α



Lysates

α-CAR N-term ab.

В

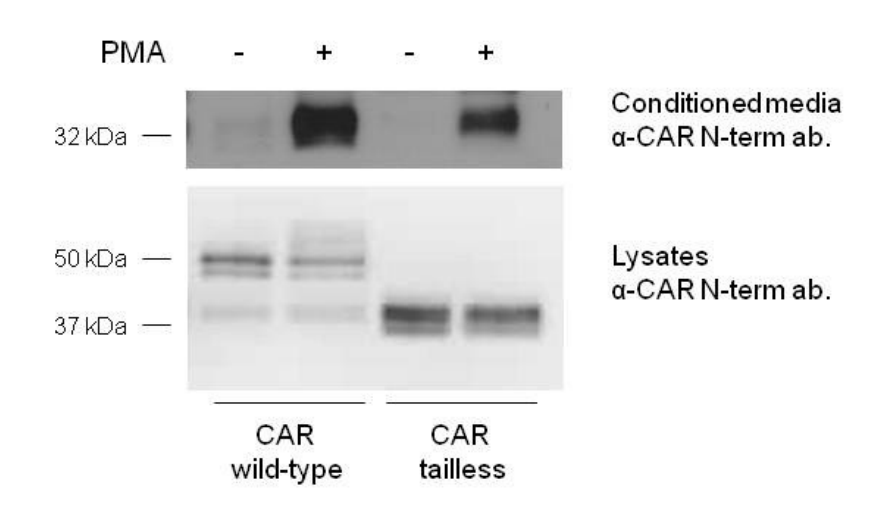


Figure 3.6: CAR ECD shedding is not stimulated by treatment of U87 CAR cells with EGF, IGF-1 or pervanadate. Serum-starved U87 CAR cells were treated with the indicated concentrations of EGF or IGF-1 overnight (A) or in the presence of PMA (1 μM, 3 hours) (200 ng/ml for EGF, 40 nM for IGF-1) (B). Treatment with these growth factors did not stimulate CAR shedding compared to the non-growth factor condition (0.1% BSA). (C) U87 CAR cells were treated for 0, 15 or 30 minutes with pervanadate as described in the materials and methods. Pervanadate did not induce CAR shedding beyond basal levels. The Western blots in these panels were performed with anti-CAR N-term. antibody 2239.

Figure 3.6

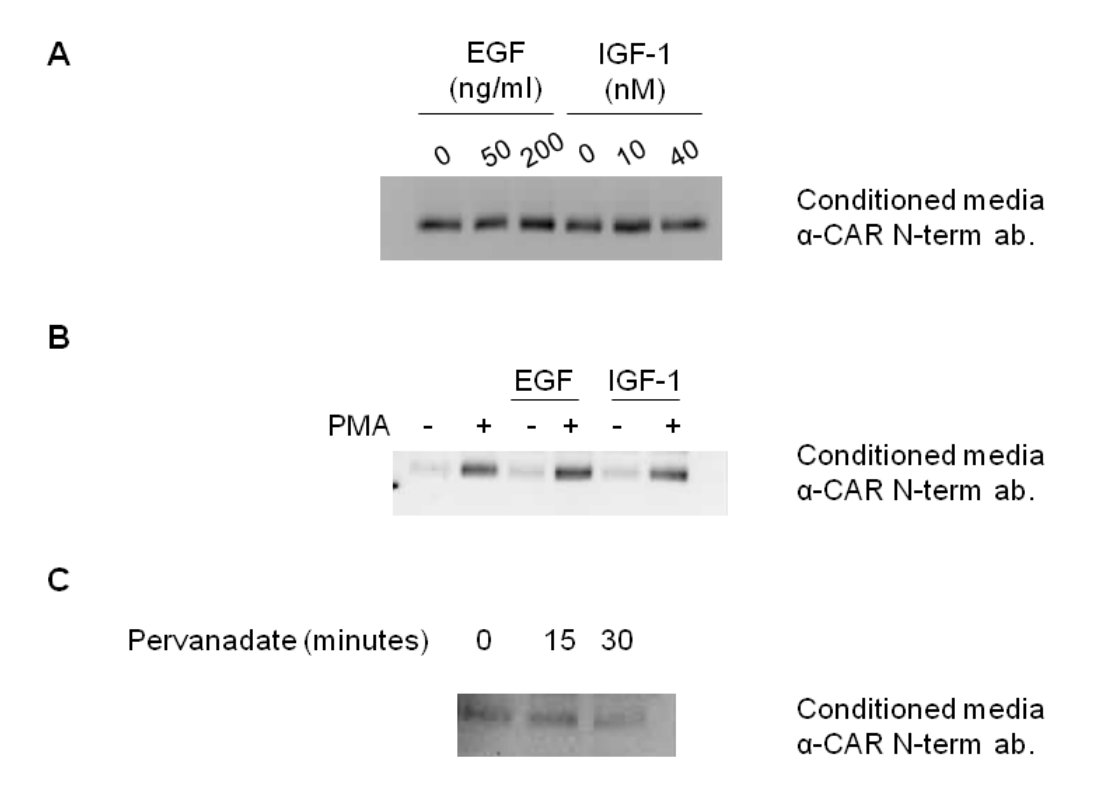


Figure 3.7: CAR shedding is inhibited by the broad-spectrum

metalloprotease inhibitor GM6001. U87 CAR cells were treated with GM6001 or its inactive analog (used as negative control), in the presence of PMA (1 μ M) or DMSO (vehicle control) for 4 hours. GM6001 inhibited PMA-stimulated CAR shedding. Note that basal shedding observed with vehicle treatment also decreased in the presence of GM6001. Western blotting was performed with the anti-CAR N-term. antibody 2240.

Figure 3.7

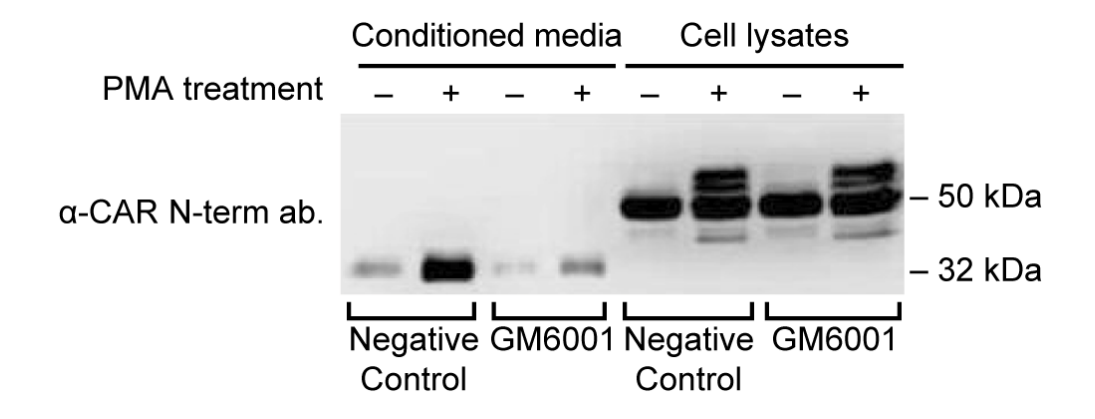


Figure 3.8: Treatment of U87 CAR cells with PMA under conditions known to trigger ADAM17-mediated shedding of proteins does not induce CAR ECD shedding. U87 CAR cells were treated with 25 ng/ml PMA for various lengths of time, as indicated. No shedding was observed within 1 hour. At this concentration, 4 hours of PMA treatment led to robust CAR ECD shedding, but remained lower than constitutive shedding (16 hours). Volumes of conditioned media loaded on SDS-PAGE were adjusted according to protein concentrations of cell lysates. Western blotting was performed using the anti-CAR N-term. antibody 2240.

Figure 3.8

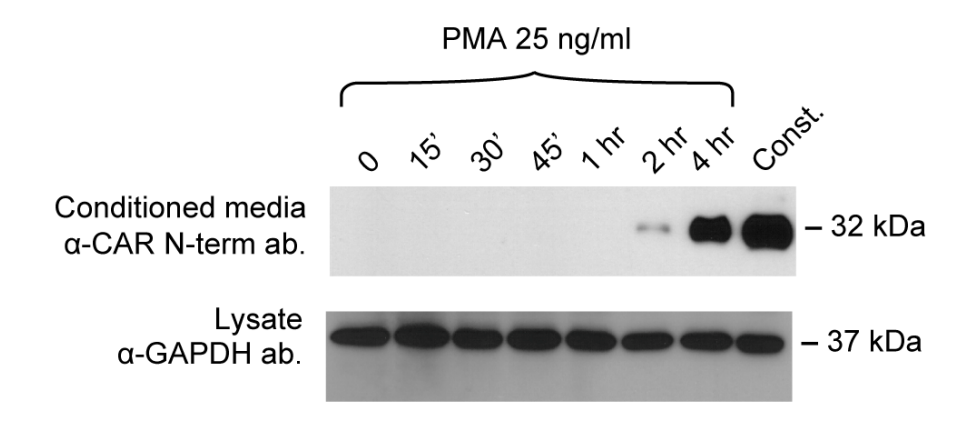
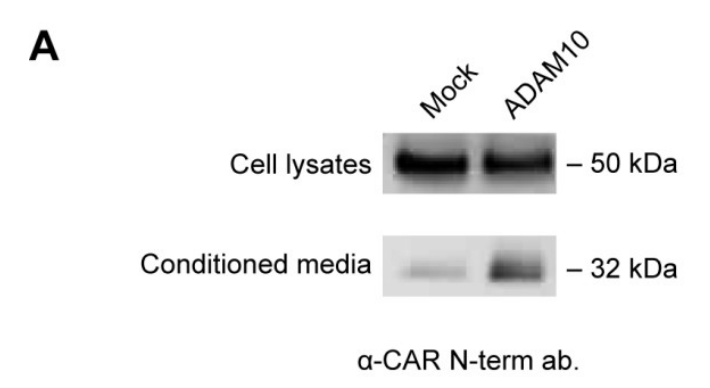


Figure 3.9: ADAM10 is involved in CAR ectodomain shedding. (A) U251N cells stably expressing CAR were transfected with empty plasmid (mock) or ADAM10 plasmid. 24 hours after transfection, cells were washed and incubated in opti-MEM for 24 hours, and conditioned media and cell lysates were analyzed with Western blots using anti-CAR N-terminus antibody (2239). Overexpression of ADAM10 increased constitutive CAR shedding. (B) U87 CAR cells were treated with 10 μM purified ADAM10 prodomain (versus an equivalent volume of buffer as a control), and conditioned media and cell lysates were collected. A Western blot for CAR extracellular domain (2240 antibody) shows that the prodomain of ADAM10, which inhibits ADAM10 activity, decreased CAR ECD shedding.

Figure 3.9



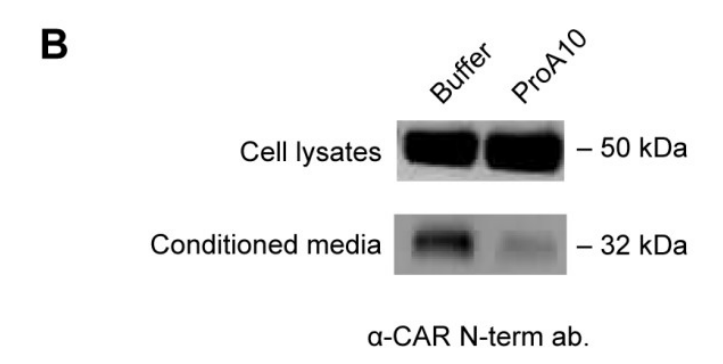
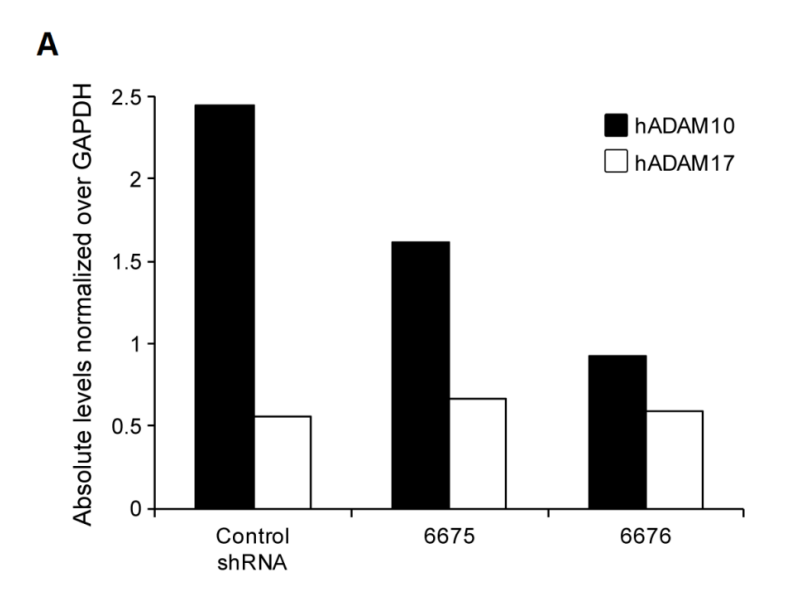


Figure 3.10: Confirmation of shRNA knockdown of ADAM10. (A) Real-time quantitative PCR for verification of knockdown of ADAM10 mRNA levels. U87 CAR stable cell lines infected with lentivirus containing control (anti-eGFP) shRNA or anti-ADAM10 (#6675 or #6676) shRNA were generated. RNAs were isolated from these cells, followed by reverse transcription to cDNA and real-time PCR in triplicates to quantify ADAM10, ADAM17 and GAPDH expression levels. The two anti-ADAM10 shRNA sequences #6675 and #6676 successfully knocked down mRNA levels of ADAM10 compared to control shRNA, without affecting expression levels of the related family member ADAM17. (B) A Western blot for ADAM10 using cell lysates of U87 CAR cells containing either control shRNA or ADAM10 (#6676) shRNA, in biological duplicates. Equal amounts of proteins were loaded on SDS-PAGE gel. The Western blot was then probed with anti-GAPDH antibody as a loading control. Quantification of mean ADAM10 band intensities normalized over GAPDH revealed a decrease of approximately 60% with anti-ADAM10 shRNA compared to control shRNA.

Figure 3.10



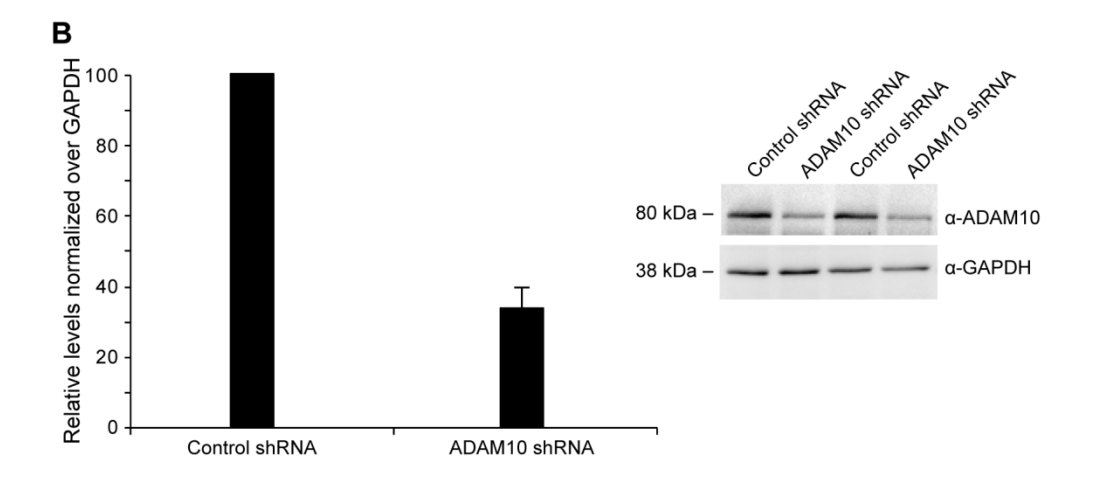
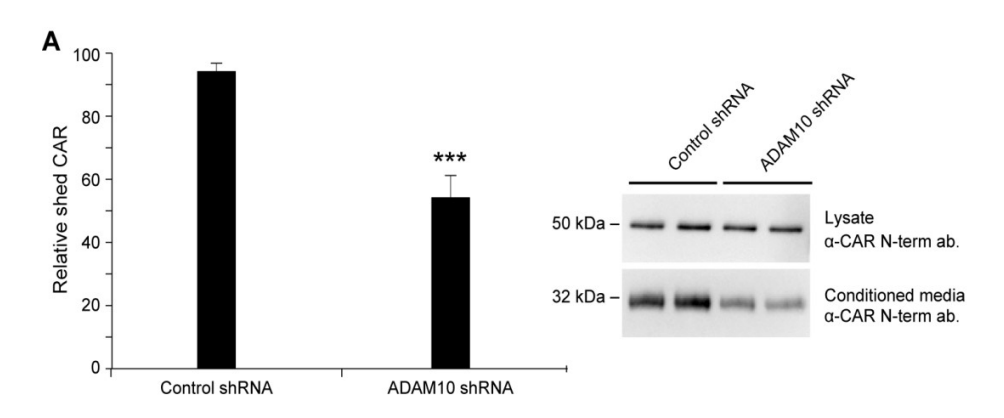
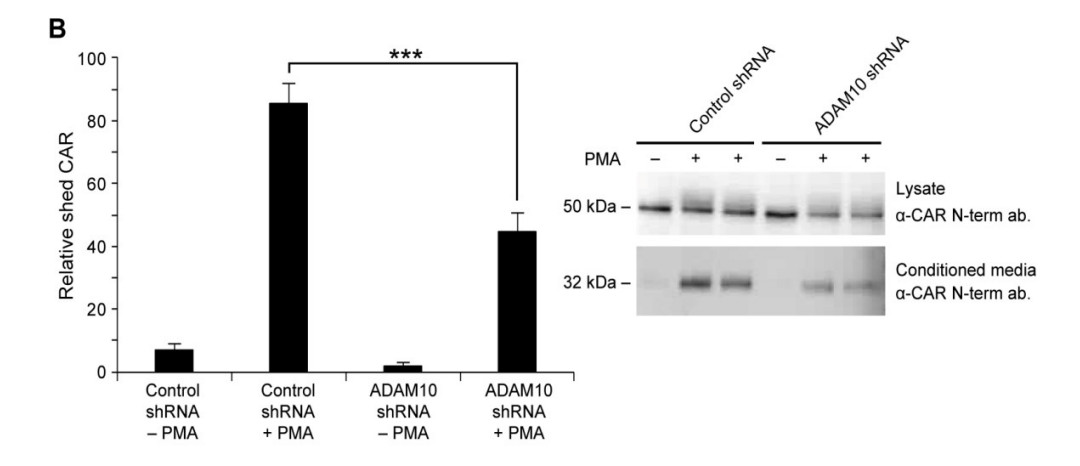


Figure 3.11: shRNA knockdown of ADAM10 decreases constitutive, PMAmediated and ionomycin-mediated CAR ECD shedding. (A) A constitutive shedding experiment was performed using U87 CAR stable cell lines containing either control shRNA or anti-ADAM10 shRNA (#6676). Conditioned media and cell lysates were collected after 24 hours of incubation of cells in opti-MEM, and Western blotting was done using the anti-CAR N-terminus antibody 2239. With anti-ADAM10 shRNA, there was a significant decrease (40%) in the levels of shed CAR. Results from 4 independent experiments performed in duplicates were quantified (unpaired t-test; p=0.0004 (***)). (B) U87 CAR cells containing either control shRNA or ADAM10 shRNA (#6676) were treated with 1 µM PMA. Conditioned media and cell lysates were collected after 3 hours, and Western blots were performed using the anti-CAR N-terminus antibody 2239. With shRNA knockdown of ADAM10, there was a significant decrease of 41% in levels of shed CAR compared to control shRNA. Results from 3 independent experiments performed in duplicates were quantified (one-way ANOVA with Tukey's multiple comparison test; *** = p < 0.001). (C) U87 CAR cells containing either control shRNA or ADAM10 shRNA (#6675) were treated with 1.5 μM ionomycin for 30 minutes, followed by collection of conditioned media and cell lysates. Western blots were performed using the anti-CAR N-term. antibody 2240. With shRNA knockdown of ADAM10, there was a significant decrease of 52% in levels of shed CAR with ionomycin treatment compared to control shRNA. Results from 3 independent experiments (n = 3 per group) were

quantified (One-way ANOVA with Bonferroni's multiple comparison test; *=p < 0.05, **=p < 0.01, ***=p < 0.001).

Figure 3.11





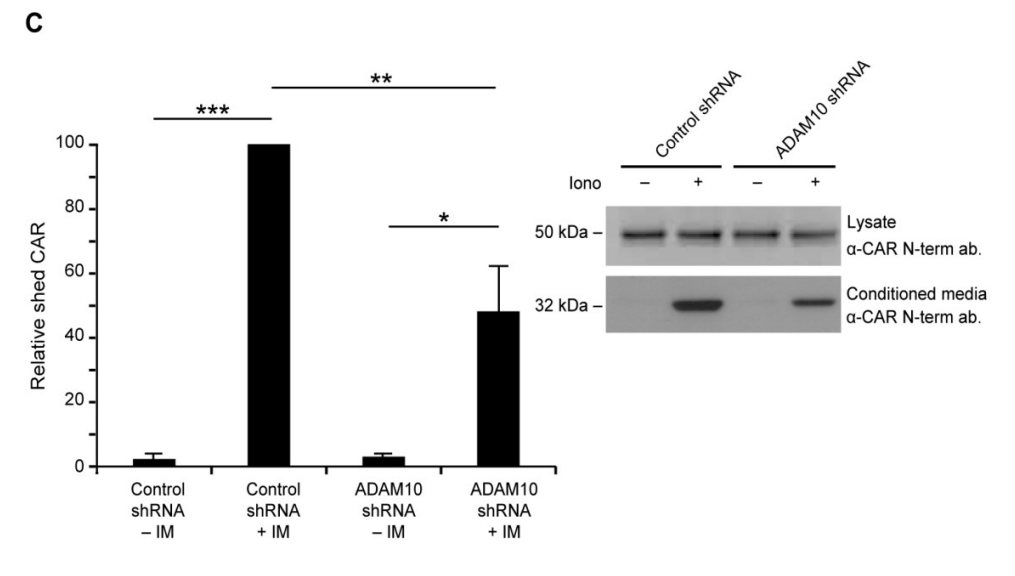
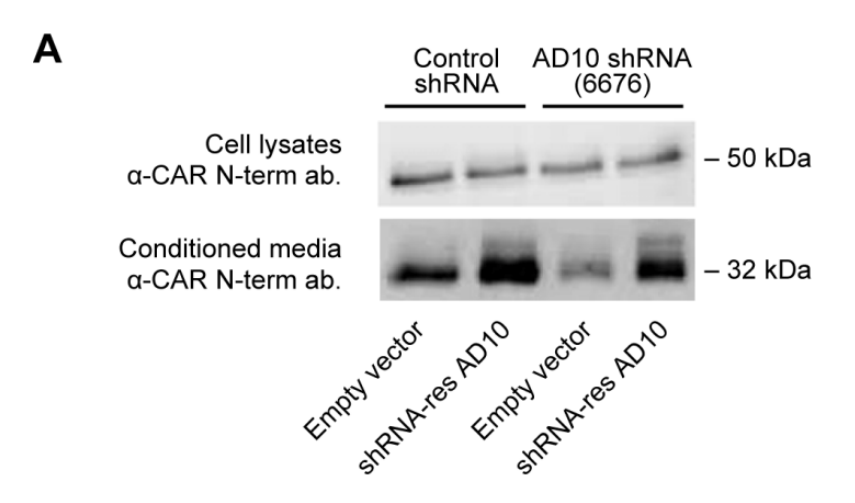


Figure 3.12: Partial rescue of shRNA-mediated loss of CAR shedding using an shRNA-resistant mutant of ADAM10. (A) shRNA stable cell lines of U251N CAR cells were transfected with either empty plasmid (mock) or an shRNA-resistant construct of ADAM10. 18-24 hours post-transfection, cells were washed and incubated in opti-MEM. Conditioned media and cell lysates were collected 24 hours later and analyzed by Western blot for CAR extracellular domain (anti-CAR antibody 2239). The shRNA-resistant ADAM10 mutant partially rescued CAR shedding in the ADAM10 (6676) shRNA cell line, compared to transfecting this cell line with empty plasmid (third and fourth Western blot bands from the left). (B) The band intensities of shed CAR detected by Western blot were quantified from 4 independent experiments (One-way ANOVA with Newman-Keuls multiple comparison test; * = p < 0.05, * = p < 0.01, * = p < 0.001).

Figure 3.12



В

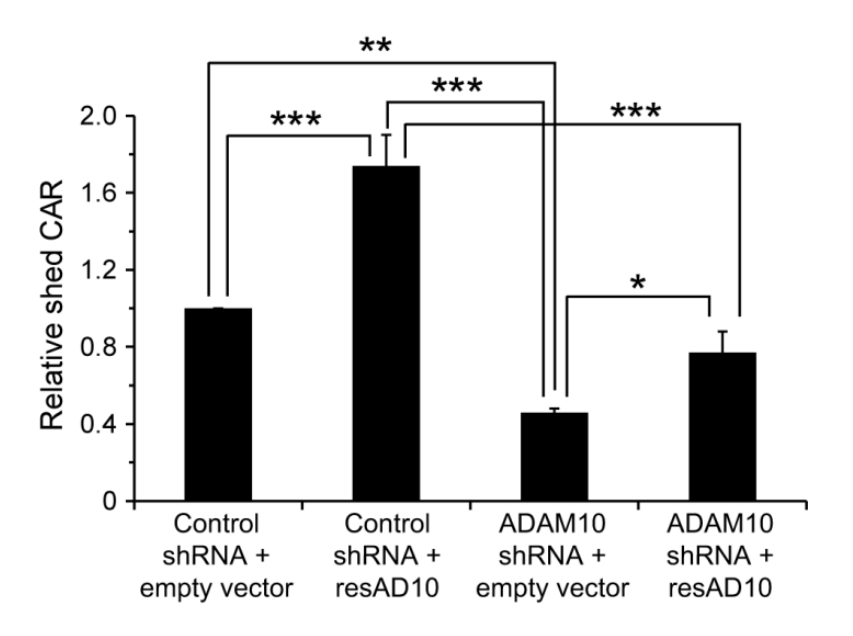


Figure 3.13: Mapping the sites of ectodomain cleavage on CAR. A 20-amino acid peptide (VGSDQCMLRLDVVPPSNRAG) representing the juxtamembrane region in CAR ectodomain was digested with recombinant human ADAM10 at 37°C for 4 or 16 hours, along with 3 controls (recombinant ADAM10 only, 16 hours; peptide only, 16 hours; peptide and recombinant ADAM10; 0 hours). Samples were analyzed by MALDI-MS. Two unique peaks (shaded grey) at (A) 1008 m/z and (B) 1393 m/z were found that were not present in the 3 controls. Further analysis was done with MS/MS in order to deduce the identities of the amino acids in each peptide fragment. These results represent 2 independent experiments.

Figure 3.13

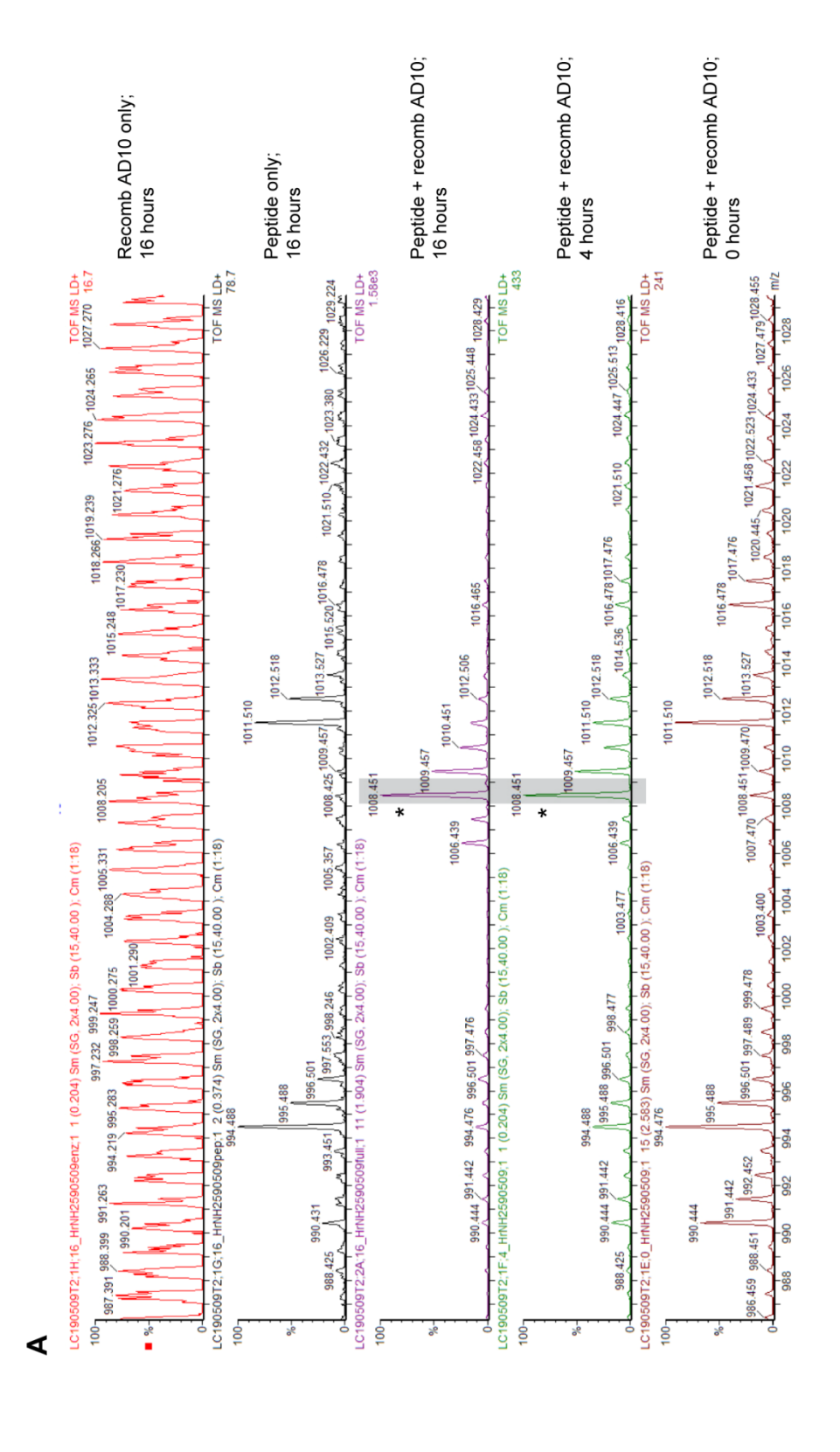


Figure 3.13 (continued)

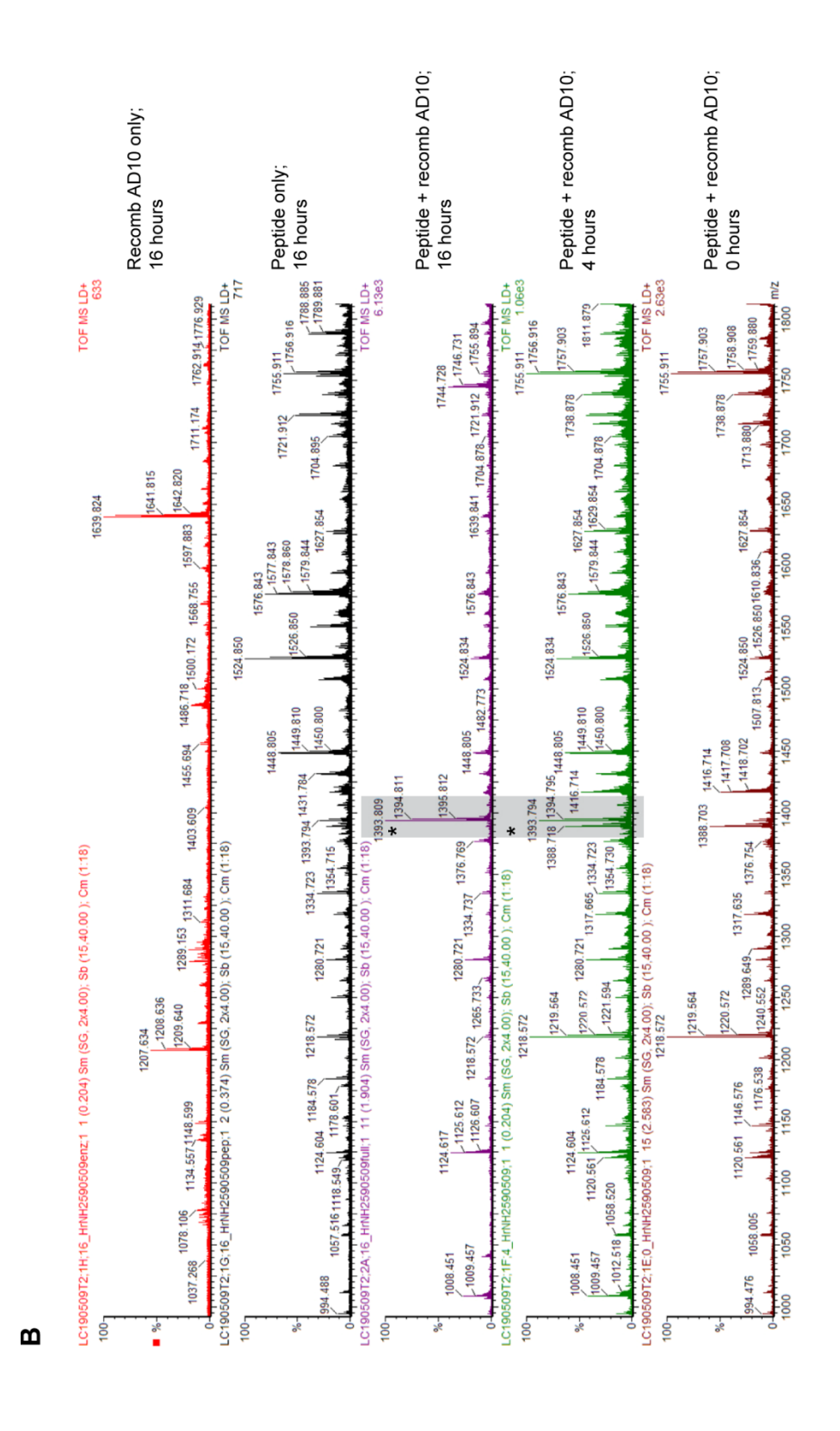
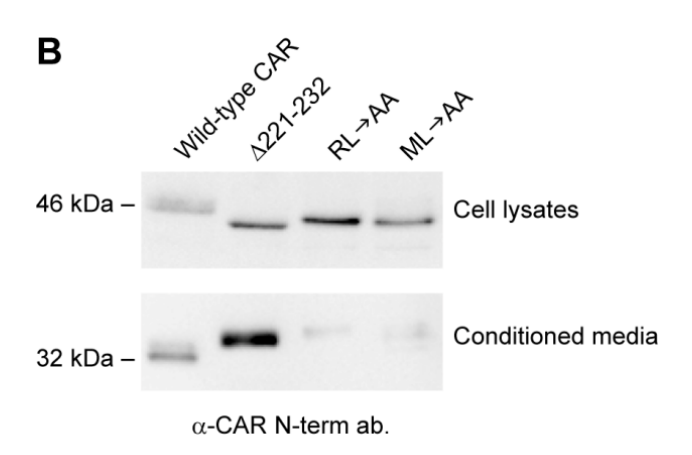


Figure 3.14: Expression of CAR ECD mutants in human glioma U251N cells.

(A) A schematic showing the putative ADAM10 cleavage sites on CAR's extracellular domain (arrows), as obtained from *in vitro* digestion studies and mass spectrometry. (B) 3 mutants were generated from wild-type CAR in pcDNA3 plasmid, and all constructs were stably expressed in U251N cells. Constitutive shedding of CAR and the mutants was assayed. Mutating pairs of amino acids to alanine (ML→AA and RL→AA) led to a decrease in CAR shedding, although not consistent over subsequent passages of the cell lines. Deletion of 12 amino acids (Δ221-232) containing the potential site of ectodomain cleavage resulted in a mutant that still shed its ectodomain. (C) A mutant CAR was generated in which amino acids 224-227 were changed to alanine residues (MLRL→AAAA) and stably expressed in U251N cells. Shedding of this mutant's ectodomain was abrogated.

Figure 3.14





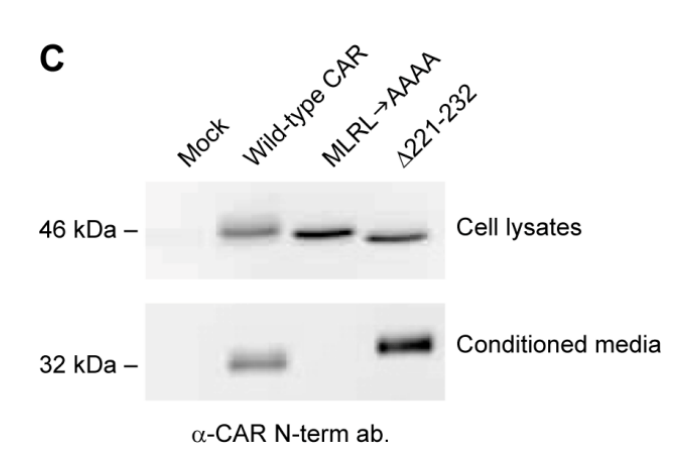
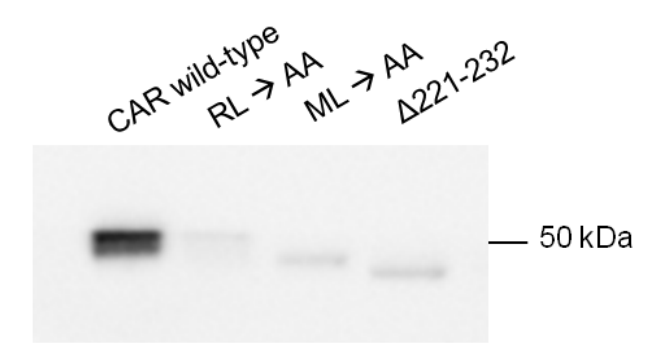


Figure 3.15: Mutations in CAR's juxtamembrane region of the ECD greatly diminish receptor levels on the surface of human glioma cells. (A) Cell surface biotinylation of human glioma U251N cells expressing wild-type CAR, the Δ 221-232 deletion mutant, the ML \rightarrow AA mutant, or the RL \rightarrow AA mutant. Cells were labeled with biotin, followed by incubation of lysates with streptavidin beads. Western blots using an antibody raised against CAR's N-terminus revealed that the deletion mutant and point mutants are expressed less than wild-type CAR at the cell surface. (B) U251N glioma stable cell lines were infected with adenovirus carrying a gene for lacZ (multiplicity of infection (MOI) of 10). Galacto-Star βgalactosidase reagent system was used to determine the amount of β -galactosidase reporter (measured in relative light units, RLUs, per mg of protein). The mutant CAR cell lines had less reporter activity compared to the wild-type CAR cell line, indicating that they are not expressed at the cell surface as well as the wild-type receptor. (C) Cell surface biotinylation of human glioma U251N cells expressing wild-type CAR, the $\Delta 221$ -232 deletion mutant, the MLRL \rightarrow AAAA mutant, or empty vector (mock). Cells were labeled with biotin, followed by incubation of lysates with streptavidin beads. Western blots using an antibody raised against CAR's N-terminus revealed that the deletion mutant and point mutant are expressed less than wild-type CAR at the cell surface. (D) U87 glioma stable cell lines were infected with adenovirus carrying a gene for lacZ at the indicated MOIs. Galacto-Star β-galactosidase reagent system was used to determine the amount of β-galactosidase reporter (measured in relative light units, RLUs, per mg of protein). The mutant CAR cell lines (MLRL \rightarrow AAAA and \triangle 221-232) had

less reporter activity compared to the wild-type CAR cell line, indicating that they are abrogated in expression at the cell surface.

Figure 3.15

Α



α-CAR N-term ab.

В

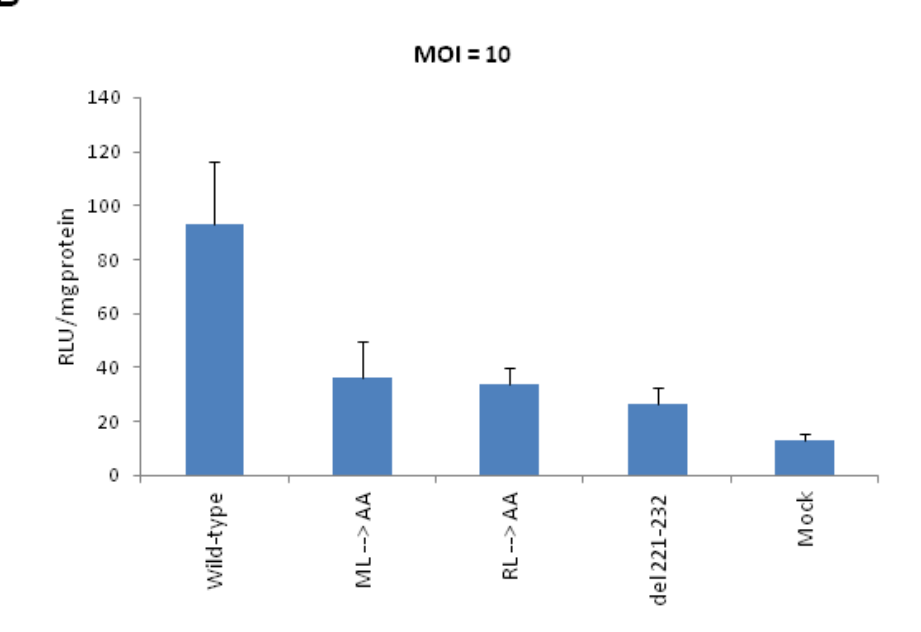


Figure 3.15 (continued)

С



α-CAR N-term ab.

D

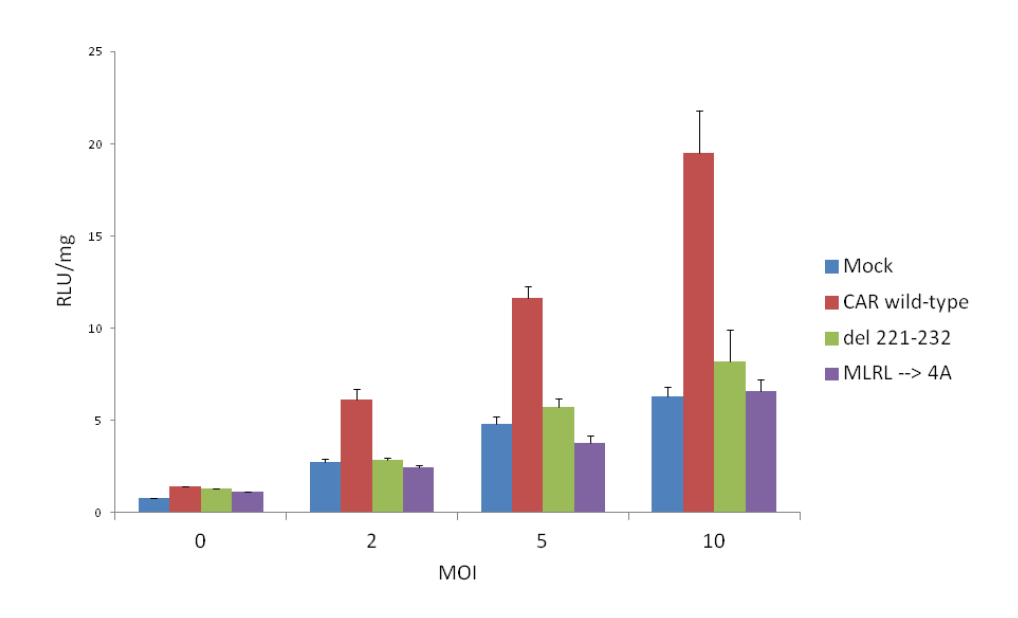
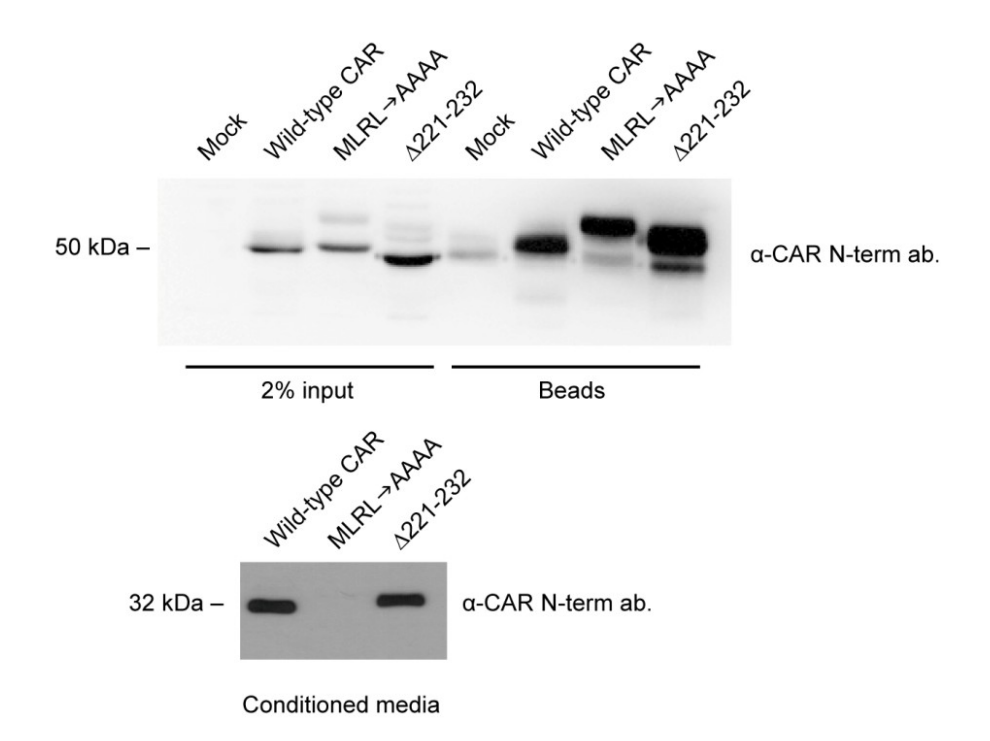


Figure 3.16: The mutants MLRL → AAAA and Δ221-232 are expressed at similar levels on the surface of HEK 293 cells as wild-type CAR. Shown are results from cell surface biotinylation and ECD shedding experiments. The MLRL → AAAA mutant is abrogated in shedding, while the Δ221-232 mutant sheds. The two mutants are expressed at similar levels on the cell surface as wild-type CAR. Note that low levels of endogenous CAR were detectable after enrichment of cell surface biotinylation (mock lane). The Western blots shown in these panels were performed with anti-CAR N-term. antibody 2240.

Figure 3.16



Chapter 4: Modulation of Shedding Does Not Affect CAR's

Inhibitory Function in Glioma

Glioblastoma multiforme (GBM), a high-grade malignant tumor of glial cells, is associated with poor patient outcome. It is locally invasive in the brain and rarely metastasizes to other organs (Wang and Jiang, 2013). The human cell line U87-MG is often used as a model for grade IV gliomas (Clark et al., 2010). U251N is another well-studied human glioma cell line (Ponten and Westermark, 1978). Our group previously reported that expression of CAR in U87-MG cells inhibits glioma migration and invasion *in vitro* and *in vivo*, as demonstrated by various techniques: tumor spheroid three-dimensional invasion in collagen, xenograft intracerebral implantation in brains of nude mice (Huang et al., 2005b), and migration of glioma cells towards a chemoattractant gradient in a modified Boyden chamber (Fok et al., 2007).

Unlike spheroid implantation in collagen or *in vivo* models, the modified Boyden chamber is a relatively fast way to quantify cell migration. We used this technique to investigate whether or not CAR ECD shedding has an effect on CAR's inhibitory function in glioma. The set up of the Boyden migration system is shown in figure 4.1.

Treatment of U87 CAR cells with the metalloprotease inhibitor GM6001 for 4 hours to inhibit CAR ECD shedding did not alter their migration compared to GM6001 negative control-treated cells (figure 4.2); neither did treatment with PMA for 4 hours (vs. DMSO vehicle) to stimulate CAR ECD shedding (figure 4.3).

The differences in cell surface expression between wild-type CAR and the ectodomain mutants MLRL→AAAA and Δ221-232 (figure 3.15) precluded the use of these mutants in direct comparison to wild-type CAR in migration experiments. However, since the mutants are similarly expressed on the cell surface, with one mutant (Δ221-232) generating a shed CAR ECD while the other (MLRL→AAAA) lacking ECD shedding (figure 3.14), we reasoned that the migration of the glioma cell lines stably expressing these constructs can be compared to one another to investigate whether or not the presence of CAR ECD in the extracellular milieu has an effect on glioma migration (perhaps by heterophilic binding to cell surface molecules besides CAR, triggering downstream cell signaling). Results from a Boyden chamber experiment are shown in figure 4.4; there were no differences in migration between U87 stable glioma cell lines expressing the MLRL→AAAA mutant or the Δ221-232 mutant.

The BioFlux migration system is yet another experimental tool employed in our laboratory to study cell migration. Whereas cell numbers are quantified in Boyden migration experiments, the BioFlux system has the advantage of quantifying migration distance and direction. The setup of a BioFlux experiment is shown in figure 4.5. Two experimental groups are compared at a time, and migration of cells in the serum-starvation condition is tracked, with most cells moving towards the conditioned (chemoattractant) medium.

Figure 4.6 shows migrated mean accumulated distance and mean Euclidean (shortest) distance with direction for U87 glioma cells expressing the shedding-defective mutant MLRL \rightarrow AAAA or the Δ 221-232 mutant that sheds. There were no significant differences in migration distances between the two cell lines.

Our group previously reported a requirement for CAR's cytoplasmic domain in inhibition of glioma migration and invasion, as U87 cells expressing a CAR mutant lacking the cytoplasmic domain (U87 CAR tailless) displayed significantly greater migration and invasion than U87 cells expressing full-length CAR (Huang et al., 2005b). To confirm the initial results obtained from collagen invasion assays and tumor xenograft models, BioFlux migration experiments were carried out. Figure 4.7A shows that the U87 CAR tailless cell line migrates more than U87 CAR cells (and similarly to U87 LNCX cells). As shown in figure 4.7B, this CAR tailless mutant sheds its ECD (although not as effectively as the wild-type receptor), suggesting that the release of CAR ECD into environment of glioma cells has no impact on their migration.

Taken together, data obtained from several experimental approaches indicate that CAR ECD shedding is not involved in CAR-mediated inhibition of glioma migration.

Figure 4.1: The modified Boyden chamber cell migration assay. An illustration for the setup of Boyden migration experiments. The top part of transwell inserts with 8 μm pores are coated with a thin layer of Matrigel basement membrane matrix. Serum-starved human glioma cells are seeded in the upper chamber and are attracted by chemotactic media in the lower chamber. Migration of cells is measured by counting the number of cells that migrated to the bottom side of the insert.

Figure 4.1

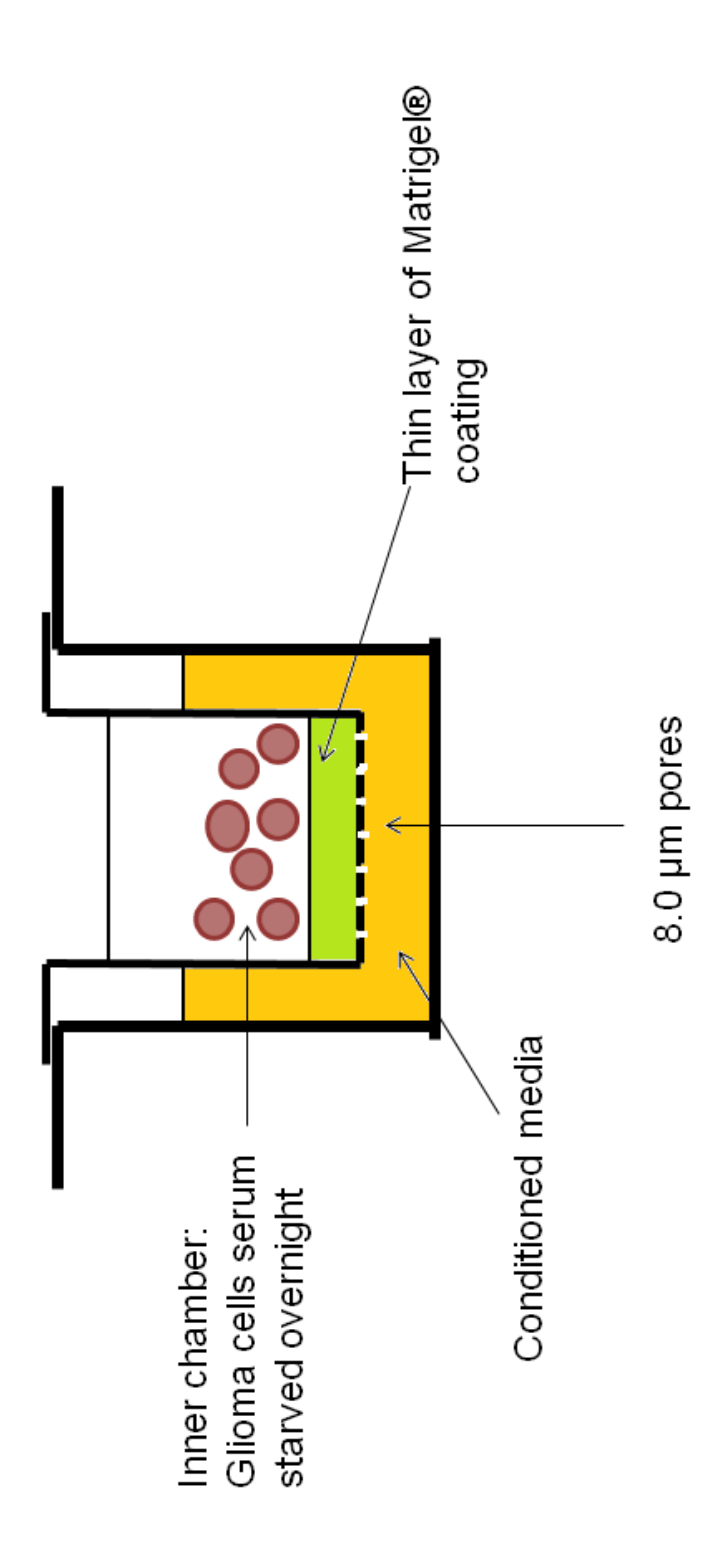


Figure 4.2: Inhibition of CAR ECD shedding does not affect migration of CAR-expressing glioma cells. 5,000 serum-starved U87 CAR cells were seeded per insert, with two experimental groups (GM6001-treated or negative control-treated, final concentration 25 μ M). Glioma cells were allowed to migrate for 4 hours before stopping the experiment. Data shown are means obtained from one independent experiment (n = 6 chambers per group). Similar results were obtained from 3 independent experiments.

Figure 4.2

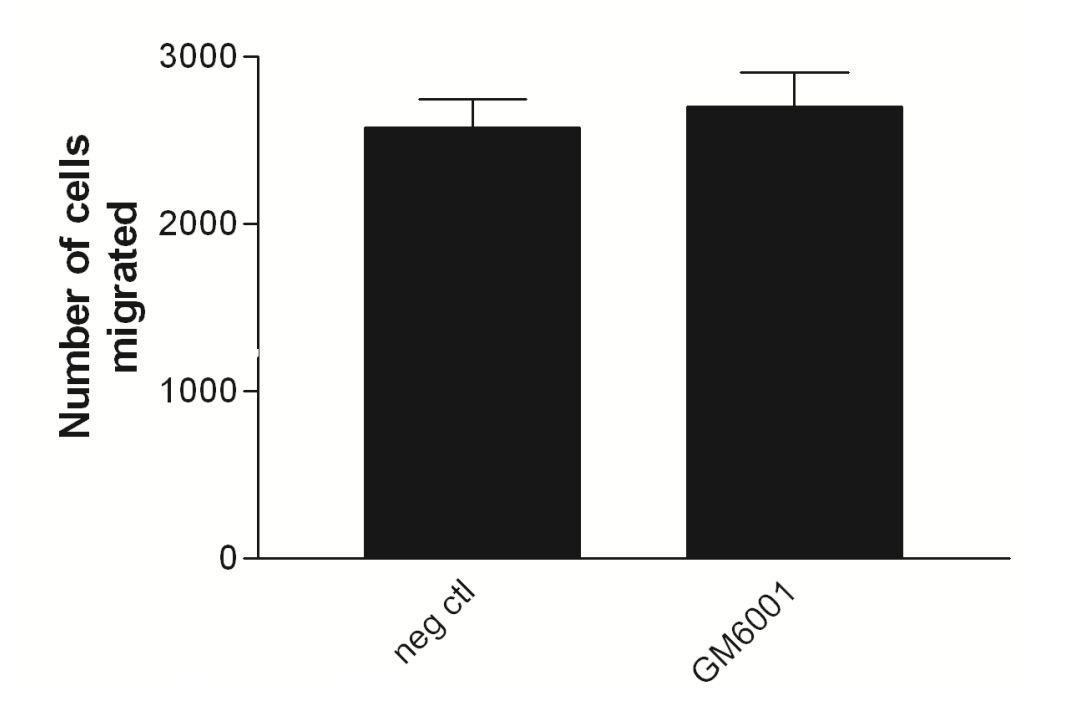


Figure 4.3: Stimulation of CAR ECD shedding with PMA does not change CAR's effect on glioma migration. A Boyden migration experiment with U87 LNCX and U87 CAR cells. 1,500 serum-starved glioma cells were seeded per insert. PMA was used at a concentration of 1 μM, which triggers robust CAR ECD shedding. Cells were allowed to migrate for 4 hours before stopping the experiment. Cells that migrated through the pores to the other side of the membrane were fixed and quantified. In the DMSO condition, U87 CAR cells migrated significantly less than control cells (U87 LNCX), as expected and as previously shown by our group (Fok et al., 2007). However, PMA treatment did not affect CAR's inhibition of U87 glioma migration. Data shown are means from 1 independent experiment (n = 6 chambers per group). Similar data were obtained from 3 independent experiments.

Figure 4.3

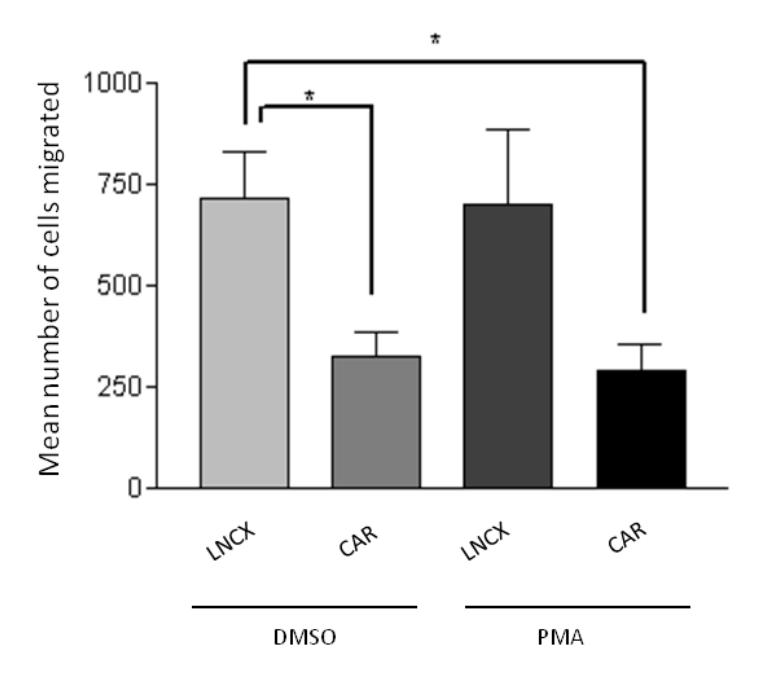


Figure 4.4: Glioma cells expressing a shedding-defective CAR mutant or a CAR mutant that sheds its ectodomain migrate similarly. 1,500 serum-starved glioma cells (U87 Δ 221-232 or U87 MLRL \rightarrow AAAA) were seeded per insert and allowed to migrate overnight. Conditioned media used as chemoattractant in the lower chambers came from each respective cell line. There were no significant differences in migration between the two groups. Results shown are from 1 independent experiment (n=5 chambers for U87 Δ 221-232 and n=6 chambers for U87 MLRL \rightarrow AAAA).

Figure 4.4

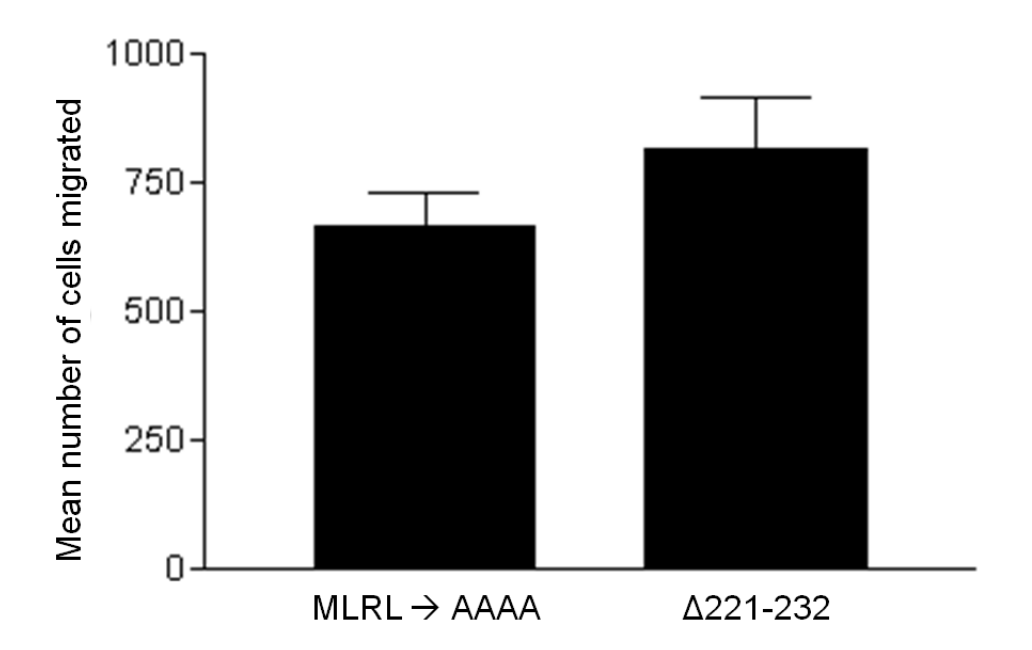


Figure 4.5: The BioFlux cell migration assay. The BioFlux live cell migration and imaging system allows for time-lapse video capture of two separate chambers containing cells that are exposed to a chemoattractant gradient. Cell movement is tracked from the serum starvation area to the conditioned media area. The image shown is an example at time 0 (start of an experiment). Migration is measured every hour, for 7 hours, to generate data on distance and direction.

Figure 4.5

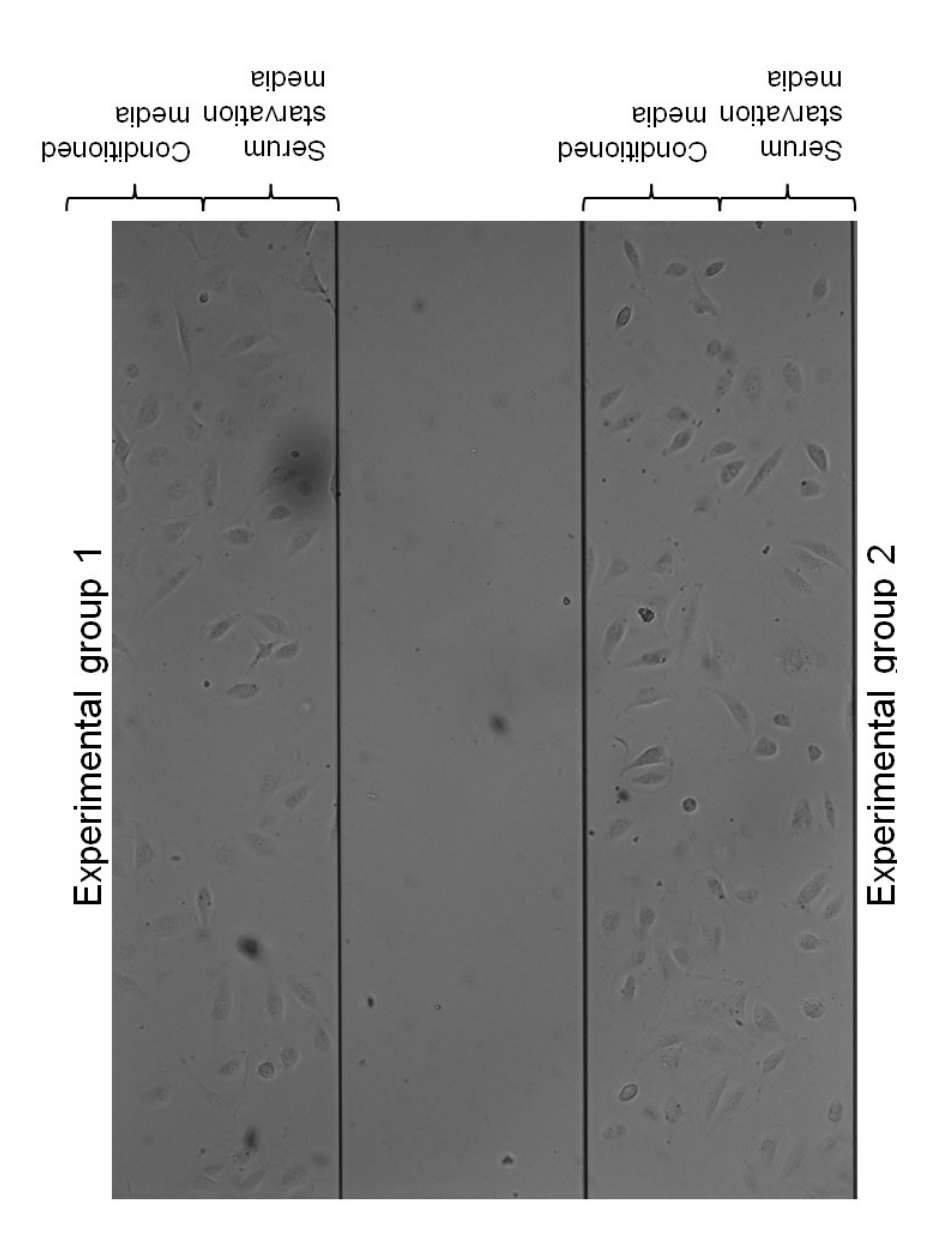


Figure 4.6: BioFlux migration of U87 cells expressing the $\Delta 221$ -232 mutant or the MLRL \rightarrow AAAA mutant. There was no significant difference between the two groups in total accumulated distance or in Euclidean (shortest) distance with direction. The means of each type of measurement are indicated. The graphs show the movement of each cell tracked per experimental group. The black paths indicate movement in a positive direction towards conditioned media, while the red paths indicate movement away from it. Data shown are from 1 independent experiment (n = 18 cells for MLRL \rightarrow AAAA, n = 25 cells for $\Delta 221$ -232).

Figure 4.6

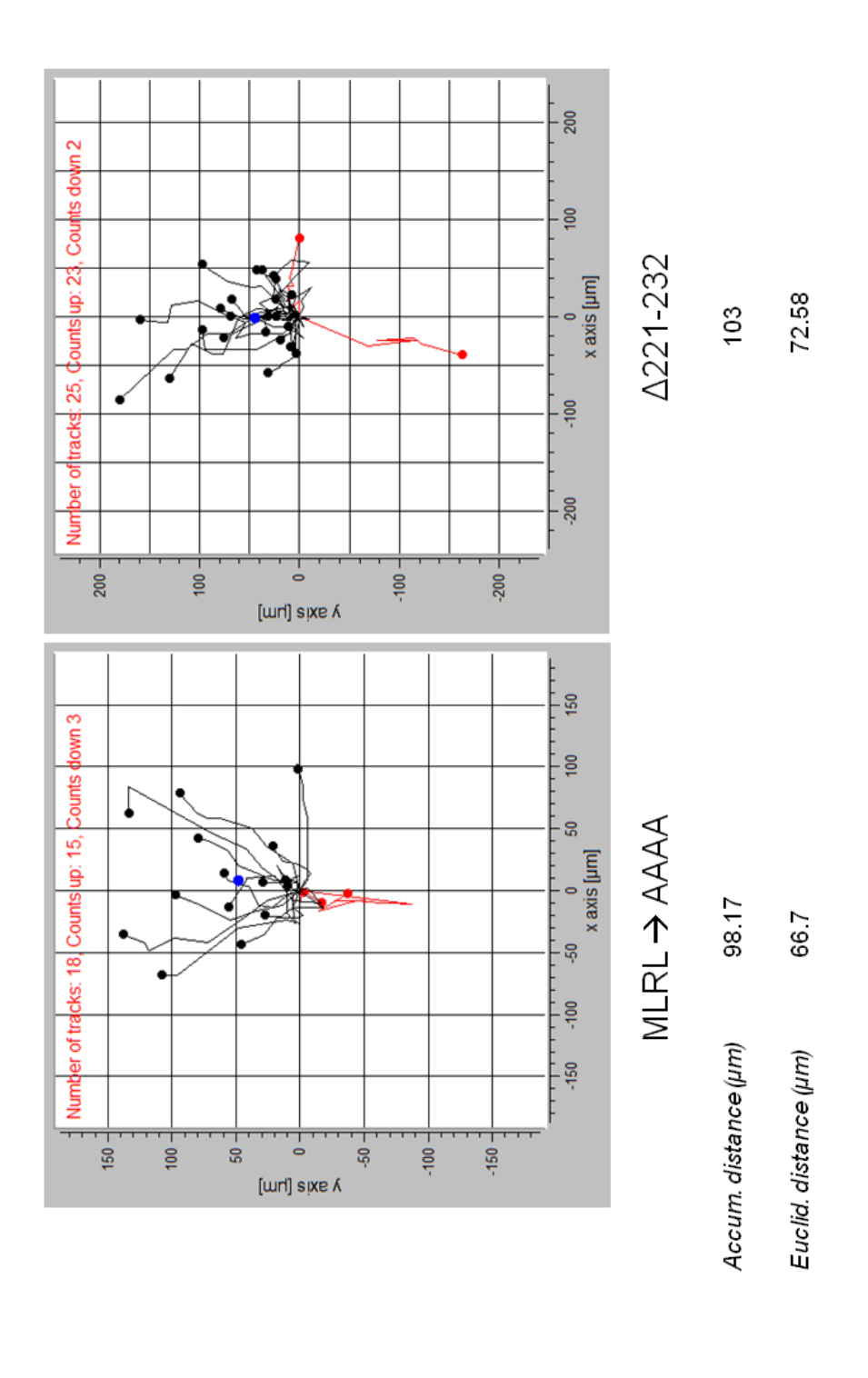
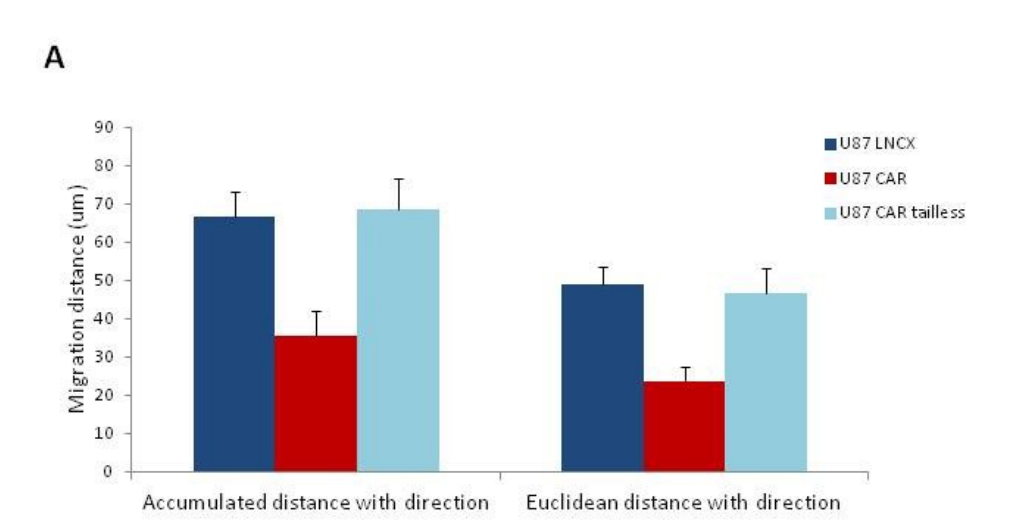
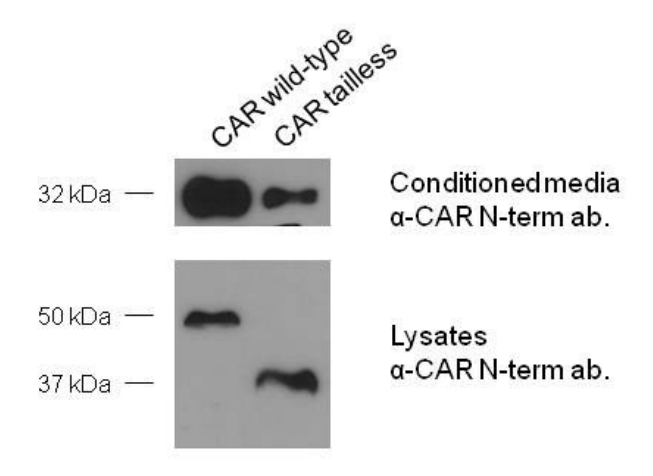


Figure 4.7: Tailless CAR, a mutant lacking CAR cytoplasmic domain and which does not inhibit glioma migration, sheds its ectodomain. (A) BioFlux migration experiments were performed on the U87 LNCX, U87 CAR (wild-type) and U87 CAR tailless cell lines. Data were compiled from 3 independent experiments for the U87 LNCX and U87 CAR tailless cell lines, and from 7 independent experiments for the U87 CAR cell line (U87 LNCX: n=99; U87 CAR: n=213; U87 CAR tailless: n=101). Error bars represent the standard error of the means. (B) A representative constitutive shedding experiment using U87 CAR (wild-type) and U87 CAR tailless cells. Conditioned media and cell lysates were analyzed by Western blot using an anti-CAR N-term antibody (CAR 2240). Like wild-type CAR, the tailless CAR mutant sheds its ectodomain, although to a lesser extent.

Figure 4.7



В



Chapter 5: Ectodomain Shedding of CAR From Developing

Neurons

CAR ECD is shed from developing cortical neurons constitutively as well as in a regulated manner

CAR is a cell adhesion molecule (CAM) highly expressed in the brain during development (Honda et al., 2000, Hotta et al., 2003). It mediates neurite extension on extracellular matrix proteins (Patzke et al., 2010) as well as on a substrate of CAR ectodomain (CAR ECD) (Huang, 2008). CAR is enriched in neuronal growth cones (Huang et al., 2007, Huang, 2008), and perturbation of the actin or microtubule networks disturbs its localization in developing neurons (Huang, 2008). Furthermore, it localizes to lipid rafts of neuronal growth cones, where it associates with neuronal nitric oxide synthase (nNOS). nNOS is required for neurite extension on CAR ECD substrate, as knockout of nNOS in a transgenic mouse line or pharmacological inhibition of nNOS activity abolished this effect of CAR ECD (Huang, 2008).

Proteolysis of CAMs is involved in the regulation of CAM-mediated neuronal outgrowth and synaptic plasticity (Bajor and Kaczmarek, 2013). With this in mind, we set out to investigate CAR proteolysis within the context of neuronal development. Preliminary data from our laboratory indicated that CAR ECD is shed from developing hippocampal neurons (Huang, 2008). Here, we present results from experiments performed using developing cortical neurons.

Conditioned media were collected from cultures of murine embryonic cortical neurons (approximately embryonic day 17, 7-9 days *in vitro*) and assayed for CAR ECD shedding. Media were found to contain shed CAR ECD migrating at approximately 32 kDa (figure 5.1A), and the presence of this shed fragment required metalloprotease activity (figure 5.2B). Full-length CAR (50 kDa) was detected from cortical neuronal lysate, as expected. The 37 kDa lower molecular weight band detected from neuronal lysate is likely a shorter CAR isoform rather than a product of degradation (figure 5.1C).

Shedding of CAR ECD from embryonic cortical neuronal cultures was upregulated by treatments with PMA, ionomycin and KCl at the indicated concentrations and lengths of time (figure 5.2). Thus, in addition to constitutive shedding, CAR ECD can be shed via the DAG-PKC pathway (PMA), Ca²⁺ transport across biological membranes (ionomycin), and neuronal cell depolarization (KCl).

Neurite outgrowth mediated by a substrate of CAR ECD requires metalloprotease activity

Studies in our laboratory have revealed that outgrowth of embryonic hippocampal neurons is enhanced on a substrate of CAR ECD, and that this effect requires expression of endogenous CAR in neurons, suggesting the involvement of homophilic CAR-CAR interactions in this process (Huang, 2008). These

experiments were performed using substrates of purified His-tagged CAR ECD or fusion protein of Fc-CAR, coated on poly-d-lysine (PDL). The structure of Fc-CAR is shown in figure 5.3A.

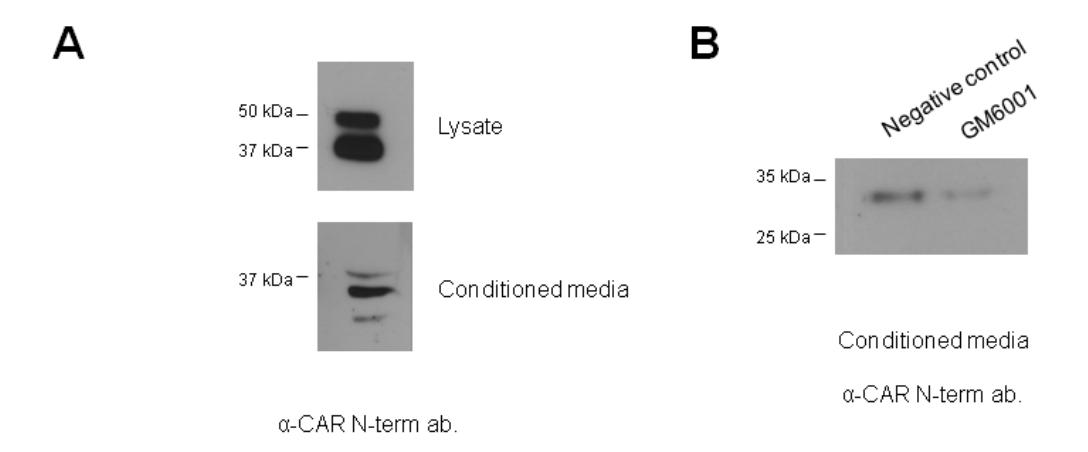
To investigate the possibility that proteolytic activity is involved in CAR-mediated neurite outgrowth, microexplants were prepared from cerebella of embryonic mice and plated on PDL vs. PDL + Fc-CAR. Similarly to dissociated hippocampal neurons, the presence of Fc-CAR ECD as a coated substrate enhanced neurite length from the cerebellar microexplants (figure 5.3B, comparison of 1st and 3rd columns from the left). Treatment with the broadspectrum metalloprotease inhibitor GM6001 abolished the effect of Fc-CAR, indicating that metalloprotease activity is required for CAR ECD-mediated neuronal outgrowth. Representative images are also shown in figure 5.3B.

ADAM10 is a sheddase of CAR in developing cortical neurons

Finally, embryonic cortical neuronal cultures were treated with ADAM10 prodomain to inhibit ADAM10 activity. Figure 5.4 shows that the prodomain treatment resulted in loss of CAR ECD from conditioned media, indicating that ADAM10 sheds CAR ECD from developing neurons similarly to our previous observations with glioma cells (presented in chapter 3 of this thesis).

shedding from cortical embryonic neurons (approx. E17) was assayed between 7 to 9 days *in vitro*. Data are representative of 3 independent neuronal cultures. (B) Cortical neurons (approx. E17) at 8 days in vitro were treated overnight with GM6001 or its negative control, and media were assayed. Shed CAR ECD decreased with inhibition of metalloprotease activity. (C) Cortical neuronal lysate samples from these experiments were probed via Western blotting with anti-CAR N-term antibody 2240 or anti-CAR C-term antibody RP291. The lower band migrating at 37 kDa was not detected with RP291 antibody, suggesting that it may be a smaller isoform of CAR rather than a product of degradation of full-length CAR.

Figure 5.1



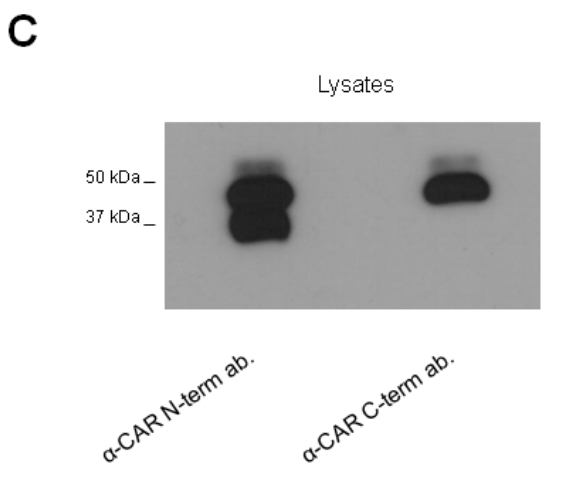


Figure 5.2: CAR ECD shedding from developing cortical neurons is stimulated by the phorbol ester PMA, by the calcium ionophore ionomycin and by KCl. Mouse embryonic cortical neurons (8-9 DIV) were treated with PMA (1 μM) vs. DMSO for 4 hours, with ionomycin (2.5 μM) vs. DMSO for 30 minutes, or with KCl (56 mM) vs. H₂O for 90 minutes. PMA, ionomycin and KCl induced CAR ECD shedding from developing neurons. Western blot bands were quantified using ImageJ and relative quantities are indicated below the blots. Results are representative of 3 independent neuronal cultures for PMA and 2 independent neuronal cultures for KCl and ionomycin.

Figure 5.2

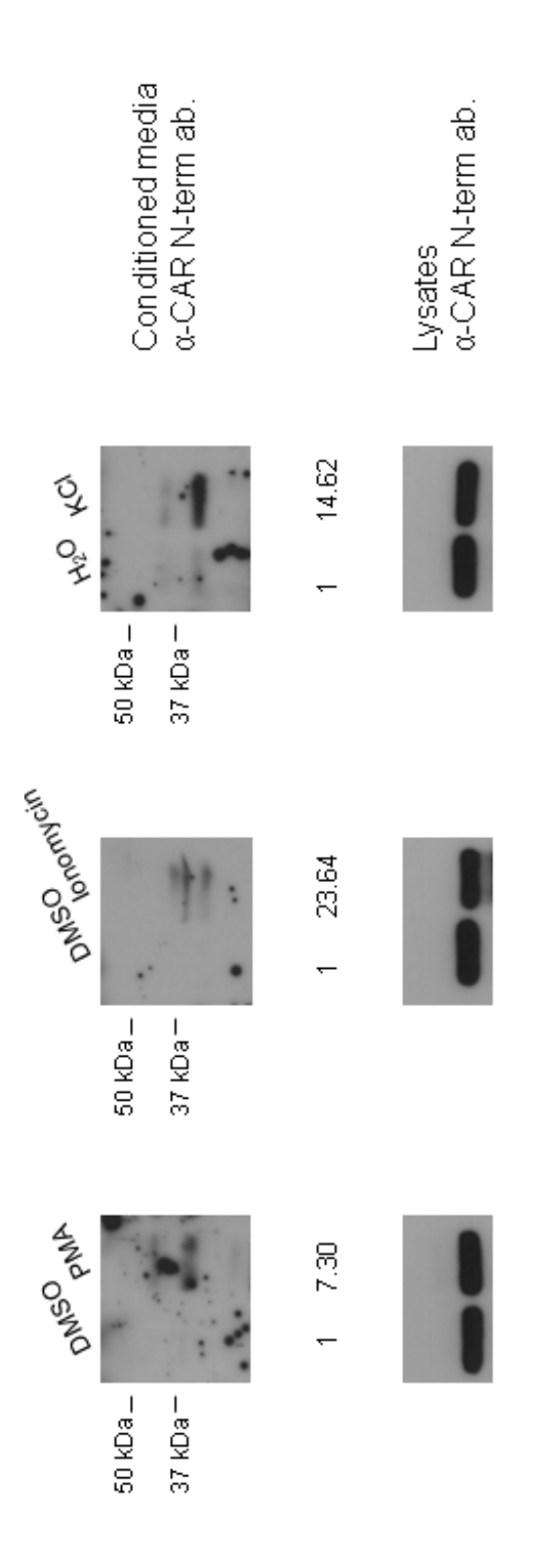


Figure 5.3: The ECD of CAR promotes neurite outgrowth from cerebellar microexplants, an effect abolished by inhibition of metalloprotease activity. (A) A schematic showing the purified Fc-tagged CAR ECD used in these studies. (B) Cerebellar microexplants were dissected and cultured as described, seeded on poly-d-lysine (PDL) or PDL plus Fc-CAR (final concentration of Fc-CAR = 0.125 µg/ml). About 16 hours later, GM6001 or its negative control was added at a final concentration of 25 µM. 24 hours later, the microexplants were fixed with 4% paraformaldehyde and stained with Coomassie blue. Pictures were taken at 100X objective, and the 5 longest neurites were quantified using the NeuronJ plugin on ImageJ software, added, and the means calculated per experimental group. Left: Means and SEMs of neurite length from the 4 experimental groups (One-way ANOVA with Bonferroni's Multiple Comparison Test; *** = p < 0.001). PDL neg ctl: n = 39; PDL GM6001: n = 35; FcCAR neg ctl: n = 38; FcCAR GM6001: n = 49. Data shown are from one independent experiment; similar data were obtained from 3 independent experiments. Right: representative images. Scale bar: 100 μm.

Figure 5.3

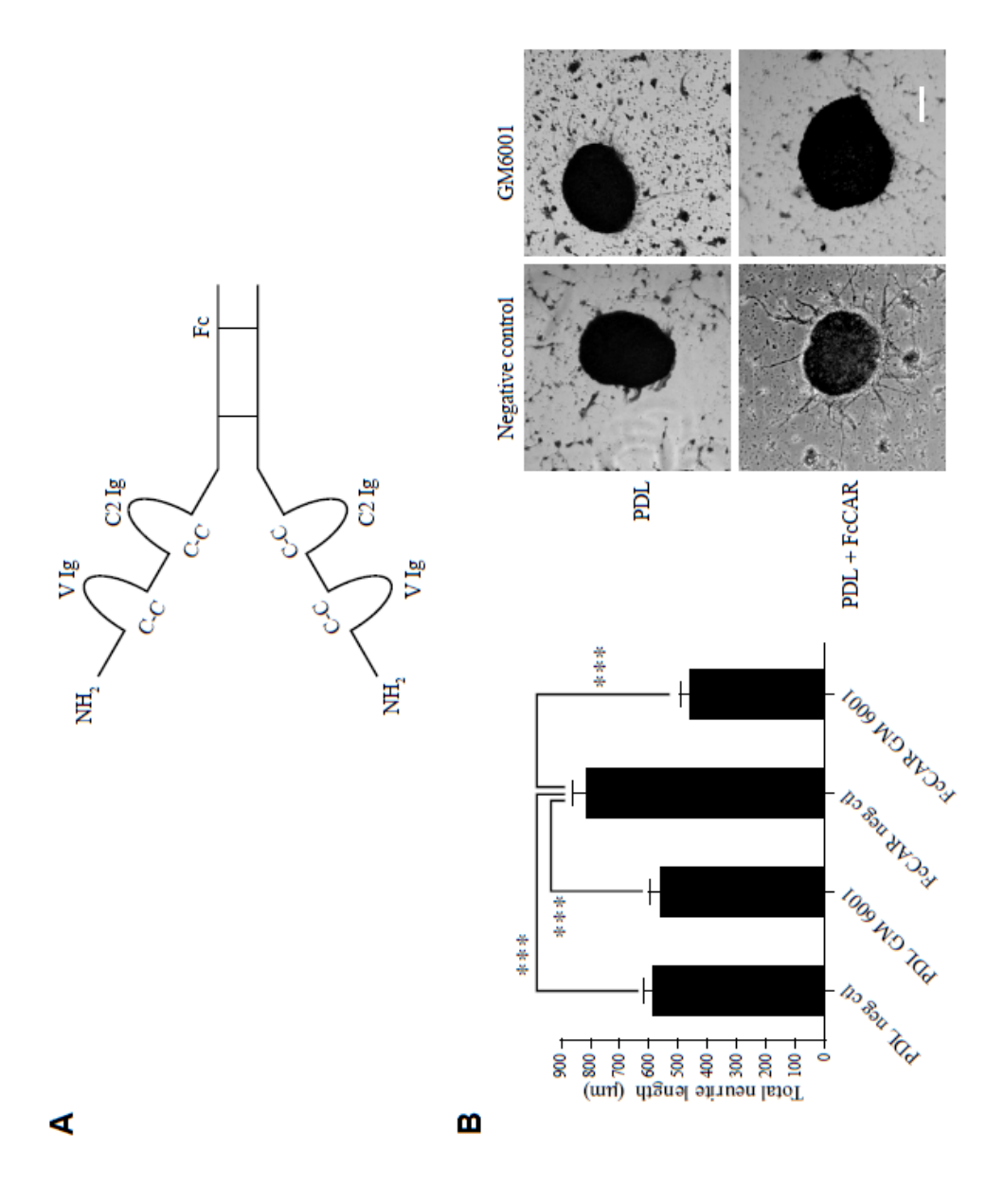
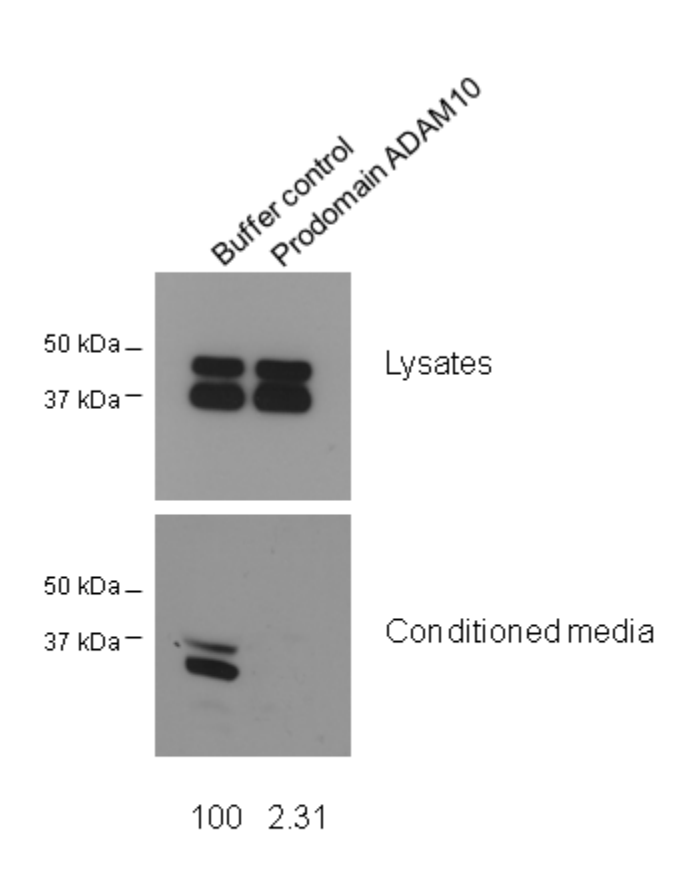


Figure 5.4: ADAM10 activity is required for basal ECD shedding of CAR from developing cortical neurons. Mouse embryonic cortical neurons were treated overnight with ADAM10 prodomain or its buffer control. Treatment with ADAM10 prodomain, which inhibits ADAM10, abolished CAR ECD shedding. Results shown are representative of 3 independent neuronal cultures. Western blot bands were quantified using ImageJ, and relative band intensities are indicated below the blot.

Figure 5.4



α-CAR N-term ab.

Chapter 6: Studies on the Intracellular Domain of CAR, a

Product of Regulated Intramembrane Proteolysis (RIP)

Cell surface proteins that undergo ectodomain shedding often also undergo regulated intramembrane proteolysis (RIP) mediated by the presenilin/γ-secretase complex. Preliminary studies, outlined in the project rational of this thesis, revealed the existence of smaller molecular weight fragments of CAR (20 kDa and 14 kDa), which were detected using antibody raised against CAR's C-terminus (figure 1.5). Treatment of U87 CAR cells with the γ-secretase inhibitors MG132 and DAPT caused accumulation of the 20 kDa fragment (CTF1) and abolished the 14 kDa fragment (CTF2). This suggested that CTF1 is the transmembrane and cytoplasmic domain stub of CAR left after its ECD is shed, whereas CTF2 is the product of RIP of CAR by the γ-secretase complex (Huang, 2008). Confirmation of the results with MG132 is shown in figure 6.1A.

Besides MG132 and DAPT, we also used Compound E, another pharmacological inhibitor of y-secretase. Treatment of U87 CAR cells with Compound E abolished the appearance of the 14 kDa CAR CTF2, while levels of the 20 kDa C-terminal fragment of CAR (CTF1) accumulated (figure 6.1B), further supporting results of experiments with MG132 and DAPT.

As presenilin is the catalytic subunit of the γ -secretase complex (Jorissen and De Strooper, 2010), we hypothesized that lack of presenilin expression would result in the absence of the CTF2 fragment. Murine embryonic fibroblast (MEF) cells,

wild-type or knockout for presenilin 1 and 2 (*PSEN1* and *PSEN2*), were infected with adenovirus to express full-length CAR. Analyzing cell lysates by Western blot using antibody raised against CAR's C-terminus revealed that the 14 kDa fragment, CAR CTF2, is indeed lost in the presenilin knockout cells (figure 6.1C).

A construct of full-length CAR with a C-terminal V5 tag was generated and stably expressed in the human glioma cells U87-MG and U251N. V5-tagged CAR was processed similarly as untagged CAR in glioma cells, as Western blots of lysates with antibody raised against the V5 tag revealed the presence of CTF1 and CTF2 fragments in addition to full-length CAR (figure 6.1D). To further support this, treatment with the γ-secretase inhibitor MG132 abolished the appearance of CAR CTF2 and led to the accumulation of CAR CTF1 (figure 6.1E).

MEF wild-type and presenilin knockout cells were infected with lentivirus to express CAR with a C-terminal V5 tag. MEF cells null for presenilin 1 and 2 had no detectable V5-tagged CAR CTF2 (figure 6.1F), further supporting the results obtained with an untagged CAR construct in figure 6.1C.

Thus, inhibition of γ -secretase activity pharmacologically or by knockout of presenilin (the catalytic component of the γ -secretase complex) prevents CAR from undergoing RIP.

We hypothesized that ECD shedding is a prerequisite for RIP of CAR. If that is the case, CAR CTF2 should be dependent on the generation of CAR CTF1. U87 CAR-V5 cells were treated for 4 hours with 25 μ M of the metalloprotease inhibitor GM6001 or its negative control. Inhibition of CAR ECD shedding was accompanied by a decrease in both CTF1 and CTF2 (figure 6.2A).

For further confirmation, ADAM10 was knocked down in U87 CAR-V5 cells (ADAM10 shRNA #6675), with control shRNA for comparison. The ADAM10 shRNA cell line had reduced amounts of the 20 kDa CTF1 fragment, as expected (figure 6.2B), since a decrease in ECD shedding should also be accompanied by lower CTF1 levels. Importantly, levels of the 14 kDa CAR CTF2 also decreased. These data indicate that RIP of CAR is dependent on ECD shedding of the full-length receptor.

Free CAR intracellular domain enters the nucleus

As the intracellular domains of some substrates translocate to the nucleus following ectodomain shedding and RIP, we wondered if that is the case for CAR. HEK 293 cells were transiently transfected with a construct of CAR containing a C-terminal V5 tag. Immunofluorescence and confocal microscopy experiments revealed the presence of V5-immunoreactive speckles inside cell nuclei (figure

6.3). However, these nuclear speckles appeared rarely and were not improved with the use of the nuclear export inhibitor leptomycin B in conjunction with PMA treatment (data not shown).

In an effort to circumvent this technical issue and to conclusively determine whether or not CAR enters the nucleus following proteolysis, a CAR intracellular domain (CAR ICD) construct with a C-terminal V5 tag was generated and transiently expressed in U87 cells. CAR ICD was detected in both the cytoplasm and nucleus (figure 6.4 and figure 6.5). Similar results were obtained in 293 cells (data not shown). This construct of CAR is derived solely from the cytoplasmic domain of the wild-type receptor and is likely to be shorter than naturally-generated CAR CTF2, as γ-secretase cleavage occurs within the transmembrane domain of substrates. As shown in figure 6.10, CAR ICD and CAR CTF2 display slightly different molecular weights.

In a proteomics and mass spectrometry screen performed in our laboratory to discover proteins that interact with CAR ICD (Fok et al., 2007), the classic nuclear import protein importin alpha was identified as a potential CAR ICD binding-protein (figure 6.6A). GST pull down experiments confirmed that CAR ICD and importin alpha interact (figure 6.6B), suggesting that CAR ICD may require importin alpha to enter the nucleus.

The online nuclear localization sequence (NLS) tool, cNLS Mapper (Kosugi et al., 2009), predicted that a sequence in CAR ICD immediately downstream of the transmembrane domain (CHRKRREEKY) may be a monopartite NLS. We attempted to generate a CAR ICD mutant that would be excluded from nuclear entry. However, lysine to alanine mutations, as well as deletion of this predicted sequence, still resulted in nuclear entry of the mutant CAR ICD constructs (data not shown), indicating that CAR ICD may not require the classic nuclear import pathway for its entry into the nucleus even though it interacts with importin alpha, directly or indirectly, as determined from GST pull down experiments (figure 6.6B).

CAR ICD is subject to proteasomal degradation

We hypothesized that CTF2, generated from CAR via RIP, is not readily detectable in nuclei due to degradation of this fragment by the proteasome. Indeed, treatment of U87 CAR-V5 cells with the proteasome inhibitor epoxomicin increased levels of CTF2 and the ratio of CTF2 to CTF1 (figure 6.7A and figure 6.7B). Levels of free CAR ICD also accumulated in the presence of the proteasome inhibitor MG132 (figure 6.7C). However, any nuclear CTF2 remained below detection level in epoxomicin-treated U87 cells stably expressing CAR-V5 (data not shown).

Studies on CAR ICD and a GAL4-dependent luciferase reporter

Since CAR ICD enters the nucleus, can it affect gene expression? One way to investigate this possibility is by using reporters such as GAL4-dependent luciferase. GAL4 is a yeast regulatory protein that binds to a DNA sequence, UAS_G (galactose upstream activation sequence), and activates genes downstream of UAS_G (Guarente et al., 1982, Giniger et al., 1985). Although GAL4 is a yeast protein, it is known to activate UAS_G-linked promoters in mammalian cells (Kakidani and Ptashne, 1988, Webster et al., 1988). In our system, expression of the luciferase gene is driven by 5 copies of UAS_G (Potter et al., 2010), and UAS_G is dependent on GAL4 binding for efficient transcription.

If CAR ICD is sufficient for transactivation of the luciferase reporter, then it should functionally replace the transactivation domains found in GAL4. We generated constructs to express GAL4 DNA-binding domain (DBD) only as well as a fusion protein of GAL4 DBD and CAR ICD. In these experiments, the positive and negative controls were full-length GAL4 and GAL4 DBD, respectively. Full-length GAL4, which contains the DBD that binds to the UAS_G sequence as well as transactivation domains, robustly induced luciferase expression, while GAL4 DBD alone did not induce luciferase expression above background levels (figure 6.8), as expected. The GAL4 DBD-CAR ICD fusion protein did not activate luciferase expression significantly and behaved similarly to the GAL4 DBD construct (figure 6.8). These results suggest that if CAR ICD

induces gene activation, it may require as yet undetermined binding partners to do so.

Interestingly, when CAR ICD was fused to full-length GAL4, it significantly inhibited GAL4-mediated luciferase expression (figure 6.9), suggesting that in this context, CAR ICD may be acting as a repressor of transcription. However, it should be noted that an alternative explanation for these results could be that CAR ICD fusion with GAL4 somehow changes GAL4's tertiary structure and prevents it from being fully functional, rather than CAR ICD behaving as a repressor.

Free CAR ICD does not inhibit glioma migration

Results of experiments presented in chapter 4 of this thesis suggest that ECD shedding may not be involved in CAR-mediated inhibition of glioma migration. We used several approaches to investigate this question, including stimulation or inhibition of CAR ECD shedding with drugs. However, it is possible that there were still sufficient levels of full-length CAR remaining in treated cells to inhibit glioma migration. Even though ECD shedding is a prerequisite for RIP of CAR, we reasoned that a reductionist approach, comparing the function of free ICD to that of full-length CAR, would be appropriate to delineate what the consequences of RIP of CAR are on glioma migration.

Past results from our laboratory have shown that intact CAR ICD is required for inhibition of glioma migration and invasion (Huang et al., 2005b). Also, CAR ICD directly interacts with, and stabilizes, the cytoskeleton (Fok et al., 2007, Huang et al., 2007), a mechanism that possibly inhibits glioma migration. We hypothesized that CAR ICD, when freed from the plasma membrane by RIP, would not inhibit glioma migration like full-length CAR.

During the course of these studies, we experienced technical difficulties in obtaining stable glioma cell lines that express detectable levels of CAR ICD. We instead used a bicistronic IRES GFP lentiviral vector (pWPI) to express V5-tagged full-length CAR or CAR ICD, with empty pWPI vector as control (figure 6.10). In addition to Western blots, immunofluorescence experiments were performed to verify expression of these constructs in U87 cells (data not shown).

Experiments using the BioFlux live cell migration system revealed that CAR ICD-expressing cells had a significantly greater mean accumulated distance of migration than cells expressing full-length CAR (figure 6.11A), similarly to control (pWPI only) cells. When taking direction (angle of migration) into account, the mean accumulated distance with direction and mean Euclidean (shortest) distance with direction were also greater for CAR ICD-expressing cells than full-length CAR-expressing cells, although these differences were not found to be statistically significant (figure 6.11B and C).

XTT cell viability assays were performed in parallel to the BioFlux migration experiments to investigate whether or not differences in migration were due to cell death. No significant differences were found for cell viability between the experimental groups (figure 6.12).

Taken together, functional studies on CAR proteolysis in chapter 3 and in this chapter indicate that while ECD shedding of CAR does not affect its inhibition of glioma migration, free CAR ICD generated from RIP loses this inhibition.

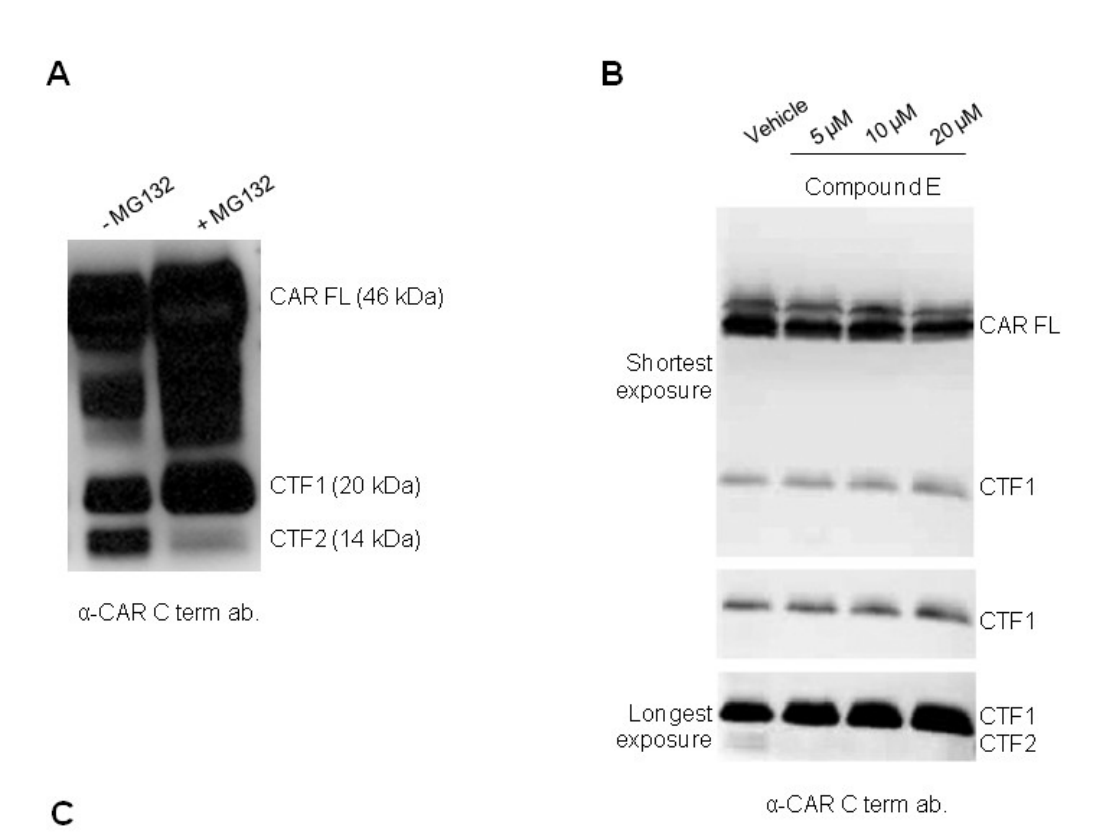
Therefore, proteolysis is ultimately a negative regulator of CAR in this context and may be a favorable factor for tumorigenesis.

Figure 6.1: RIP of CAR is mediated by the presentlin/y-secretase complex.

(A) U87 CAR cells were treated overnight with 25 µM MG132 vs DMSO vehicle. Treatment with the proteasome and y-secretase complex inhibitor MG132 resulted in accumulation of the CAR CTF1 fragment (20 kDa) and a dramatic decrease in levels of CAR CTF2 (14 kDa fragment). (B) U87 CAR cells were treated overnight with the y-secretase inhibitor Compound E at the indicated concentrations. Equal quantities of proteins from cell lysates were analyzed by SDS-PAGE and Western blot using the anti-CAR C-term antibody RP291. With increasing concentrations of Compound E, there was a corresponding accumulation of a 20 kDa fragment (CAR CTF1) and a decrease in a 14 kDa fragment (CAR CTF2). 3 different exposures of the Western blot are shown. (C) Wild-type (WT) or PS 1- and 2-knockout MEF cells (MEF PS1/2 KO) were infected with adenovirus carrying the CAR gene (AdVCAR). Lysates were analyzed by Western blot using the anti-CAR intracellular domain antibody RP291. A CAR CTF2 fragment migrating at ~14 kDa was detected from wildtype MEF cells but not from cells null for presenilin. (D) Stable cell lines of U87-MG and U251N expressing either V5 tag alone (mock) or CAR with a C-terminal V5 tag were generated. Equal amounts of cell lysates were analyzed by SDS-PAGE and Western blot using a mouse monoclonal antibody raised against the V5 tag. Full-length CAR, as well as CAR CTF1 and CTF2 fragments, were detected, as from the U87 CAR cell line. (E) U251N V5 and U251N CAR-V5 cells were treated overnight with MG132 (25 µM) or DMSO vehicle control. Equal amounts of proteins from cell lysates were used for anti-V5 Western blots.

In the case of the MG132-treated cells, CTF1 levels accumulated while CTF2 nearly disappeared, similar to previous experiments with U87 cells expressing untagged CAR. (F) MEF WT and MEF PS 1/2 KO cells were infected with lentivirus to express full-length CAR with a C-terminal V5 tag (CAR-V5 construct). Cells were lysed 3 days post-infection, and lysates were analyzed by Western blot using antibody raised against the V5 tag. MEF WT cells, but not MEF PS 1/2 KO cells, contained CAR CTF2, indicating that presentlin is required for generation of the 14 kDa CTF2 fragment.

Figure 6.1



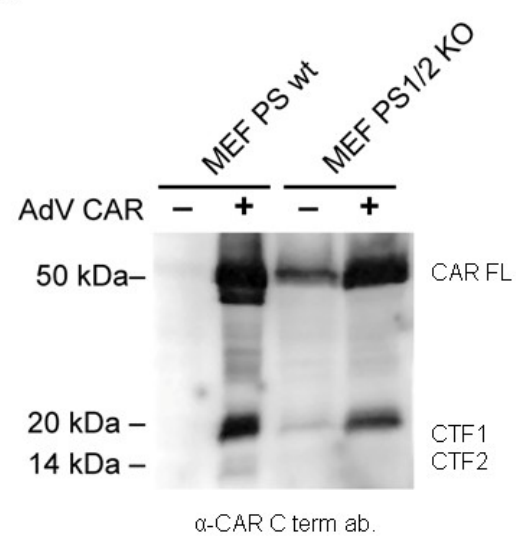
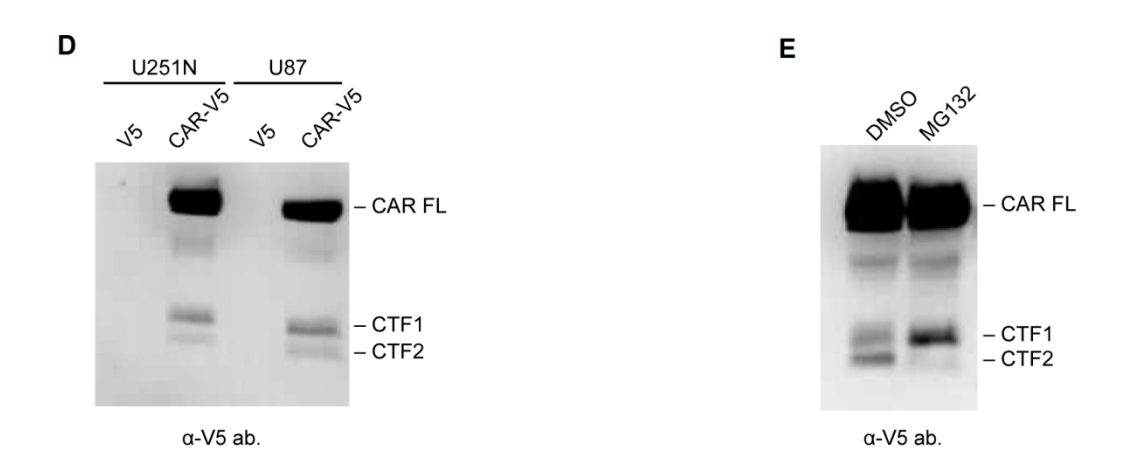


Figure 6.1 (continued)



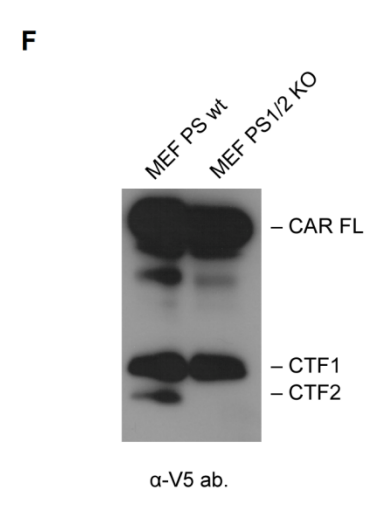


Figure 6.2: Generation of CAR CTF1 precedes CTF2 production. (A) U87 CAR-V5 cells were treated with 25 µM of the metalloprotease inhibitor GM6001 or its negative control for 4 hours. Conditioned media and lysates were collected and analyzed by Western blot using anti-CAR N-term. antibody 2240 (for conditioned media) and anti-V5 tag antibody (lysates). GM6001 treatment inhibited CAR ECD shedding, as expected. There was a small decrease in levels of both CAR CTF1 and CTF2 with GM6001 treatment. (B) U87 CAR-V5 stable cells were infected with lentivirus containing control (anti-eGFP) shRNA or ADAM10 shRNA (#6675) and assayed for knockdown (see ADAM10 and GAPDH Western blots). Lysates were analyzed by Western blot using antibody raised against the V5 tag. The ADAM10 shRNA stable cell line had a loss in CAR CTF1 level, as expected, since a decrease in ADAM10-mediated CAR ECD shedding should be accompanied by less CTF1 being generated. Importantly, CAR CTF2 levels also decreased, indicating that ectodomain shedding is a prerequisite for the RIP of CAR.

Figure 6.2

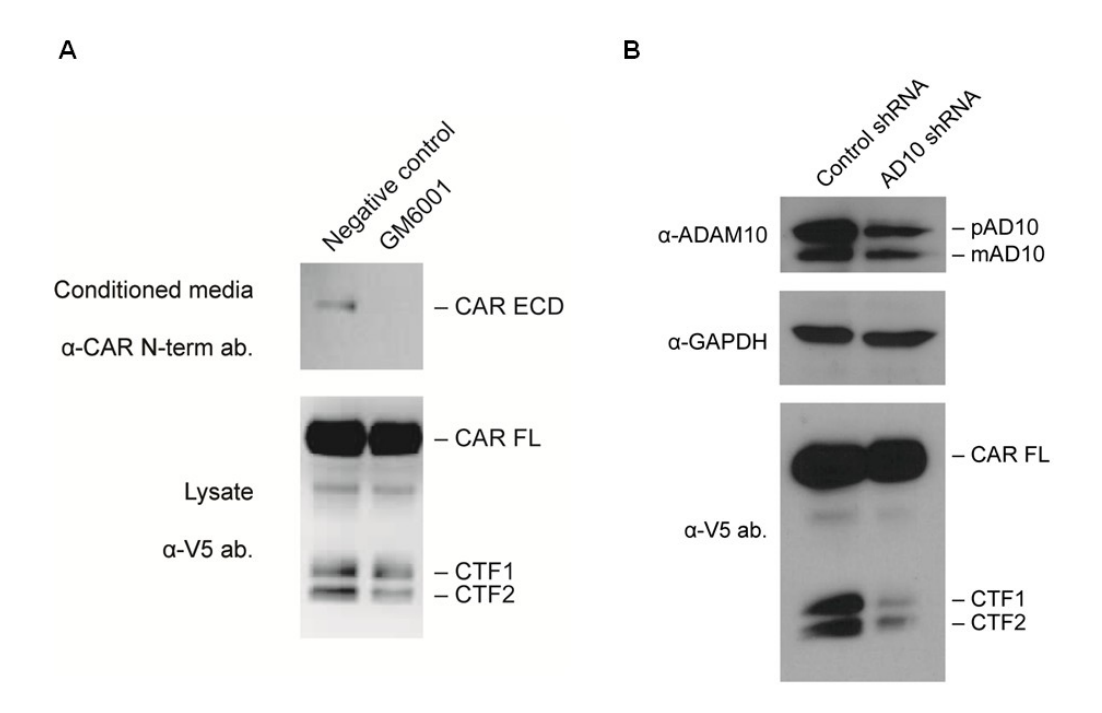


Figure 6.3: Detection of V5 tag immunoreactive speckles in nuclei of 293 cells transiently transfected with full-length CAR-V5. Immunofluorescence and confocal microscopy revealed the presence of V5-immunoreactive speckles in nuclei of 293 cells, possibly CTF2 fragments that had translocated to the nucleus following RIP of CAR. Green = anti-V5, blue = DRAQ5 nuclear stain. The white arrows point to the speckles in the green channel. Scale bar: 5 μ m.

Figure 6.3

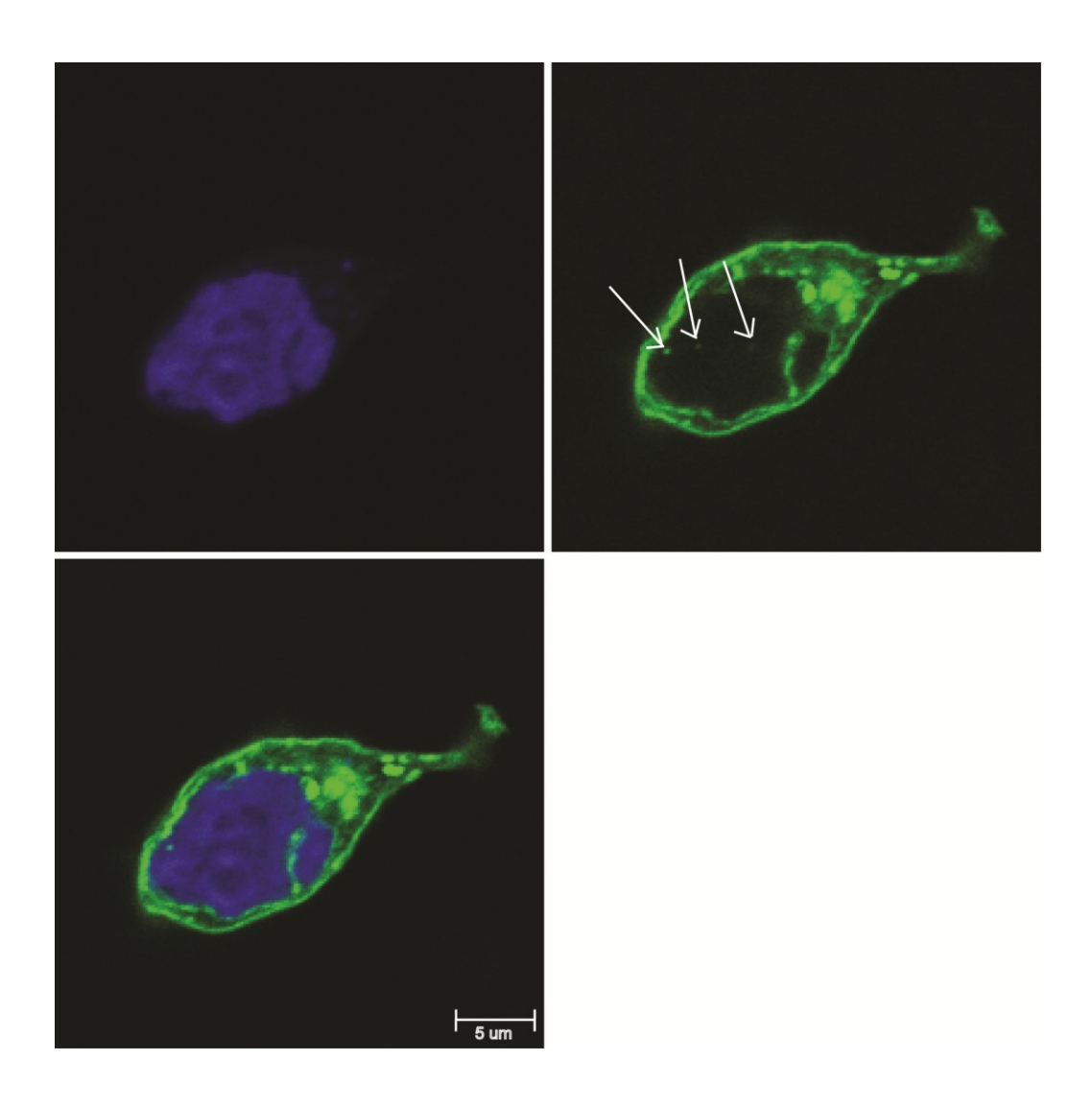


Figure 6.4: CAR intracellular domain (ICD) enters the nucleus.

Immunofluorescence and confocal microscopy images showing the presence of CAR ICD in nuclei of U87-MG cells. U87-MG cells were transiently transfected with empty pcDNA3.1 V5/His plasmid, full-length CAR-V5 plasmid or with CAR ICD-V5 plasmid. Immunofluorescence staining was performed 24-48 hours post-transfection using anti-V5 tag antibody and Alexa Fluor 555 secondary antibody (red). Nuclei were stained with DRAQ5 (blue). Images were acquired with a confocal microscope (63x oil objective). Images are representative of at least 3 independent experiments. Scale bars: 5 μm.

Figure 6.4

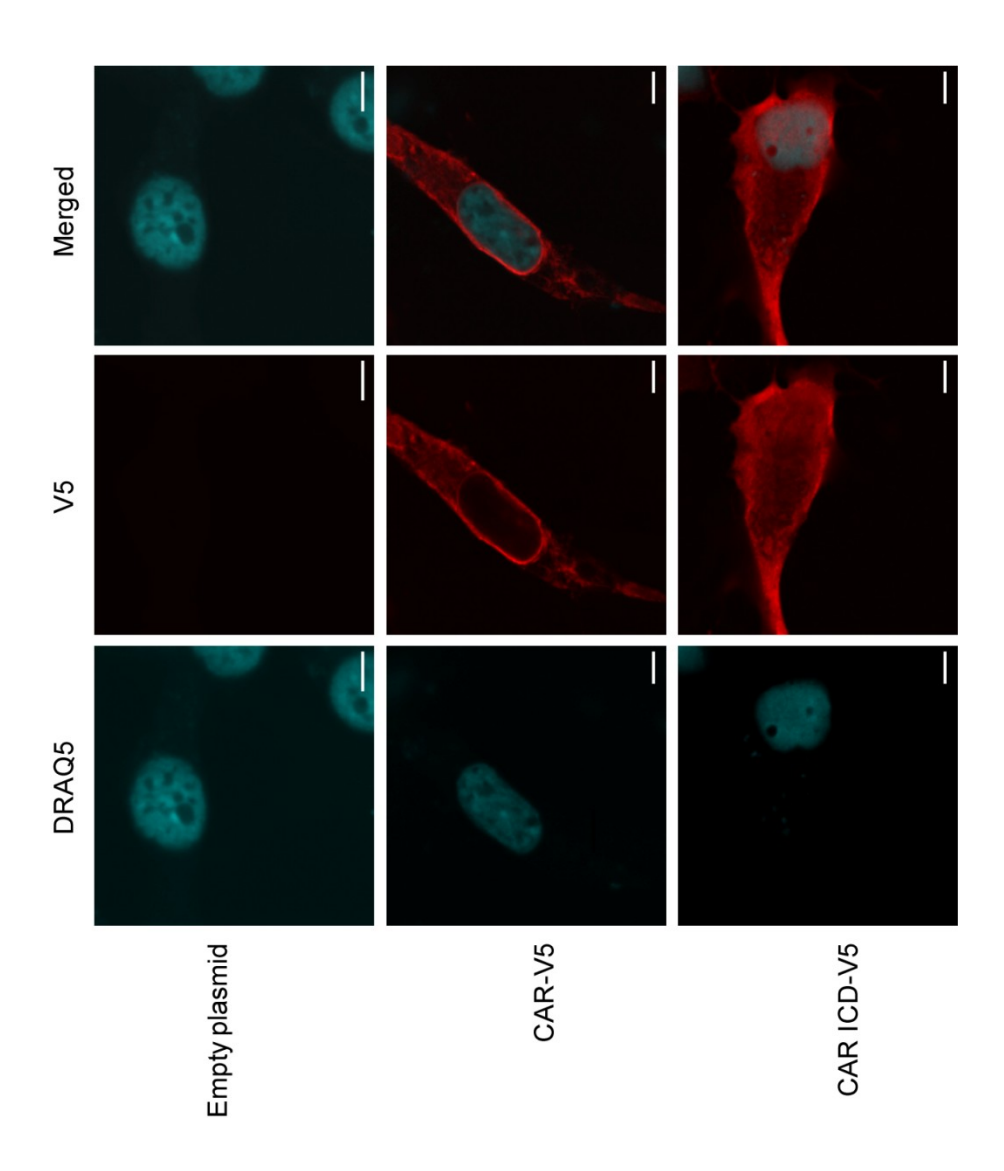


Figure 6.5: Confocal microscopy Z stack images of a U87 cell transiently expressing V5-tagged CAR ICD. Green = anti-V5 tag, blue = DRAQ5 (nuclear stain). Shown are 18 slices representing a total thickness of 5.93 μ m. Scale bar: 5 μ m.

Figure 6.5

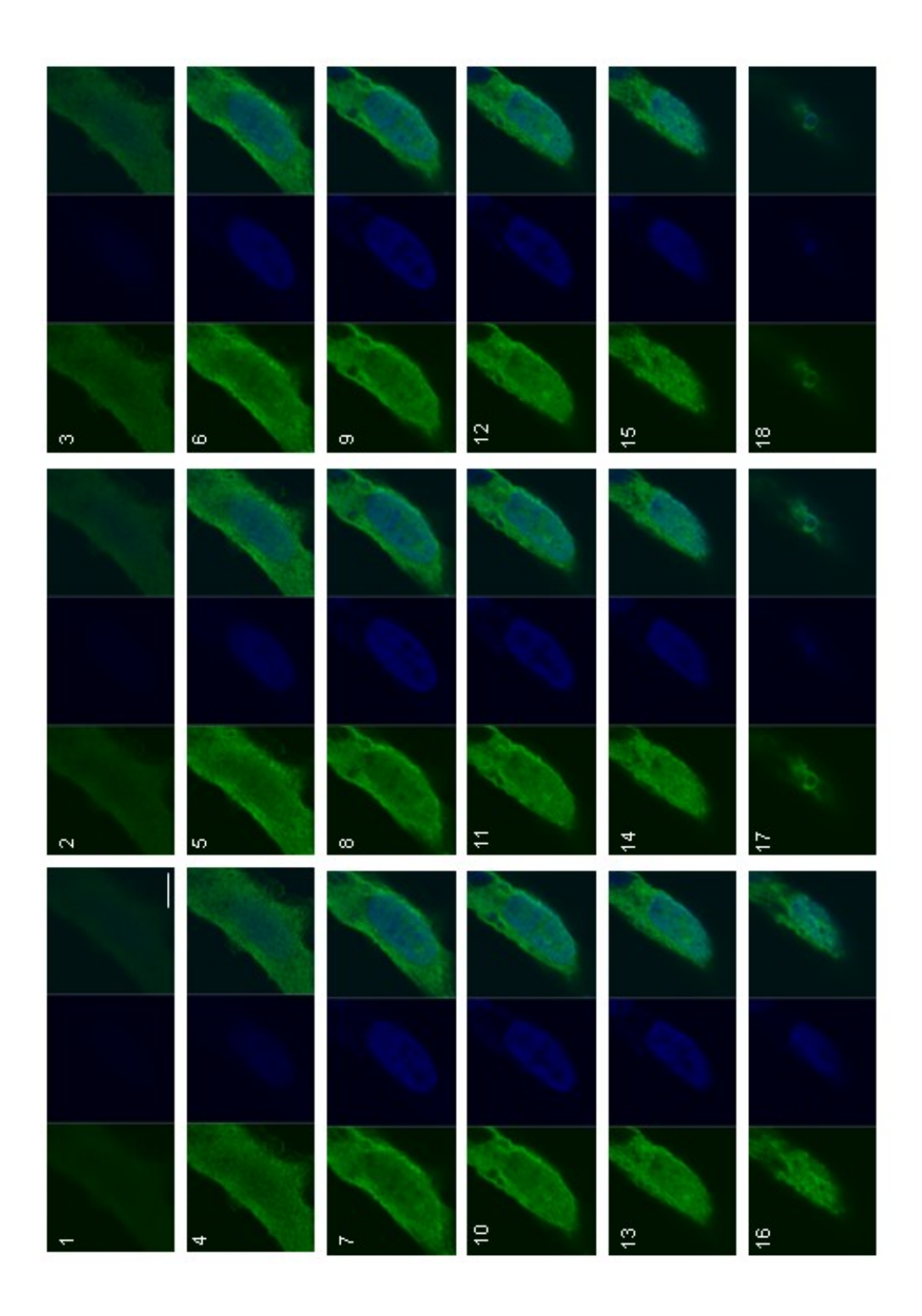


Figure 6.6: CAR ICD binds the nuclear import protein importin alpha. (A) A proteomics screen performed in our laboratory (Fok et al., 2007) identified the nuclear import protein importin alpha as a potential interactor with CAR ICD. Highlighted is the peptide fragment of importin alpha that was detected. The ion score was 89, with scores greater than 39 considered significant. (B) GST pull-down experiments were performed, and samples were analyzed by SDS-PAGE and Western blot. The Western blot shows that GST-CAR ICD fusion protein, but not GST (control), pulls down importin alpha.

Figure 6.6

Α

10 20 30 40 50 60 MTTPGKENFR LKSYKNKSLN PDEMRRREE EGLQLRKQKR EEQLFKRRNV ATAEEETEEE 70 80 90 100 110 120 VMSDGGFHEA QISNMEMAPG GVITSDMIEM IFSKSPEQQL SATQKFRKLL SKEPNPPIDE 130 140 150 160 170 180 VISTPGVVAR FVEFLKRKEN CTLQFESAWV LTNIASGNSL QTRIVIQAGA VPIFIELLSS 190 200 210 220 230 240 EFEDVQEQAV WALGNIAGDS TMCRDYVLDC NILPPLLQLF SKQNRLTMTR NAVWALSNLC 250 260 270 280 290 300 RGKSPPPEFA KVSPCLNVLS WLLFVSDTDV LADACWALSY LSDGPNDKIQ AVIDAGVCRR 310 320 330 340 350 360 LVELLMHNDY KVVSPALRAV GNIVTGDDIQ TQVILNCSAL QSLLHLLSSP KESIKKEACW 370 380 <td< th=""><th></th><th></th><th></th><th></th><th></th><th></th></td<>						
70 80 90 100 110 120 VMSDGGFHEA QISNMEMAPG GVITSDMIEM IFSKSPEQQL SATQKFRKLL SKEPNPPIDE 130 140 150 160 170 180 VISTPGVVAR FVEFLKRKEN CTLQFESAWV LTNIASGNSL QTRIVIQAGA VPIFIELLSS 190 200 210 220 230 240 EFEDVQEQAV WALGNIAGDS TMCRDYVLDC NILPPLLQLF SKQNRLTMTR NAVWALSNLC 250 260 270 280 290 300 RGKSPPPEFA KVSPCLNVLS WLLFVSDTDV LADACWALSY LSDGPNDKIQ AVIDAGVCRR 310 320 330 340 350 360 LVELLMHNDY KVVSPALRAV GNIVTGDDIQ TQVILNCSAL QSLLHLLSSP KESIKKEACW 370 380 390 400 410 420 TISNITAGNR AQIQTVIDAN IFPALISILQ TAEFRTRKEA AWAITNATSG GSAEQIKYLV 430 440	1 <u>0</u>	2 <u>0</u>	3 <u>0</u>	4 <u>0</u>	5 <u>0</u>	6 <u>0</u>
VMSDGGFHEA QISNMEMAPG GVITSDMIEM IFSKSPEQQL SATQKFRKLL SKEPNPPIDE 130 140 150 160 170 180 VISTPGVVAR FVEFLKRKEN CTLQFESAWV LTNIASGNSL QTRIVIQAGA VPIFIELLSS 190 200 210 220 230 240 EFEDVQEQAV WALGNIAGDS TMCRDYVLDC NILPPLLQLF SKQNRLTMTR NAVWALSNLC 250 260 270 280 290 300 RGKSPPPEFA KVSPCLNVLS WLLFVSDTDV LADACWALSY LSDGPNDKIQ AVIDAGVCRR 310 320 330 340 350 360 LVELLMHNDY KVVSPALRAV GNIVTGDDIQ TQVILNCSAL QSLLHLLSSP KESIKKEACW 370 380 390 400 410 420 TISNITAGNR AQIQTVIDAN IFPALISILQ TAEFRTRKEA AWAITNATSG GSAEQIKYLV 430 440 450 460 470 480 ELGCIKPLCD LLT	MTTPGKENFR	LKSYKNKSLN	PDEMRRREE	EGLQLRKQKR	EEQLFKRRNV	ATAEEETEEE
130	7 <u>0</u>	8 <u>0</u>	9 <u>0</u>	10 <u>0</u>	11 <u>0</u>	12 <u>0</u>
TISNITAGNR AQIQTVIDAN GULLERS CTLQFESAWV LTNIASGNSL QTRIVIQAGA VPIFIELLSS CFEDVARD FOR A QUALTURA STORY COLOR COLO	VMSDGGFHEA	QISNMEMAPG	GVITSDMIEM	IFSKSPEQQL	SATQKFRKLL	SK <mark>EPNPPIDE</mark>
190 200 210 220 230 240 EFEDVQEQAV WALGNIAGDS TMCRDYVLDC NILPPLLQLF SKQNRLTMTR NAVWALSNLC 250 260 270 280 290 300 RGKSPPPEFA KVSPCLNVLS WLLFVSDTDV LADACWALSY LSDGPNDKIQ AVIDAGVCRR 310 320 330 340 350 360 LVELLMHNDY KVVSPALRAV GNIVTGDDIQ TQVILNCSAL QSLLHLLSSP KESIKKEACW 370 380 390 400 410 420 TISNITAGNR AQIQTVIDAN IFPALISILQ TAEFRTRKEA AWAITNATSG GSAEQIKYLV 430 440 450 460 470 480 ELGCIKPLCD LITVMDSKIV QVALNGLENI LRLGEQEAKR NGTGINPYCA LIEEAYGLDK	13 <u>0</u>	14 <u>0</u>	15 <u>0</u>	16 <u>0</u>	17 <u>0</u>	18 <u>0</u>
EFEDVQEQAV WALGNIAGDS TMCRDYVLDC NILPPLLQLF SKQNRLTMTR NAVWALSNLC 250 260 270 280 290 300 RGKSPPPEFA KVSPCLNVLS WLLFVSDTDV LADACWALSY LSDGPNDKIQ AVIDAGVCRR 310 320 330 340 350 360 LVELLMHNDY KVVSPALRAV GNIVTGDDIQ TQVILNCSAL QSLLHLLSSP KESIKKEACW 370 380 390 400 410 420 TISNITAGNR AQIQTVIDAN IFPALISILQ TAEFRTRKEA AWAITNATSG GSAEQIKYLV 430 440 450 460 470 480 ELGCIKPLCD LLTVMDSKIV QVALNGLENI LRLGEQEAKR NGTGINPYCA LIEEAYGLDK	VISTPGVVAR	FVEFLKRKEN	CTLQFESAWV	LTNIASGNSL	QTRIVIQAGA	VPIFIELLSS
250 260 270 280 290 300 RGKSPPPEFA KVSPCLNVLS WLLFVSDTDV LADACWALSY LSDGPNDKIQ AVIDAGVCRR 310 320 330 340 350 360 LVELLMHNDY KVVSPALRAV GNIVTGDDIQ TQVILNCSAL QSLLHLLSSP KESIKKEACW 370 380 390 400 410 420 TISNITAGNR AQIQTVIDAN IFPALISILQ TAEFRTRKEA AWAITNATSG GSAEQIKYLV 430 440 450 460 470 480 ELGCIKPLCD LLTVMDSKIV QVALNGLENI LRLGEQEAKR NGTGINPYCA LIEEAYGLDK 490 500 510 520 530	19 <u>0</u>	20 <u>0</u>	21 <u>0</u>	22 <u>0</u>	23 <u>0</u>	24 <u>0</u>
RGKSPPPEFA KVSPCLNVLS WLLFVSDTDV LADACWALSY LSDGPNDKIQ AVIDAGVCRR 310 320 330 340 350 360 LVELLMHNDY KVVSPALRAV GNIVTGDDIQ TQVILNCSAL QSLLHLLSSP KESIKKEACW 370 380 390 400 410 420 TISNITAGNR AQIQTVIDAN IFPALISILQ TAEFRTRKEA AWAITNATSG GSAEQIKYLV 430 440 450 460 470 480 ELGCIKPLCD LLTVMDSKIV QVALNGLENI LRLGEQEAKR NGTGINPYCA LIEEAYGLDK	EFEDVQEQAV	WALGNIAGDS	TMCRDYVLDC	NILPPLLQLF	SKQNRLTMTR	NAVWALSNLC
310 320 330 340 350 360 LVELLMHNDY KVVSPALRAV GNIVTGDDIQ TQVILNCSAL QSLLHLLSSP KESIKKEACW 370 380 390 400 410 420 TISNITAGNR AQIQTVIDAN IFPALISILQ TAEFRTRKEA AWAITNATSG GSAEQIKYLV 430 440 450 460 470 480 ELGCIKPLCD LLTVMDSKIV QVALNGLENI LRLGEQEAKR NGTGINPYCA LIEEAYGLDK	25 <u>0</u>	26 <u>0</u>	27 <u>0</u>	28 <u>0</u>	29 <u>0</u>	30 <u>0</u>
LVELLMHNDY KVVSPALRAV GNIVTGDDIQ TQVILNCSAL QSLLHLLSSP KESIKKEACW 370 380 390 400 410 420 TISNITAGNR AQIQTVIDAN IFPALISILQ TAEFRTRKEA AWAITNATSG GSAEQIKYLV 430 440 450 460 470 480 ELGCIKPLCD LLTVMDSKIV QVALNGLENI LRLGEQEAKR NGTGINPYCA LIEEAYGLDK	RGKSPPPEFA	KVSPCLNVLS	WLLFVSDTDV	LADACWALSY	LSDGPNDKIQ	AVIDAGVCRR
370 380 390 400 410 420 TISNITAGNR AQIQTVIDAN IFPALISILQ TAEFRTRKEA AWAITNATSG GSAEQIKYLV 430 440 450 460 470 480 ELGCIKPLCD LLTVMDSKIV QVALNGLENI LRLGEQEAKR NGTGINPYCA LIEEAYGLDK	31 <u>0</u>	32 <u>0</u>	33 <u>0</u>	34 <u>0</u>	35 <u>0</u>	36 <u>0</u>
TISNITAGNR AQIQTVIDAN IFPALISILQ TAEFRTRKEA AWAITNATSG GSAEQIKYLV 430 440 450 460 470 480 ELGCIKPLCD LLTVMDSKIV QVALNGLENI LRLGEQEAKR NGTGINPYCA LIEEAYGLDK 490 500 510 520 530	LVELLMHNDY	KVVSPALRAV	GNIVTGDDIQ	TQVILNCSAL	QSLLHLLSSP	KESIKKEACW
430 440 450 460 470 480 ELGCIKPLCD LLTVMDSKIV QVALNGLENI LRLGEQEAKR NGTGINPYCA LIEEAYGLDK 490 500 510 520 530	37 <u>0</u>	38 <u>0</u>	39 <u>0</u>	40 <u>0</u>	41 <u>0</u>	42 <u>0</u>
ELGCIKPLCD LLTVMDSKIV QVALNGLENI LRLGEQEAKR NGTGINPYCA LIEEAYGLDK 490 500 510 520 530	TISNITAGNR	AQIQTVIDAN	IFPALISILQ	TAEFRTRKEA	AWAITNATSG	GSAEQIKYLV
49 <u>0</u> 50 <u>0</u> 51 <u>0</u> 52 <u>0</u> 53 <u>0</u>	43 <u>0</u>	44 <u>0</u>	45 <u>0</u>	46 <u>0</u>	47 <u>0</u>	48 <u>0</u>
	ELGCIKPLCD	LLTVMDSKIV	QVALNGLENI	LRLGEQEAKR	NGTGINPYCA	LIEEAYGLDK
IEFLQSHENQ EIYQKAFDLI EHYFGTEDED SSIAPQVDLN QQQYIFQQCE APMEGFQL	49 <u>0</u>	50 <u>0</u>	51 <u>0</u>	52 <u>0</u>	53 <u>0</u>	
	IEFLQSHENQ	EIYQKAFDLI	EHYFGTEDED	SSIAPQVDLN	QQQYIFQQCE	APMEGFQL

Figure 6.6 (continued)

В

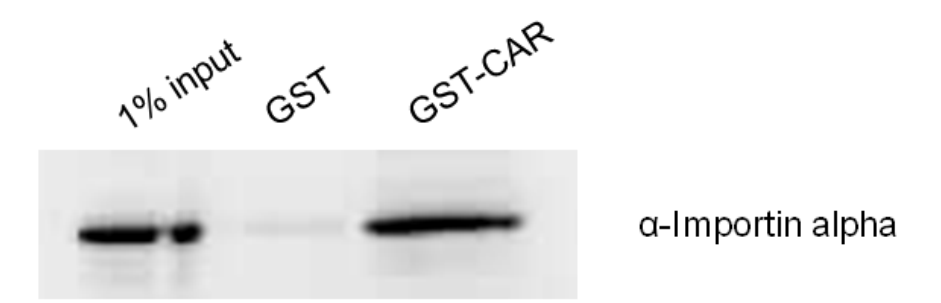


Figure 6.7: CAR ICD is subject to proteasomal degradation. (A) U87 CAR-V5 cells were treated for 16 hours with the proteasome inhibitor epoxomicin (1 μ M or 5 μ M) vs. DMSO vehicle. Shown is a representative Western blot performed using antibody raised against the V5 tag. (B) CTF1 and CTF2 band intensities were quantified from Western blots, and ratios of CTF2/CTF1 were calculated. The graph represents mean CTF2/CTF1 ratios obtained from 3 independent experiments (n=3 per group). One-way ANOVA with Bonferroni post-test, * = p < 0.05. (C) U87 cells transiently expressing V5-tagged CAR ICD were treated overnight with the proteasome inhibitor MG132 (25 μ M) or DMSO vehicle control. Samples were analyzed by Western blotting for GAPDH and the V5 tag. Treatment with MG132 led to an accumulation of CAR ICD levels.

Figure 6.7

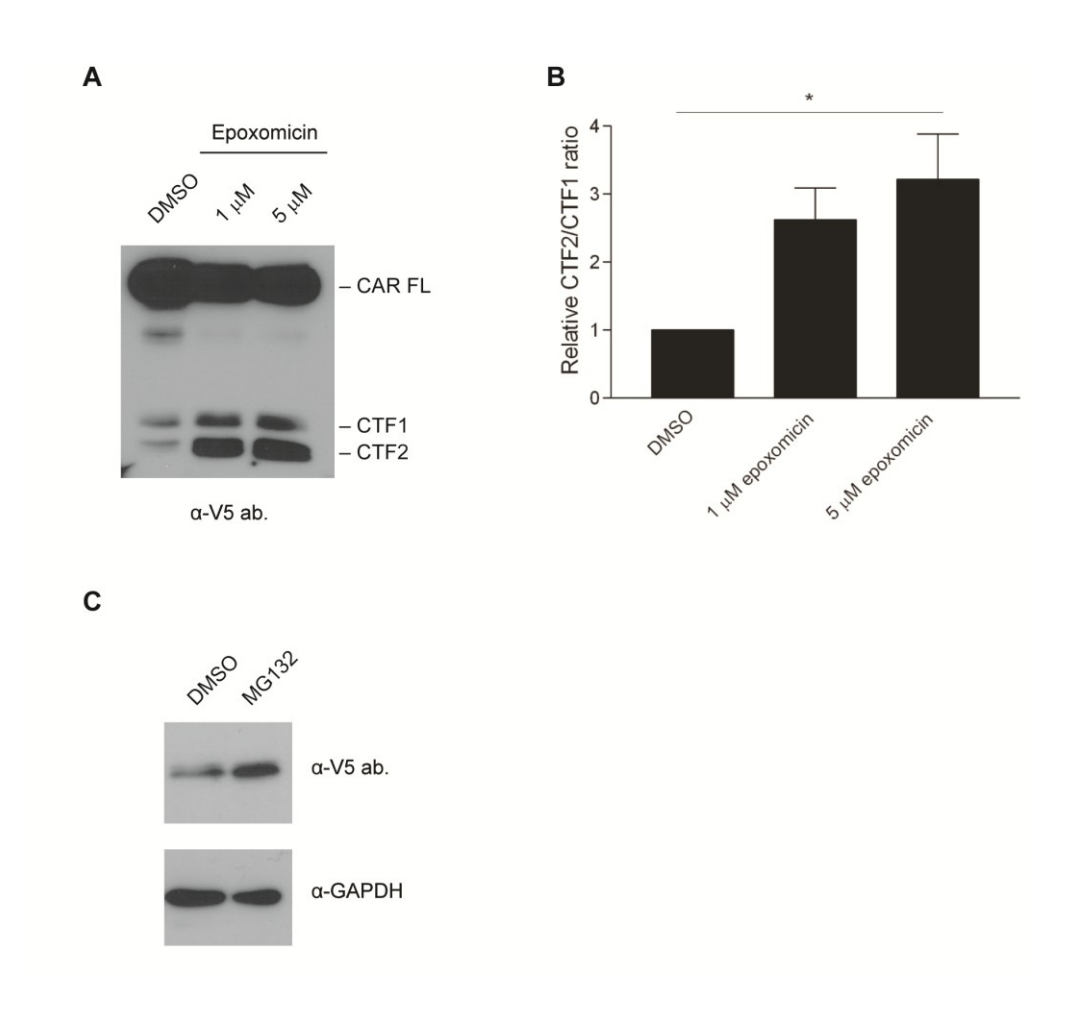
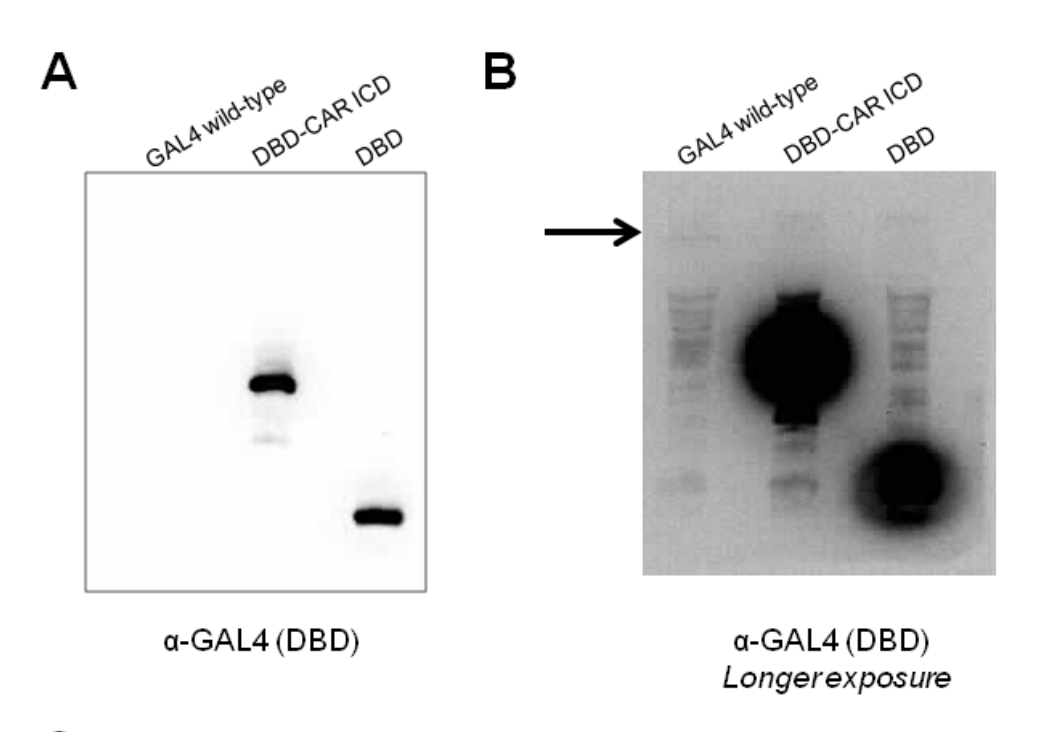


Figure 6.8: CAR ICD fused to GAL4 DNA-binding domain (DBD) does not induce expression of a GAL4-dependent luciferase reporter. U87 cells were transiently transfected with pUAS-luciferase plasmid plus pCMV-GAL4, pCMV-GAL4 DBD or pCMV-GAL4 DBD-CAR ICD plasmid. Western blots performed with an anti-GAL4 DBD antibody are shown in (A) and (B) (where panel (B) is a longer exposure time to visualize full-length GAL4; see arrow). (C) Luciferase reporter assays were performed. As expected, full-length GAL4, which contains a DBD as well as activation domains, robustly induced expression of GAL4-driven luciferase reporter (positive control). GAL4 DBD alone was not sufficient to activate luciferase expression, as expected (negative control). The presence of CAR ICD as a fusion protein with GAL4 DBD did not induce luciferase expression above background levels. The graph shows means from 3 biological triplicates, expressed in relative luminescence units (RLU), from one experiment (One-way ANOVA with Bonferroni's multiple comparison test; *** = p < 0.001). Similar results were obtained from 3 independent experiments.

Figure 6.8



С

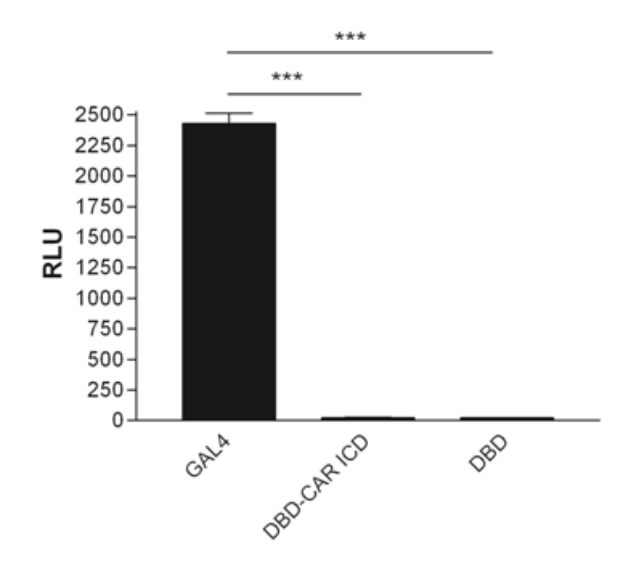
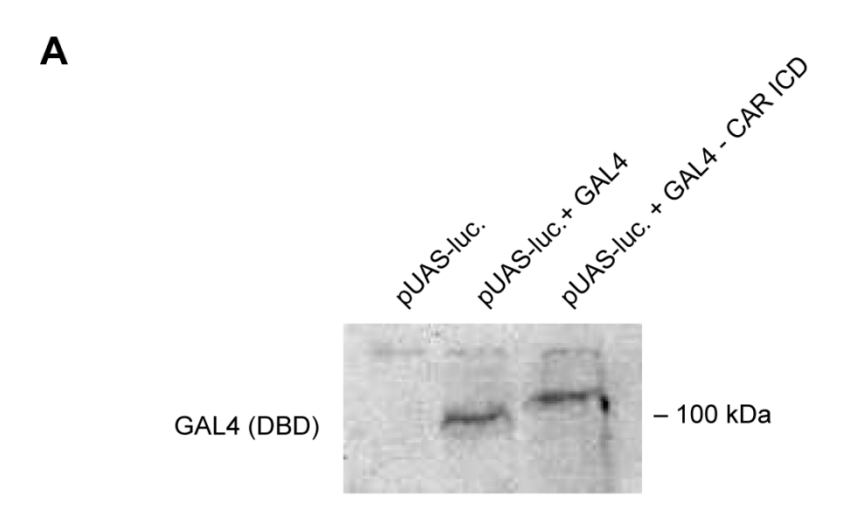


Figure 6.9: CAR ICD inhibits luciferase expression induction by full-length GAL4. U87-MG cells were transiently transfected with pUAS-luciferase plasmid alone, with equal amounts of pUAS-luciferase and pCMV-GAL4 plasmids, or with equal amounts of pUAS-luciferase and pCMV-GAL4-CAR ICD plasmids.

(A) A Western blot for GAL4's DNA-binding domain showing similar expression levels between wild-type GAL4 and the GAL4-CAR ICD fusion protein. (B) Luciferase activity was assayed 24-48 hours post-transfection. The GAL4-CAR ICD fusion protein significantly decreased luciferase reporter activity (by 85.4%) compared to wild-type GAL4. The graph shows means from 3 biological triplicates, expressed in relative luminescence units (RLU), from one experiment (One-way ANOVA with Bonferroni's multiple comparison test; *** = p <0.001). Similar results were obtained from at least 3 independent experiments.

Figure 6.9



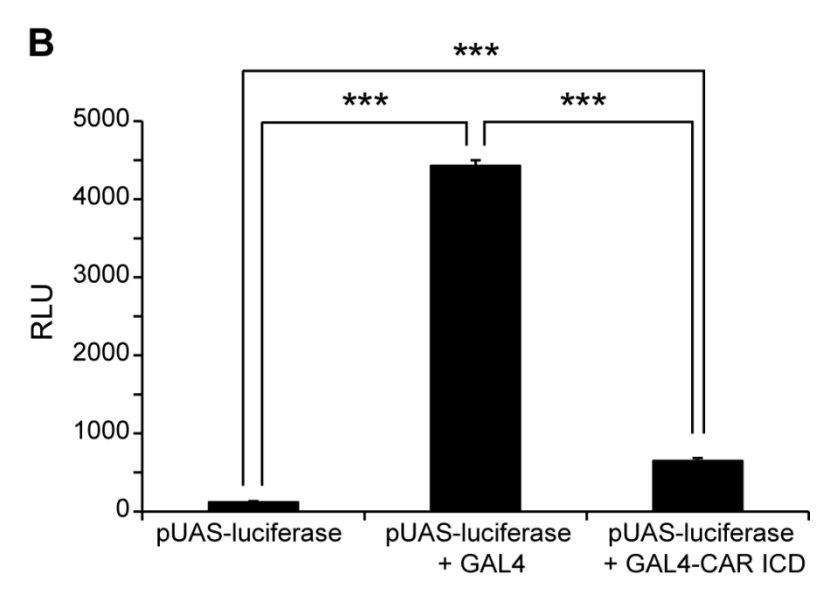


Figure 6.10: Lentiviral-mediated expression of V5-tagged full-length CAR and CAR ICD. U87-MG cells were infected with lentivirus carrying an IRES GFP bicistronic plasmid (pWPI), pWPI with CAR-V5 or pWPI with ICD-V5. Shown are Western blots for (A) GFP and (B) V5 tag.

Figure 6.10

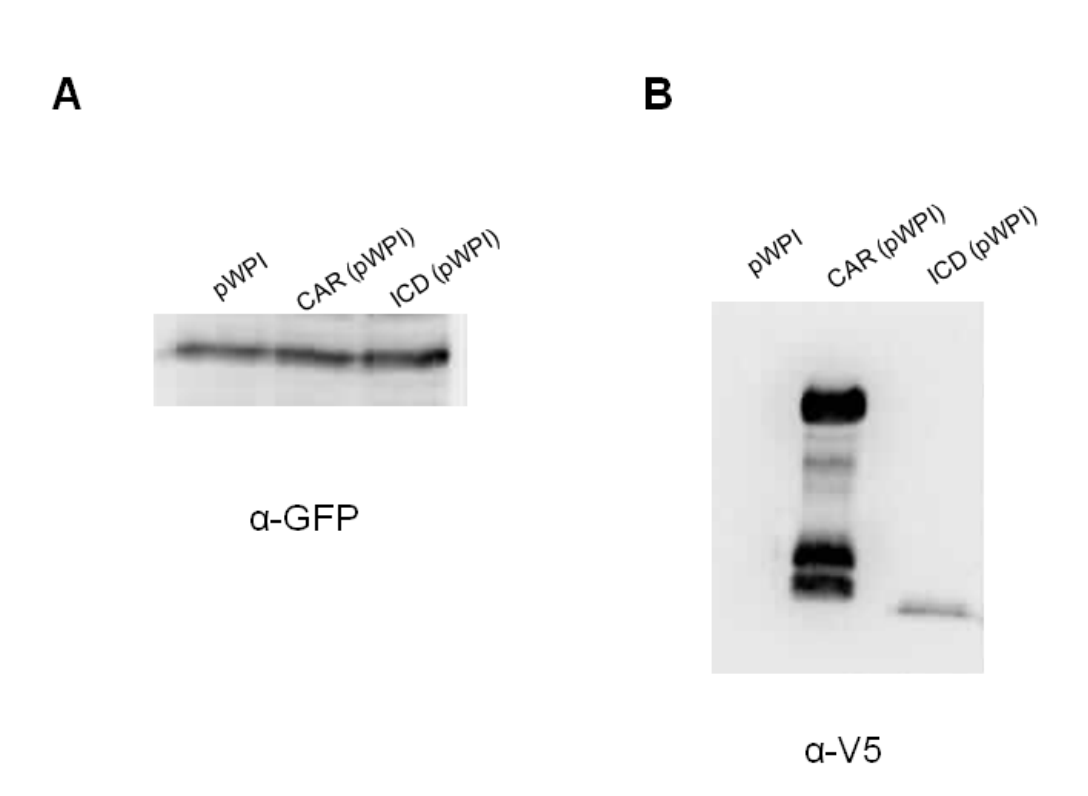
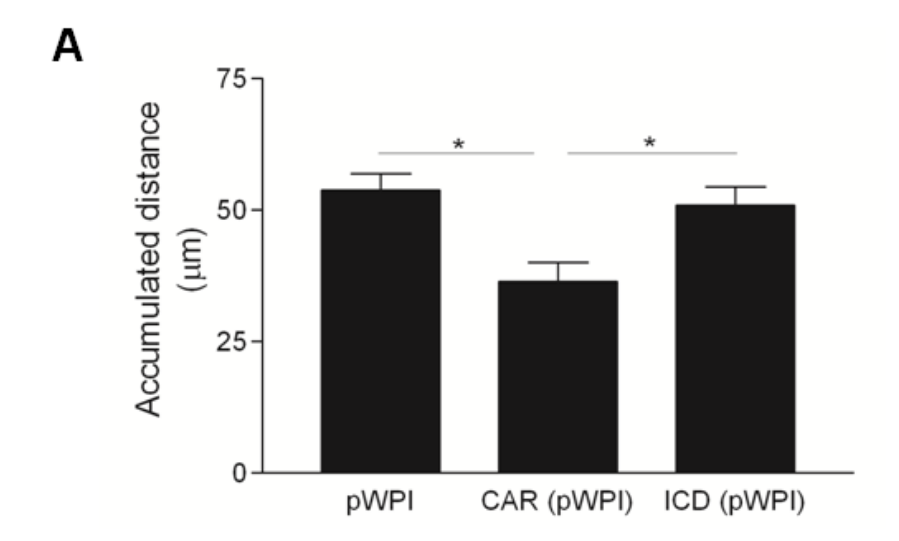
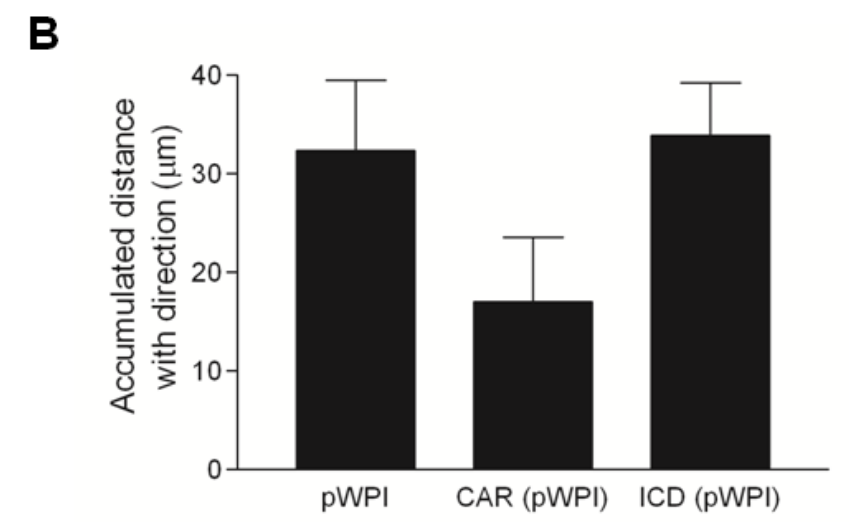


Figure 6.11: BioFlux migration assays comparing U87 cells expressing full-length CAR, CAR ICD or control. Results shown are mean values (in μ m) from 7 independent experiments for (A) accumulated distance, (B) accumulated distance with direction, and (C) Euclidean distance with direction. CAR ICD-expressing glioma cells had significantly greater accumulated distance than glioma cells expressing wild-type CAR, indicating that free ICD does not inhibit glioma migration. One-Way ANOVA with Bonferroni post-test, * = p < 0.05. Mean migration distances for accumulated distance with direction and Euclidean distance with direction were also higher for CAR ICD-expressing cells than for CAR-expressing cells, however these differences were not statistically significant.

Figure 6.11





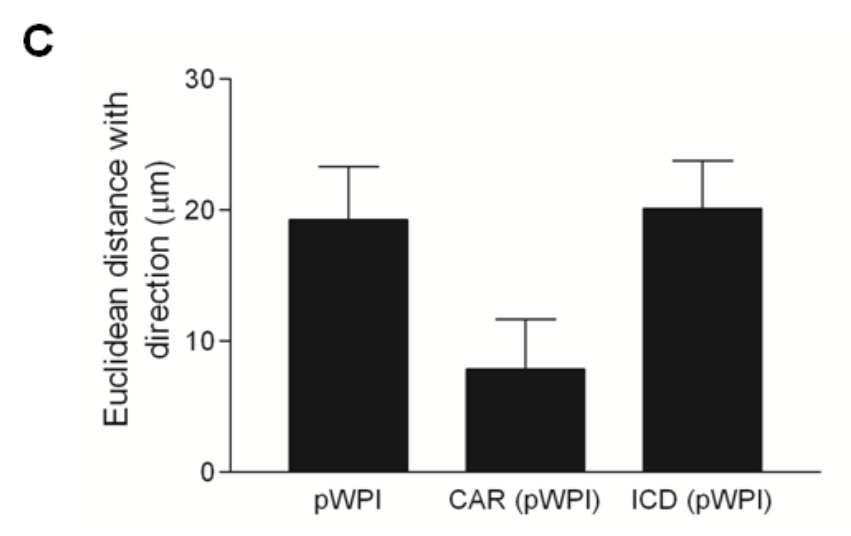
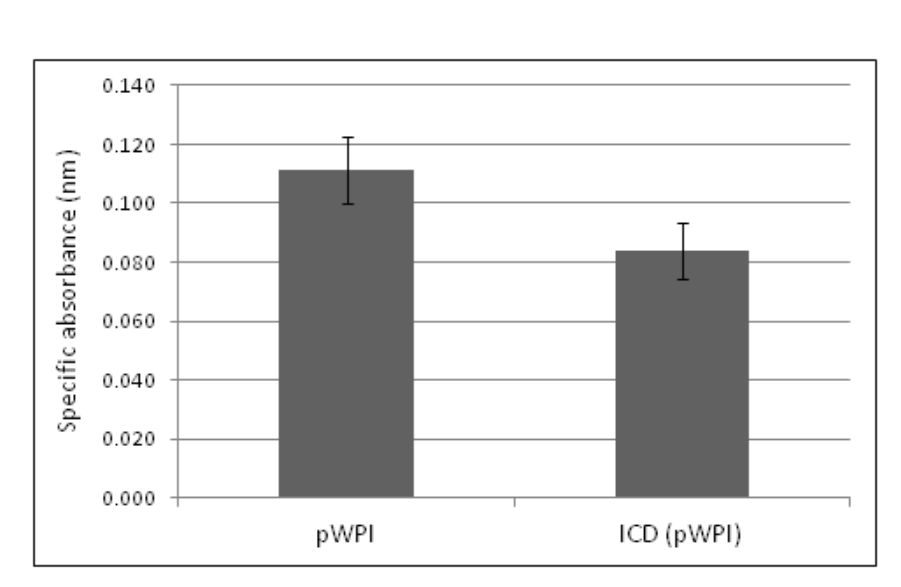


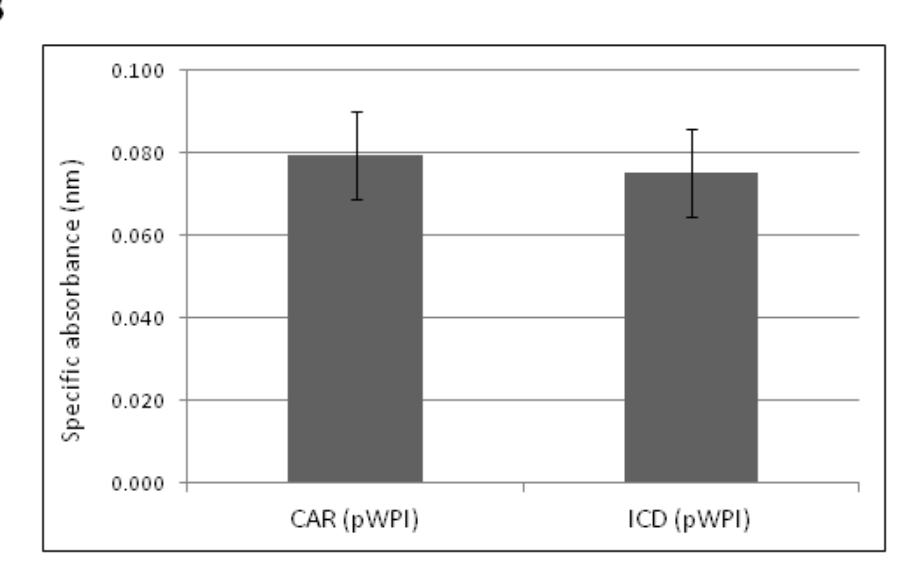
Figure 6.12: XTT cell proliferation assays on U87 cells expressing control pWPI, pWPI-CAR-V5 or pWPI-ICD-V5 constructs. XTT cell proliferation assays were performed on lentivirus-infected cells in parallel to the BioFlux migration experiments in order to determine if any differences observed in glioma migration may be due to changes in cell viability. There were no significant differences in proliferation between (A) pWPI (control) and pWPI-ICD cells, or (B) pWPI-CAR and pWPI-ICD cells. Means shown in each graph are from one independent experiment (n=12 wells per group), and data are representative of at least 3 independent experiments.

Figure 6.12





В



Chapter 7: Discussion

A wide variety of cell surface proteins, including CAMs, shed their ECDs and also undergo RIP (Edwards et al., 2008, Lichtenthaler et al., 2011). In this work, we report that the CAM and virus receptor CAR undergoes these processing events.

CAR ECD sheds from glioma cells ectopically expressing CAR (figure 3.1A) and from developing cortical neurons with endogenous CAR expression (figure 5.1). In addition to constitutive (basal) shedding, CAR ECD shedding is also triggered in a regulated manner via the DAG-PKC pathway using the phorbol ester PMA under pleiotropic conditions (figures 3.1B, 3.3 and 5.2), via increases in intracellular Ca²⁺ using the calcium ionophore ionomycin (figures 3.4 and 5.2), and in the case of neurons, by depolarization using potassium chloride (figure 5.2). As ionomycin may have pleiotropic effects on cells, one possible way to verify the link between calcium and CAR shedding would be to use an intracellular calcium releaser such as Thapsigargin to trigger CAR shedding. Metalloprotease activity is required for CAR shedding, as treatment of U87 CAR cells with the broad-spectrum metalloprotease inhibitors O-phenanthroline, TAPI-1 (Huang, 2008) and GM6001 (figure 3.7) inhibits CAR ECD shedding.

PKC isoforms are important in a wide range of cellular processes including regulation of the cytoskeleton (subsequently affecting cellular migration and

neurite outgrowth), cell-cell interactions and cell polarity (Larsson, 2006, Rosse et al., 2010). Calcium signaling too plays diverse roles in cellular processes, including regulation of neurite outgrowth (Kiryushko et al., 2004, Bolsover, 2005) and promotion of tumorigenesis by regulating migration, invasion and proliferation of cancer cells (Monteith et al., 2012, Chen et al., 2013). CAR is involved in the regulation of cell migration (Huang et al., 2005b, Fok et al., 2007) and neurite outgrowth (Huang, 2008), and also directly interacts with the actin and microtubule cytoskeleton (Fok et al., 2007, Huang et al., 2007). Thus, it is plausible that regulation of its proteolysis by the PKC and calcium signaling pathways may have implications on its role as a cell adhesion molecule in normal cells (including epithelial cells and developing neurons) and cancerous cells such as gliomas.

Shedding of CAR ECD is accompanied by a decrease in levels of full-length receptor on the cell surface (figure 3.2A), and also results in host cells being less susceptible to adenovirus infection (figure 3.2B). Thus, shedding of CAR directly affects its function as a virus receptor.

Interestingly, soluble isoforms of CAR, arising from alternative splicing, have been reported to act as decoys. Soluble isoforms bind to CAR and to coxsackie B3 viruses (CVB3), and addition of the isoform CAR4/7 to culture media inhibits infection of HeLa cells by CVB3 (Dorner et al., 2004). Recombinant CAR ECD binds to CAR and also inhibits infection by CVB3 when added to culture medium

(Dorner et al., 2004, Yanagawa et al., 2004, Goodfellow et al., 2005). Intravenous injection of soluble recombinant CAR ECD into mice infected with CVB3 confers protection against virus-induced myocarditis and pancreatitis (Yanagawa et al., 2004). A 31 kDa soluble fragment of CAR, possibly shed ECD, has been detected from malignant pleural effusions of lung cancer patients, and its removal from media improves adenovirus infection (Bernal et al., 2002). Thus, it is possible that the shedding of CAR ECD may lead to protection of host cells from infection by coxsackieviruses and adenoviruses, but may also interfere with the efficacy of adenovirus-mediated gene therapy.

CAR's cytoplasmic domain is involved in shedding but is not absolutely necessary. Its presence promotes optimal levels of constitutive and PMA-stimulated ECD shedding, as a mutant of CAR lacking the cytoplasmic domain sheds less than the full-length receptor (figures 3.5B and 4.7). This effect is unlikely to be due to differences in expression, as the U87 stable cell lines used in these experiments have similar levels of CAR and truncated (tailless) mutant on the cell surface (Huang et al., 2005b). Unlike for CAR, deletion of the cytoplasmic domain from angiotensin-converting enzyme (ACE) greatly enhances its basal shedding; however, phorbol ester-induced shedding of the truncated ACE mutant is minimal relative to basal levels, suggesting that the cytoplasmic domain is required for optimal phorbol ester-stimulated shedding but not basal shedding of ACE (Chubb et al., 2004). On the other hand, phorbol ester-stimulated shedding of human growth hormone receptor (hGHR) is not dependent on the

presence of its cytoplasmic domain (Amit et al., 2001). Perhaps in the case of CAR, the presence of the cytoplasmic domain provides the best conformation for substrate recognition, or the cytoplasmic domain interacts with yet undetermined adaptor proteins that bring CAR to metalloproteases.

Interestingly, PMA-stimulated shedding, but not constitutive or ionomycininduced shedding, is accompanied by phosphorylation of CAR in its cytoplasmic domain (figure 3.5). This effect is dependent on the PKC pathway (figure 3.3) but not on metalloprotease activity (figure 3.7). Similar to CAR, TNFR is phosphorylated with PMA treatment, and deletion of its cytoplasmic domain somewhat decreases its shedding (Crowe et al., 1993). On the other hand, the cytoplasmic domain of HB-EGF is phosphorylated at Ser207 by treatment with phorbol ester or calcium ionophore, yet mutagenesis studies revealed that phosphorylation is not necessary for shedding of this growth factor, although this mutation inhibited HB-EGF's tumorigenic effect in liver cells injected into nude mice (Wang et al., 2006). It remains to be determined whether or not phosphorylation of CAR's cytoplasmic domain is required for PMA-stimulated ECD shedding, and which residues (tyrosine and/or serine/threonine amino acids) are involved if that is the case. It has been proposed that protein tyrosine kinases phosphorylate proteins that are involved in optimal shedding of substrates, rather than the substrates themselves being required to be phosphorylated for shedding to occur (Hayashida et al., 2010). It may be the case that proteins that interact

with CAR are required to be phosphorylated for optimal CAR ECD shedding, and that phosphorylation of CAR is a non-specific by-effect.

ADAM10 is a sheddase of CAR

The TIMP inhibition profile (Huang, 2008) suggested that ADAM10 was a possible candidate metalloprotease for CAR shedding. Also, ionomycinstimulated shedding is generally mediated by ADAM10 (figure 3.4) (Horiuchi et al., 2007, Le Gall et al., 2009). Furthermore, the results shown in figure 3.8 suggested that the involvement of ADAM17, another well-studied metalloprotease, was unlikely at least in our system. With these pieces of evidence in mind, we chose to focus on ADAM10 as a candidate metalloprotease involved in CAR ECD shedding.

We show that ADAM10 is indeed a sheddase of CAR using a variety of methods: overexpression of wild-type ADAM10 (figure 3.9A), inhibition of ADAM10 activity with prodomain (figures 3.9B and 5.4), shRNA knockdown of ADAM10 (figures 3.10 and 3.11), and rescue of ADAM10 expression in shRNA cell lines (figure 3.12). ADAM10 is involved in constitutive shedding as well as regulated shedding of CAR ECD, with the latter involving treatment of cells with PMA under chronic conditions or with ionomycin (figure 3.11). Thus, CAR shedding is mediated by ADAM10 like for a wide diversity of other substrates, including

APP, Notch, CD44, ErbB2, VE-cadherin, JAM-A, IL-6R, Pcdhy, N-cadherin, L1 and Ephrins (Pruessmeyer and Ludwig, 2009).

Although ADAM10 is clearly a sheddase of CAR in our experimental systems, it is possible that other metalloproteases, whether from the ADAM family or other metzincin families, are also capable of shedding CAR. For example, the cell adhesion molecule L1 is shed by both ADAM10 and ADAM17, although via different stimuli (Maretzky et al., 2005b). The hyaluronan receptor CD44 is shed by ADAM10, ADAM17 (Nagano et al., 2004) and the matrix metalloproteinases MMP-9 (Chetty et al., 2012) and MMP-14 (Kajita et al., 2001). Different proteases mediate ECD shedding of the same substrates in different cell types (Tousseyn et al., 2006, Murphy, 2010), suggesting redundancy in some cases. Thus, CAR shedding could be mediated by metalloproteases other than ADAM10 depending on the cell types and perhaps even the developmental stages assayed.

It is thought that ADAMs do not have consensus recognition sites on substrates, although ADAM10 and ADAM17 seem to have different amino acid preferences in the cleavage sites of their substrates (Caescu et al., 2009). To map the area of ADAM10 cleavage within CAR's ECD, we used a similar strategy as described by other groups (Cheng et al., 2003, Hinkle et al., 2003, Gardiner et al., 2007, Lemieux et al., 2007). A peptide consisting of 20 amino acids of CAR ECD, upstream of the transmembrane domain, was digested with recombinant ADAM10. Mass spectrometry of the digestion products revealed two possible

cleavage sites: between M224 and L225, and between R226 and L227 (figures 3.13 and 3.14A).

The mutant MLRL \rightarrow AAAA stably expressed in HEK293 cells does not shed its ECD into conditioned media (figure 3.16), indicating that amino acids 224-227 are important for CAR ECD shedding. Interestingly, deletion of a larger area consisting of amino acids 221-232 resulted in a mutant that sheds its ECD (figure 3.16), although we had expected this mutant not to shed as it lacks the cleavage area determined from the *in vitro* studies. The effect with the $\Delta 221-232$ mutant may be due to a change in receptor conformation, as the region targeted by deletion contains a cysteine that participates in a disulfide bridge (Jiang and Caffrey, 2007). Perhaps additional sites are exposed by this deletion, allowing cleavage of the $\Delta 221$ -232 mutant by ADAM10 or other proteases. Unlike in HEK 293 cells, the mutants Δ 221-232 and MLRL \rightarrow AAAA are not expressed on the surface of glioma cells at comparable levels to wild-type receptor (figures 3.14) and 3.15), possibly due to differences in post-translational modification or protein folding of these mutants in U87 and U251N cells, precluding the use of these mutant CAR stable cell lines in direct comparison to wild-type CAR-expressing glioma cells.

In polarized epithelial cells, CAR participates in the formation of tight junctions, where its expression is associated with lower cell permeability (Cohen et al., 2001b, Raschperger et al., 2006). It also localizes to cell-cell contacts in non-

polarized epithelial cells (Cohen et al., 2001b). ADAM10 localizes mainly to adherens junctions, and to a limited extent tight junctions, of polarized epithelial cells, and its proper targeting to adherens junctions promotes cell migration in a wound healing assay (Wild-Bode et al., 2006). Perhaps ADAM10 or other metalloproteases can access CAR in tight junctions and promote shedding of its ECD. In this scenario, proteolytic processing of CAR may negatively affect the integrity of epithelial cell tight junctions.

CAR proteolysis and neurite outgrowth

During the development of the nervous system, it is crucial that neurons find their appropriate synaptic targets for proper wiring (Goodman, 1996). This function is performed by growth cones, actin-rich structures on the tips of neuronal extensions, which sense environmental cues (Goodman, 1996). The cues are in the form of contact-mediated attraction, contact-mediated repulsion, chemoattraction and chemorepulsion, and they result in neurite outgrowth and directional guidance (Goodman, 1996). Thus, communication between neurons and other cells (or with the extracellular matrix (ECM)) occurs via direct contact or through long-range, secreted attractive or repulsive cues (Goodman, 1996). Growth cones respond dynamically to the environment using receptors on their surface, resulting in second messenger cascades and regulation of the cytoskeleton, leading to formation or retraction of their lamellipodia and filopodia (Goodman, 1996, Mueller, 1999).

Ig CAMs, including L1, DCC and NCAM, are one group of guidance molecules expressed on growth cones, and generally they mediate contact-dependent, attractive cues although there are exceptions (Goodman, 1996, Walsh and Doherty, 1997). CAR is a relatively novel CAM of the nervous system (Honda et al., 2000), mediating outgrowth of developing neurons via homophilic interactions (Huang, 2008) as well as via heterophilic interactions with ECM proteins such as laminin and fibronectin (Patzke et al., 2010).

ADAM and MMP metalloproteases regulate neurite outgrowth during development (Yang et al., 2006). Treatment of retinal ganglion cells (RGCs) with the hydroxamate-based metalloprotease inhibitors GM6001 and BB-94 leads to mistargeting by RGC axons and their failure to reach the optic tectum (Webber et al., 2002). Pharmacological inhibition of ADAM10 or ADAM17 results in a decrease in outgrowth of neurites from cerebellar microexplants on a substrate of L1 ECD (Maretzky et al., 2005b). Media of COS-7 cells containing ADAM8-cleaved CHL1 ECD stimulate outgrowth of developing cerebellar neurons; this effect was abolished with the metalloprotease inhibitor BB-94 or when COS-7 cells were transfected with ADAMs that do not cleave CHL1 (Naus et al., 2004). Proteolysis of NCAM in hippocampal neurons promotes their outgrowth (Hubschmann et al., 2005, Kalus et al., 2006). However, NCAM proteolysis and addition of soluble NCAM ECD inhibits outgrowth of cortical neurons (Hinkle et

al., 2006, Brennaman and Maness, 2008), suggesting that the effect of metalloproteases on neuronal CAMs could be context-dependent.

Metalloprotease activity is required for neurite outgrowth mediated by CAR ECD, as treatment of cerebellar microexplants with GM6001 significantly decreased neurite outgrowth on a substrate of CAR ECD (figure 5.3). Thus, CAR's function as a neuronal CAM is regulated by metalloproteases (possibly ADAM10; figure 5.4), similarly to L1, NCAM, and others. It may be expected that inhibition of metalloprotease activity would promote the presence of more full-length CAR and consequently, enhanced outgrowth on Fc-CAR substrate as a result of greater adhesiveness. However, substrate-mediated neurite outgrowth likely requires a continuous and dynamic regulation of CAR via metalloprotease-mediated ECD shedding as a mechanism of remodeling cell surface adhesiveness of elongating neurites.

RIP of CAR requires presentlin/y-secretase and occurs after ECD shedding

Using chemical inhibitors and knockout cells (figure 6.1), we show that CAR undergoes RIP by the presenilin/γ-secretase complex. There are over 90 known such substrates (Haapasalo and Kovacs, 2011) and the list keeps growing as more substrates are discovered, especially since many more proteins are known to shed their ECDs.

The intracellular fragments generated upon RIP of substrates may be capable of participating in signaling pathways, such as membrane-to-nucleus signaling, apoptosis, neurite outgrowth, regulation of tight junctions, and cell migration, although the function of many ICDs arising from RIP are unknown (McCarthy et al., 2009, Bajor and Kaczmarek, 2013). Alternatively, RIP may be a mechanism for interrupting signal transduction or for turnover of substrates at the membrane, perhaps by proteasomal degradation (Kopan and Ilagan, 2004, McCarthy et al., 2009).

RIP of CAR occurs after ECD shedding (figure 6.2). Such a step-wise process has been reported for other substrates including L1 (Maretzky et al., 2005b), N-cadherin (Uemura et al., 2006), protein-tyrosine kinase 7 (PTK7) (Na et al., 2012), and the epidermal growth factor-like betacellulin precursor (Stoeck et al., 2010). This sequential process appears to be a general mechanism for γ-secretase substrates. It is thought that removal of the ECD by shedding relieves steric inhibition and allows nicastrin, a member of the γ-secretase complex, to recognize RIP substrates (Shah et al., 2005, Dries et al., 2009) and to promote maturation of the γ-secretase complex (Chavez-Gutierrez et al., 2008, Dries et al., 2009). Furthermore, substrates must have permissive transmembrane and cytoplasmic domains for RIP to occur following ECD shedding (Hemming et al., 2008). Thus, RIP of substrates is tightly controlled by ECD shedding, which in turn is regulated by intracellular signaling pathways or by external cues such as ligand binding. This step-wise process has been described for other classes of I-CLiPs, the SPP

and S2P families, while a fourth class, the rhomboids, do not seem to have this requirement (Dries and Yu, 2009).

CAR ICD enters the nucleus

Some intracellular domain products of γ-secretase cleavage translocate to the nucleus (Haapasalo and Kovacs, 2011, Lichtenthaler et al., 2011). This phenomenon has been described for at least 30 substrates (Haapasalo and Kovacs, 2011) including Notch (Mumm and Kopan, 2000), APP (Pardossi-Piquard and Checler, 2012), and even ADAM10 (Tousseyn et al., 2009).

C-terminal domain immunoreactive speckles of CAR were detected in nuclei of transiently transfected HEK 293 cells (figure 6.3). However, since these speckles were found in a small proportion of CAR-expressing cells (<10%), we overexpressed a construct of CAR consisting of its ICD only and found that it indeed enters the nucleus (figures 6.4 and 6.5). Thus, CAR is a new substrate of γ -secretase cleavage with a product that enters the nucleus.

If γ-secretase cleavage-mediated RIP of CAR occurs readily (figure 6.1), why is it so difficult to detect the product (CAR CTF2) in cell nuclei? One possible explanation may be that CAR CTF2 fragments are subject to rapid proteasomal degradation, as determined from experiments using the proteasome inhibitors epoxomicin and MG132 (figure 6.7). Degradation of RIP-generated ICD

fragments has been reported for other γ -secretase substrates including Notch, syndecan-3, nectin-1 α , p75, DCC and members of the APP family (Walsh et al., 2003, Fryer et al., 2004, Kopan and Ilagan, 2004, Tagami et al., 2008). It has been proposed that not all RIP products participate in signal transduction, and that RIP could lead to proteasomal degradation of ICD products and abrogation of signaling (Kopan and Ilagan, 2004); this may be the case for CAR ICD.

There are at least 2 different species of ICD generated from RIP of Notch-1 receptor with different metabolic stabilities (Tagami et al., 2008). The more stable NICD is the product of cleavage between Gly1743 and Val1744, while the less stable NICD is the product of cleavage between Leu1746 and Ser1747 (Tagami et al., 2008). This observation follows the "N-end degradation rule" which states that proteins with a valine residue at the N-terminus are more stable than those with a N-terminal serine (Gonda et al., 1989), although there are other amino acids that are more destabilizing than serine in eukaryotes (Varshavsky, 1997). It is tempting to speculate that there could be multiple species of CAR CTF2 with different stabilities. Although there are no serines in the transmembrane domain of murine CAR isoform 1 (the isoform employed in our studies), γ-secretase cleavage may predominantly generate CTF2 products that have other destabilizing amino acids at the N-terminus.

Even though epoxomic treatment significantly increases the amount of CAR CTF2 and the ratio of CTF2 to CTF1 as determined by Western blot (figure 6.7A

and B), epoxomicin-treated U87 CAR-V5 stable cells do not have CAR-positive nuclei when assayed by immunofluorescence (data not shown). Perhaps the higher levels of CTF2 that accumulate with epoxomicin treatment are still not enough for detection via immunofluorescence. Nevertheless, ICD products of RIP may still impart cellular effects in the nucleus at expression levels below detection. A Notch NICD construct with N-terminal V1744 significantly induces reporter expression driven by *HES* (a gene target of NICD), yet very small amounts of NICD are sufficient for this effect (Schroeter et al., 1998).

Another possible explanation for the difficulty in visualizing CAR CTF2 in the nucleus may be its retention at the plasma membrane due to palmitoylation. Cysteine palmitoylation of CAR at amino acids 259 and 260 is required for proper cell surface targeting of the receptor (van't Hof and Crystal, 2002). These cysteines are the first two amino acids in CAR's cytoplasmic domain. Since RIP of CAR likely occurs upstream of these residues within the transmembrane domain, perhaps the resulting CTF2 fragments remain tethered to the plasma membrane. As palmitoylation is a dynamic and reversible modification (Iwanaga et al., 2009, Salaun et al., 2010), a fraction of CTF2 fragments could be depalmitoylated and freed from the plasma membrane to enter the nucleus (alternatively, de-palmitoylation of some CAR molecules could occur before γ-secretase cleavage and CTF2 generation).

Based on a proteomics screen performed in our laboratory, a putative interaction between CAR ICD and the classic nuclear import protein importin α (figure 6.6), and a predicted NLS within the ICD of mCAR1 (amino acids 260-269), we expected that CAR ICD would require an NLS for entry into the nucleus. However, lysine to alanine mutations within, or complete deletion of, the predicted NLS sequence resulted in a mutant with expression pattern indistinguishable from non-mutated ICD (data not shown). Unless there is some other NLS within CAR's ICD that is recognized by importin α , it is possible that CAR may not require an NLS to translocate to the nucleus following proteolytic processing. Many small proteins under 40 kDa in molecular weight can enter and exit the nucleus by diffusion and do not require assistance to do so, unlike for larger proteins (Xu et al., 2010). Table 7.1 illustrates this concept for some known ICD products of y-secretase cleavage. In general, smaller molecular weight ICDs are found in both the cytoplasm and nucleus, while relatively large ICDs tend to be predominantly nuclear. For some ICDs, such as Notch (Kopan et al., 1994), the NLS is known.

To investigate the possibility that CAR ICD can induce gene expression, we employed a GAL4-dependent luciferase reporter system. GAL4-dependent reporter assays have been used in previous studies to investigate the effects of γ -secretase cleavage products on gene expression. The intracellular domain of APP fused to GAL4's DBD activates GAL4-dependent luciferase reporter expression, an effect that is greatly enhanced with co-expression of the nuclear adaptor

protein and APP ICD interactor Fe65 (Cao and Sudhof, 2001). Similar observations were reported for the β-amyloid precursor-like protein 1 and 2 (APLP1 and APLP2) (Scheinfeld et al., 2002). Insertion of the GAL4 DBD in between the transmembrane and cytoplasmic domains of full-length DCC produces a γ-secretase cleavage product that induces GAL4-dependent luciferase expression, indicating translocation of DCC ICD to the nucleus (Taniguchi et al., 2003). A kinase domain deletion mutant of the receptor tyrosine kinase ErbB4's ICD activated GAL4-dependent luciferase expression, and this effect is inhibited by the nuclear corepressor and ErbB4 interactor KAP1 (Gilmore-Hebert et al., 2010). GAL4 fusion proteins were used to identify the transactivation domain in Notch1 (Kurooka et al., 1998). Binding of Delta, Serrate, and Lag-2 (DSL) ligands to full-length Notch receptor triggers ECD shedding and RIP of Notch, resulting in NICD converting the CSL corepression complex to a coactivator complex, and the expression of Notch target genes such the HES and HEY families of transcription factors (reviewed in (Mumm and Kopan, 2000)).

A fusion protein of GAL4 DBD and CAR ICD does not induce GAL4-dependent luciferase expression significantly greater than GAL4 DBD alone (figure 6.8). This suggests that CAR ICD may not have an intrinsic gene transactivation property. If CAR ICD is capable of inducing changes in gene expression, it is possible that it requires nuclear partners, such as transcription factors, to do so.

Interestingly, a fusion protein of full-length GAL4 (a considerably large protein at 880 amino acids) and CAR ICD significantly inhibits activation of GAL4-dependent luciferase (figure 6.9). In this context, CAR ICD may be preventing full-length GAL4 from binding to DNA or interacting with the transcription machinery.

It remains to be determined which genes are upregulated and/or downregulated as a result of CAR ICD entry into the nucleus, and whether or not there may be tissue-specific differences. A technical limitation has been the lack of successful production of stable cell lines expressing CAR ICD to be used for microarray analyses. Transient infections with lentivirus carrying the ICD construct (versus control and full-length CAR) is not a suitable approach as it would be difficult to minimize variability between independent experiments. One possible approach could be the use of a tetracycline- or doxycycline-inducible system. It should be kept in mind that overexpression of ICDs to study changes in gene expression may represent pathological, rather than normal, physiology, since the real effects of ICDs could be occurring at small amounts. Ideally, gene expression results would be verified with mutagenesis and knock-out and rescue approaches in both cell culture and animals (Kopan and Ilagan, 2004).

CAR proteolysis and inhibition of glioma migration

MMP and ADAM metalloproteases are involved in the initiation and progression of a wide variety of cancers, participating in angiogenesis, ECM degradation, tumor cell proliferation and evasion of the immune system, loss of cell-cell adhesion, and metastasis (Duffy et al., 2009, Pruessmeyer and Ludwig, 2009, Saftig and Reiss, 2011, Shuman Moss et al., 2012). Various ADAMs are upregulated in cancer, often correlating with poor outcome (Duffy et al., 2009). For example, ADAM10 expression is upregulated in cancers of the stomach, colon, prostate and uterine, in leukemia and in gliomas (Kataoka, 2009, Formolo et al., 2011, Saftig and Reiss, 2011, Mohanan et al., 2013).

In gliomas, ADAMs and MMPs degrade the ECM and basal lamina, promoting the highly invasive properties of these tumor cells, and also regulate growth and chemotactic factors and their receptors, resulting in angiogenesis and tumor growth and survival (Dwyer and Matthews, 2011, Mentlein et al., 2012).

ADAM10 and ADAM17 are overexpressed in glioblastomas as well as in stem-like tumor cell populations, and pharmacological inhibition of ADAM10 and ADAM17 counteracts glioma tumorigenesis (Bulstrode et al., 2012).

Relevant substrates of metalloproteases in cancer progression include HER/EGFR ligands and receptors, TNF-α, the tumor antigens MICA and CD30, and CAMs (Duffy et al., 2009, Kataoka, 2009, Pruessmeyer and Ludwig, 2009). Several CAMs have been reported to participate in tumorigenesis. Cleaved CD44 (heparan sulfate proteoglycan) is found in various cancers including glioma,

breast carcinoma, NSCL carcinoma, ovarian carcinoma and colon carcinoma (Okamoto et al., 2002). Soluble CD44 is a potential tumor marker (Guo et al., 1994), and it is associated with metastasis and poor patient outcome, likely due to decreased cell-cell adhesion (reviewed in (Pruessmeyer and Ludwig, 2009)).

Soluble L1 is highly elevated in ovarian and endometrial cancers (Altevogt and Fogel, 2004), and it stimulates cell migration via $\alpha v \beta 5$ integrin (Mechtersheimer et al., 2001). L1 shedding promotes glioma cell migration and invasion, possibly via L1 ECD binding to integrins, activation of focal adhesion kinase (FAK) and turnover of focal complexes (Yang et al., 2011).

Processing of N-cadherin is elevated in glioblastomas compared to normal astrocytes, and inhibition of N-cadherin shedding leads to decreased tumor cell migration (Kohutek et al., 2009). On the other hand, proteolysis of E-cadherin or loss of E-cadherin expression generally promote tumorigenesis (reviewed in (Reiss et al., 2006a)).

We wondered if CAR ECD shedding plays a role in its function as a suppressor of glioma migration. If so, then inhibition or stimulation of shedding would be expected to change the behavior of CAR-expressing U87-MG cells. Treatment of U87 CAR cells with GM6001 or with PMA have no effect on the migration and invasion of U87 CAR cells (figures 4.2 and 4.3).

The ECD mutants are not expressed on the surface of glioma cells as well as the wild-type receptor (figure 3.15). Given that the deletion mutant $\Delta 221$ -232 sheds its ECD (figure 3.14), we reasoned that comparing $\Delta 221$ -232 to the shedding-defective mutant MLRL \rightarrow AAAA would be helpful in determining whether or not soluble CAR ECD has an effect on cell migration, possibly via heterophilic interactions. However, there is no difference in migration between the mutant glioma cell lines (figures 4.4 and 4.6).

Although the presence of the cytoplasmic domain results in optimal levels of ECD shedding, the tailless CAR mutant nevertheless does shed its ECD to a certain extent (figure 4.7). In both cell culture and animal models, glioma cells expressing the tailless mutant migrate and invade similarly to control cells and significantly more than CAR-expressing cells (Huang et al., 2005b, Fok et al., 2007). Taken together, these data indicate that the presence of CAR cytoplasmic domain is required for CAR-mediated inhibition of glioma, and that soluble CAR ECD may not be participating in this process.

Interestingly, overexpression of free CAR ICD is not sufficient to inhibit migration of U87-MG glioma cells (figure 6.11). This suggests that mere presence of the cytoplasmic domain is not enough for glioma inhibition, and that it is required to be tethered to the plasma membrane. As CAR's cytoplasmic domain interacts directly with the cytoskeleton (Fok et al., 2007, Huang et al., 2007), it is possible that free ICD, generated upon RIP of CAR, may not be able to bind to

and stabilize the cytoskeleton. Thus, while ECD shedding itself does not appear to participate in regulation of CAR-mediated glioma inhibition, proteolysis would ultimately abolish CAR's effect. However, as CAR's role within cancers is context-dependent and sometimes confounding, the effect of proteolysis should be examined on a case-by-case basis.

Conclusion

The characterization of proteolytic processing of CAR presented in this work promotes our understanding of this fascinating cell adhesion molecule and virus receptor. We demonstrate that these processing events regulate some of CAR's known functions in normal physiology and pathophysiology. Thus, examining the effects of ECD shedding and RIP within the context of other known CAR functions is warranted. Future studies will "shed" more light on whether or not other metalloproteases act on CAR, what the site(s) of γ-secretase-mediated cleavage are, and whether or not the ICD produced upon RIP of CAR can participate in signal transduction.

Table 7.1: Molecular weight of the ICDs of some proteins known to undergo γ -secretase-mediated RIP. Generally, ICDs with molecular weights > 50 kDa are located mostly or exclusively in the nucleus, while relatively small ICDs have a mixed distribution.

Table 7.1: ICD molecular weights and cellular distribution

Origin of ICD	ICD molecular weight (kDa)	Cellular distribution of ICD as visualized by immunofluorescence microscopy	Reference
Robo-1	100	Predominantly nuclear	(Seki et al., 2010)
Notch receptors 1-4	70-80	Predominantly nuclear	(Kopan et al., 1994, Saxena et al., 2001)
Leukocyte- common antigen- related (LAR) receptor tyrosine phosphatase	70	Predominantly nuclear	(Haapasalo et al., 2007)
Receptor protein tyrosine phosphatase (RPTP) κ	70	Nuclear	(Anders et al., 2006)
Ire1 β	60	Predominantly nuclear	(Niwa et al., 1999)
Insulin receptor tyrosine kinase	47	Predominantly nuclear	(Kasuga et al., 2007)
Ephrin receptor (EphA4)	40	Cytoplasmic and nuclear	(Inoue et al., 2009)
Growth hormone receptor	< 40	Cytoplasmic; accumulates in nucleus when proteasome inhibitors are used	(Cowan et al., 2005)
EpCAM	26	Cytoplasmic and nuclear	(Maetzel et al., 2009)
Alcadein α1	25	Predominantly cytoplasmic when overexpressed alone; predominantly nuclear when co-expressed with Fe65	(Araki et al., 2004)
Receptor for advanced glycation endproducts (RAGE)	12	Cytoplasmic and nuclear	(Galichet et al., 2008)
Syndecan-3	7-10	Cytoplasmic and nuclear	(Schulz et al., 2003)
APP	6	Cytoplasmic and nuclear when overexpressed alone; increased number of nuclear speckles when co-expressed with Fe65	(Konietzko et al., 2010)

References

Adlerz L, Holback S, Multhaup G, Iverfeldt K (2007) IGF-1-induced processing of the amyloid precursor protein family is mediated by different signaling pathways. The Journal of biological chemistry 282:10203-10209.

Altevogt P, Fogel M (2004) The role of L1 in the progression of ovarian carcinomas. Zentralblatt fur Gynakologie 126:323-325.

Amit T, Amit T, Hochberg Z, Yogev-Falach M, Youdim MB, Youdim MB, Barkey RJ (2001) Shedding of growth hormone-binding protein is inhibited by hydroxamic acid-based protease inhibitors: proposed mechanism of activation of growth hormone-binding protein secretase. The Journal of endocrinology 169:397-407.

Anders L, Mertins P, Lammich S, Murgia M, Hartmann D, Saftig P, Haass C, Ullrich A (2006) Furin-, ADAM 10-, and gamma-secretase-mediated cleavage of a receptor tyrosine phosphatase and regulation of beta-catenin's transcriptional activity. Molecular and cellular biology 26:3917-3934.

Anders M, Christian C, McMahon M, McCormick F, Korn WM (2003) Inhibition of the Raf/MEK/ERK pathway up-regulates expression of the coxsackievirus and adenovirus receptor in cancer cells. Cancer research 63:2088-2095.

Anders M, Vieth M, Rocken C, Ebert M, Pross M, Gretschel S, Schlag PM, Wiedenmann B, Kemmner W, Hocker M (2009) Loss of the coxsackie and adenovirus receptor contributes to gastric cancer progression. British journal of cancer 100:352-359.

Araki Y, Miyagi N, Kato N, Yoshida T, Wada S, Nishimura M, Komano H, Yamamoto T, De Strooper B, Yamamoto K, Suzuki T (2004) Coordinated metabolism of Alcadein and amyloid beta-protein precursor regulates FE65-dependent gene transactivation. The Journal of biological chemistry 279:24343-24354.

Arribas J, Borroto A (2002) Protein ectodomain shedding. Chemical reviews 102:4627-4638.

Asaoka K, Tada M, Sawamura Y, Ikeda J, Abe H (2000) Dependence of efficient adenoviral gene delivery in malignant glioma cells on the expression levels of the Coxsackievirus and adenovirus receptor. Journal of neurosurgery 92:1002-1008.

Asher DR, Cerny AM, Weiler SR, Horner JW, Keeler ML, Neptune MA, Jones SN, Bronson RT, Depinho RA, Finberg RW (2005) Coxsackievirus and adenovirus receptor is essential for cardiomyocyte development. Genesis 42:77-85.

Auer D, Reimer D, Porto V, Fleischer M, Roessler J, Wiedemair A, Marth C, Muller-Holzner E, Daxenbichler G, Zeimet AG (2009) Expression of coxsackie-adenovirus receptor is related to estrogen sensitivity in breast cancer. Breast cancer research and treatment 116:103-111.

Bajor M, Kaczmarek L (2013) Proteolytic remodeling of the synaptic cell adhesion molecules (CAMs) by metzincins in synaptic plasticity. Neurochemical research 38:1113-1121.

Beel AJ, Sanders CR (2008) Substrate specificity of gamma-secretase and other intramembrane proteases. Cellular and molecular life sciences: CMLS 65:1311-1334.

Benilova I, Karran E, De Strooper B (2012) The toxic Abeta oligomer and Alzheimer's disease: an emperor in need of clothes. Nature neuroscience 15:349-357.

Bergelson JM (1999) Receptors mediating adenovirus attachment and internalization. Biochemical pharmacology 57:975-979.

Bergelson JM, Cunningham JA, Droguett G, Kurt-Jones EA, Krithivas A, Hong JS, Horwitz MS, Crowell RL, Finberg RW (1997) Isolation of a common receptor for Coxsackie B viruses and adenoviruses 2 and 5. Science 275:1320-1323.

Bergelson JM, Krithivas A, Celi L, Droguett G, Horwitz MS, Wickham T, Crowell RL, Finberg RW (1998) The murine CAR homolog is a receptor for coxsackie B viruses and adenoviruses. Journal of virology 72:415-419.

Bernal RM, Sharma S, Gardner BK, Douglas JT, Bergelson JM, Dubinett SM, Batra RK (2002) Soluble coxsackievirus adenovirus receptor is a putative

inhibitor of adenoviral gene transfer in the tumor milieu. Clinical cancer research : an official journal of the American Association for Cancer Research 8:1915-1923.

Bewley MC, Springer K, Zhang YB, Freimuth P, Flanagan JM (1999) Structural analysis of the mechanism of adenovirus binding to its human cellular receptor, CAR. Science 286:1579-1583.

Black RA, Rauch CT, Kozlosky CJ, Peschon JJ, Slack JL, Wolfson MF, Castner BJ, Stocking KL, Reddy P, Srinivasan S, Nelson N, Boiani N, Schooley KA, Gerhart M, Davis R, Fitzner JN, Johnson RS, Paxton RJ, March CJ, Cerretti DP (1997) A metalloproteinase disintegrin that releases tumour-necrosis factor-alpha from cells. Nature 385:729-733.

Blobel CP (2005) ADAMs: key components in EGFR signalling and development. Nature reviews Molecular cell biology 6:32-43.

Boissy P, Lenhard TR, Kirkegaard T, Peschon JJ, Black RA, Delaisse JM, del Carmen Ovejero M (2003) An assessment of ADAMs in bone cells: absence of TACE activity prevents osteoclast recruitment and the formation of the marrow cavity in developing long bones. FEBS Lett 553:257-261.

Bolsover SR (2005) Calcium signalling in growth cone migration. Cell calcium 37:395-402.

Bowles KR, Gibson J, Wu J, Shaffer LG, Towbin JA, Bowles NE (1999) Genomic organization and chromosomal localization of the human Coxsackievirus B-adenovirus receptor gene. Human genetics 105:354-359.

Bozkulak EC, Weinmaster G (2009) Selective use of ADAM10 and ADAM17 in activation of Notch1 signaling. Molecular and cellular biology 29:5679-5695.

Brennaman LH, Maness PF (2008) Developmental regulation of GABAergic interneuron branching and synaptic development in the prefrontal cortex by soluble neural cell adhesion molecule. Molecular and cellular neurosciences 37:781-793.

Brew K, Nagase H (2010) The tissue inhibitors of metalloproteinases (TIMPs): an ancient family with structural and functional diversity. Biochimica et biophysica acta 1803:55-71.

Bruning A, Runnebaum IB (2003) CAR is a cell-cell adhesion protein in human cancer cells and is expressionally modulated by dexamethasone, TNFalpha, and TGFbeta. Gene therapy 10:198-205.

Bruning A, Runnebaum IB (2004) The coxsackie adenovirus receptor inhibits cancer cell migration. Experimental cell research 298:624-631.

Bruning A, Stickeler E, Diederich D, Walz L, Rohleder H, Friese K, Runnebaum IB (2005) Coxsackie and adenovirus receptor promotes adenocarcinoma cell survival and is expressionally activated after transition from preneoplastic precursor lesions to invasive adenocarcinomas. Clinical cancer research: an official journal of the American Association for Cancer Research 11:4316-4320.

Bulstrode H, Jones LM, Siney EJ, Sampson JM, Ludwig A, Gray WP, Willaime-Morawek S (2012) A-Disintegrin and Metalloprotease (ADAM) 10 and 17 promote self-renewal of brain tumor sphere forming cells. Cancer letters 326:79-87.

Caccamo A, Oddo S, Billings LM, Green KN, Martinez-Coria H, Fisher A, LaFerla FM (2006) M1 receptors play a central role in modulating AD-like pathology in transgenic mice. Neuron 49:671-682.

Caescu CI, Jeschke GR, Turk BE (2009) Active-site determinants of substrate recognition by the metalloproteinases TACE and ADAM10. The Biochemical journal 424:79-88.

Cal S, Freije JM, Lopez JM, Takada Y, Lopez-Otin C (2000) ADAM 23/MDC3, a human disintegrin that promotes cell adhesion via interaction with the alphavbeta3 integrin through an RGD-independent mechanism. Mol Biol Cell 11:1457-1469.

Cao X, Sudhof TC (2001) A transcriptionally [correction of transcriptively] active complex of APP with Fe65 and histone acetyltransferase Tip60. Science 293:115-120.

Carey RM, Blusztajn JK, Slack BE (2011) Surface expression and limited proteolysis of ADAM10 are increased by a dominant negative inhibitor of dynamin. BMC cell biology 12:20.

Carson SD (2001) Receptor for the group B coxsackieviruses and adenoviruses: CAR. Reviews in medical virology 11:219-226.

Carson SD, Chapman NN, Tracy SM (1997) Purification of the putative coxsackievirus B receptor from HeLa cells. Biochem Biophys Res Commun 233:325-328.

Carvajal-Gonzalez JM, Gravotta D, Mattera R, Diaz F, Perez Bay A, Roman AC, Schreiner RP, Thuenauer R, Bonifacino JS, Rodriguez-Boulan E (2012) Basolateral sorting of the coxsackie and adenovirus receptor through interaction of a canonical YXXPhi motif with the clathrin adaptors AP-1A and AP-1B. Proc Natl Acad Sci U S A 109:3820-3825.

Castagna M, Takai Y, Kaibuchi K, Sano K, Kikkawa U, Nishizuka Y (1982) Direct activation of calcium-activated, phospholipid-dependent protein kinase by tumor-promoting phorbol esters. The Journal of biological chemistry 257:7847-7851.

Cavallaro U, Dejana E (2011) Adhesion molecule signalling: not always a sticky business. Nature reviews Molecular cell biology 12:189-197.

Chavez-Gutierrez L, Tolia A, Maes E, Li T, Wong PC, de Strooper B (2008) Glu(332) in the Nicastrin ectodomain is essential for gamma-secretase complex maturation but not for its activity. The Journal of biological chemistry 283:20096-20105.

Chen JW, Zhou B, Yu QC, Shin SJ, Jiao K, Schneider MD, Baldwin HS, Bergelson JM (2006) Cardiomyocyte-specific deletion of the coxsackievirus and adenovirus receptor results in hyperplasia of the embryonic left ventricle and abnormalities of sinuatrial valves. Circ Res 98:923-930.

Chen YF, Chen YT, Chiu WT, Shen MR (2013) Remodeling of calcium signaling in tumor progression. Journal of biomedical science 20:23.

Cheng QC, Tikhomirov O, Zhou W, Carpenter G (2003) Ectodomain cleavage of ErbB-4: characterization of the cleavage site and m80 fragment. The Journal of biological chemistry 278:38421-38427.

Chetty C, Vanamala SK, Gondi CS, Dinh DH, Gujrati M, Rao JS (2012) MMP-9 induces CD44 cleavage and CD44 mediated cell migration in glioblastoma xenograft cells. Cellular signalling 24:549-559.

Cho C (2012) Testicular and epididymal ADAMs: expression and function during fertilization. Nature reviews Urology 9:550-560.

Chretien I, Marcuz A, Courtet M, Katevuo K, Vainio O, Heath JK, White SJ, Du Pasquier L (1998) CTX, a Xenopus thymocyte receptor, defines a molecular family conserved throughout vertebrates. European journal of immunology 28:4094-4104.

Chubb AJ, Schwager SL, van der Merwe E, Ehlers MR, Sturrock ED (2004) Deletion of the cytoplasmic domain increases basal shedding of angiotensin-converting enzyme. Biochem Biophys Res Commun 314:971-975.

Clark MJ, Homer N, O'Connor BD, Chen Z, Eskin A, Lee H, Merriman B, Nelson SF (2010) U87MG decoded: the genomic sequence of a cytogenetically aberrant human cancer cell line. PLoS genetics 6:e1000832.

Cohen CJ, Gaetz J, Ohman T, Bergelson JM (2001a) Multiple regions within the coxsackievirus and adenovirus receptor cytoplasmic domain are required for basolateral sorting. The Journal of biological chemistry 276:25392-25398.

Cohen CJ, Shieh JT, Pickles RJ, Okegawa T, Hsieh JT, Bergelson JM (2001b) The coxsackievirus and adenovirus receptor is a transmembrane component of the tight junction. Proc Natl Acad Sci U S A 98:15191-15196.

Cowan JW, Wang X, Guan R, He K, Jiang J, Baumann G, Black RA, Wolfe MS, Frank SJ (2005) Growth hormone receptor is a target for presentilin-dependent gamma-secretase cleavage. The Journal of biological chemistry 280:19331-19342.

Coyne CB, Bergelson JM (2006) Virus-induced Abl and Fyn kinase signals permit coxsackievirus entry through epithelial tight junctions. Cell 124:119-131.

Coyne CB, Voelker T, Pichla SL, Bergelson JM (2004) The coxsackievirus and adenovirus receptor interacts with the multi-PDZ domain protein-1 (MUPP-1) within the tight junction. The Journal of biological chemistry 279:48079-48084.

Crowe PD, VanArsdale TL, Goodwin RG, Ware CF (1993) Specific induction of 80-kDa tumor necrosis factor receptor shedding in T lymphocytes involves the cytoplasmic domain and phosphorylation. Journal of immunology 151:6882-6890.

De Strooper B, Annaert W, Cupers P, Saftig P, Craessaerts K, Mumm JS, Schroeter EH, Schrijvers V, Wolfe MS, Ray WJ, Goate A, Kopan R (1999) A presenilin-1-dependent gamma-secretase-like protease mediates release of Notch intracellular domain. Nature 398:518-522.

De Strooper B, Saftig P, Craessaerts K, Vanderstichele H, Guhde G, Annaert W, Von Figura K, Van Leuven F (1998) Deficiency of presenilin-1 inhibits the normal cleavage of amyloid precursor protein. Nature 391:387-390.

Dello Sbarba P, Rovida E (2002) Transmodulation of cell surface regulatory molecules via ectodomain shedding. Biological chemistry 383:69-83.

Dho SE, Jacob S, Wolting CD, French MB, Rohrschneider LR, McGlade CJ (1998) The mammalian numb phosphotyrosine-binding domain. Characterization of binding specificity and identification of a novel PDZ domain-containing numb binding protein, LNX. The Journal of biological chemistry 273:9179-9187.

Diaz-Rodriguez E, Montero JC, Esparis-Ogando A, Yuste L, Pandiella A (2002) Extracellular signal-regulated kinase phosphorylates tumor necrosis factor alphaconverting enzyme at threonine 735: a potential role in regulated shedding. Mol Biol Cell 13:2031-2044.

Dorner A, Xiong D, Couch K, Yajima T, Knowlton KU (2004) Alternatively spliced soluble coxsackie-adenovirus receptors inhibit coxsackievirus infection. The Journal of biological chemistry 279:18497-18503.

Dorner AA, Wegmann F, Butz S, Wolburg-Buchholz K, Wolburg H, Mack A, Nasdala I, August B, Westermann J, Rathjen FG, Vestweber D (2005) Coxsackievirus-adenovirus receptor (CAR) is essential for early embryonic cardiac development. Journal of cell science 118:3509-3521.

Dries DR, Shah S, Han YH, Yu C, Yu S, Shearman MS, Yu G (2009) Glu-333 of nicastrin directly participates in gamma-secretase activity. The Journal of biological chemistry 284:29714-29724.

Dries DR, Yu G (2009) Rip exposed: how ectodomain shedding regulates the proteolytic processing of transmembrane substrates. Proc Natl Acad Sci U S A 106:14737-14738.

Duffy MJ, McKiernan E, O'Donovan N, McGowan PM (2009) Role of ADAMs in cancer formation and progression. Clinical cancer research: an official journal of the American Association for Cancer Research 15:1140-1144.

Dwyer CA, Matthews RT (2011) The Neural Extracellular Matrix, Cell Adhesion Molecules and Proteolysis in Glioma Invasion and Tumorigenicity.

Edwards DR, Handsley MM, Pennington CJ (2008) The ADAM metalloproteinases. Molecular aspects of medicine 29:258-289.

Esch FS, Keim PS, Beattie EC, Blacher RW, Culwell AR, Oltersdorf T, McClure D, Ward PJ (1990) Cleavage of amyloid beta peptide during constitutive processing of its precursor. Science 248:1122-1124.

Esler WP, Kimberly WT, Ostaszewski BL, Diehl TS, Moore CL, Tsai JY, Rahmati T, Xia W, Selkoe DJ, Wolfe MS (2000) Transition-state analogue inhibitors of gamma-secretase bind directly to presenilin-1. Nature cell biology 2:428-434.

Excoffon KJ, Gansemer N, Traver G, Zabner J (2007) Functional effects of coxsackievirus and adenovirus receptor glycosylation on homophilic adhesion and adenoviral infection. Journal of virology 81:5573-5578.

Excoffon KJ, Gansemer ND, Mobily ME, Karp PH, Parekh KR, Zabner J (2010) Isoform-specific regulation and localization of the coxsackie and adenovirus receptor in human airway epithelia. PLoS One 5:e9909.

Excoffon KJ, Hruska-Hageman A, Klotz M, Traver GL, Zabner J (2004) A role for the PDZ-binding domain of the coxsackie B virus and adenovirus receptor (CAR) in cell adhesion and growth. Journal of cell science 117:4401-4409.

Excoffon KJ, Kolawole AO, Kusama N, Gansemer ND, Sharma P, Hruska-Hageman AM, Petroff E, Benson CJ (2012) Coxsackievirus and adenovirus receptor (CAR) mediates trafficking of acid sensing ion channel 3 (ASIC3) via PSD-95. Biochem Biophys Res Commun 425:13-18.

Excoffon KJ, Traver GL, Zabner J (2005) The role of the extracellular domain in the biology of the coxsackievirus and adenovirus receptor. American journal of respiratory cell and molecular biology 32:498-503.

Fanning AS, Mitic LL, Anderson JM (1999) Transmembrane proteins in the tight junction barrier. Journal of the American Society of Nephrology: JASN 10:1337-1345.

Fechner H, Haack A, Wang H, Wang X, Eizema K, Pauschinger M, Schoemaker R, Veghel R, Houtsmuller A, Schultheiss HP, Lamers J, Poller W (1999) Expression of coxsackie adenovirus receptor and alphav-integrin does not correlate with adenovector targeting in vivo indicating anatomical vector barriers. Gene therapy 6:1520-1535.

Fischer OM, Hart S, Gschwind A, Ullrich A (2003) EGFR signal transactivation in cancer cells. Biochemical Society transactions 31:1203-1208.

Fok PT, Huang KC, Holland PC, Nalbantoglu J (2007) The Coxsackie and adenovirus receptor binds microtubules and plays a role in cell migration. The Journal of biological chemistry 282:7512-7521.

Formolo CA, Williams R, Gordish-Dressman H, MacDonald TJ, Lee NH, Hathout Y (2011) Secretome signature of invasive glioblastoma multiforme. Journal of proteome research 10:3149-3159.

Freimuth P, Springer K, Berard C, Hainfeld J, Bewley M, Flanagan J (1999) Coxsackievirus and adenovirus receptor amino-terminal immunoglobulin V-related domain binds adenovirus type 2 and fiber knob from adenovirus type 12. Journal of virology 73:1392-1398.

Fryer CJ, White JB, Jones KA (2004) Mastermind recruits CycC:CDK8 to phosphorylate the Notch ICD and coordinate activation with turnover. Molecular cell 16:509-520.

Fuxe J, Liu L, Malin S, Philipson L, Collins VP, Pettersson RF (2003) Expression of the coxsackie and adenovirus receptor in human astrocytic tumors and xenografts. International journal of cancer 103:723-729.

Galichet A, Weibel M, Heizmann CW (2008) Calcium-regulated intramembrane proteolysis of the RAGE receptor. Biochem Biophys Res Commun 370:1-5.

Gardiner EE, Karunakaran D, Shen Y, Arthur JF, Andrews RK, Berndt MC (2007) Controlled shedding of platelet glycoprotein (GP)VI and GPIb-IX-V by ADAM family metalloproteinases. Journal of thrombosis and haemostasis: JTH 5:1530-1537.

Gaultier A, Cousin H, Darribere T, Alfandari D (2002) ADAM13 disintegrin and cysteine-rich domains bind to the second heparin-binding domain of fibronectin. The Journal of biological chemistry 277:23336-23344.

Gilmore-Hebert M, Ramabhadran R, Stern DF (2010) Interactions of ErbB4 and Kap1 connect the growth factor and DNA damage response pathways. Molecular cancer research: MCR 8:1388-1398.

Giniger E, Varnum SM, Ptashne M (1985) Specific DNA binding of GAL4, a positive regulatory protein of yeast. Cell 40:767-774.

Ginsberg HS (1996) The ups and downs of adenovirus vectors. Bulletin of the New York Academy of Medicine 73:53-58.

Gonda DK, Bachmair A, Wunning I, Tobias JW, Lane WS, Varshavsky A (1989) Universality and structure of the N-end rule. The Journal of biological chemistry 264:16700-16712.

Goodfellow IG, Evans DJ, Blom AM, Kerrigan D, Miners JS, Morgan BP, Spiller OB (2005) Inhibition of coxsackie B virus infection by soluble forms of its receptors: binding affinities, altered particle formation, and competition with cellular receptors. Journal of virology 79:12016-12024.

Goodman CS (1996) Mechanisms and molecules that control growth cone guidance. Annual review of neuroscience 19:341-377.

Groot AJ, Vooijs MA (2012) The role of Adams in Notch signaling. Advances in experimental medicine and biology 727:15-36.

Guarente L, Yocum RR, Gifford P (1982) A GAL10-CYC1 hybrid yeast promoter identifies the GAL4 regulatory region as an upstream site. Proc Natl Acad Sci U S A 79:7410-7414.

Guo YJ, Liu G, Wang X, Jin D, Wu M, Ma J, Sy MS (1994) Potential use of soluble CD44 in serum as indicator of tumor burden and metastasis in patients with gastric or colon cancer. Cancer research 54:422-426.

Guo YL, Bai R, Chen CX, Liu DQ, Liu Y, Zhang CY, Zen K (2009) Role of junctional adhesion molecule-like protein in mediating monocyte transendothelial migration. Arterioscler Thromb Vasc Biol 29:75-83.

Haapasalo A, Kim DY, Carey BW, Turunen MK, Pettingell WH, Kovacs DM (2007) Presenilin/gamma-secretase-mediated cleavage regulates association of leukocyte-common antigen-related (LAR) receptor tyrosine phosphatase with beta-catenin. The Journal of biological chemistry 282:9063-9072.

Haapasalo A, Kovacs DM (2011) The many substrates of presenilin/gamma-secretase. Journal of Alzheimer's disease: JAD 25:3-28.

Hartmann D, de Strooper B, Serneels L, Craessaerts K, Herreman A, Annaert W, Umans L, Lubke T, Lena Illert A, von Figura K, Saftig P (2002) The disintegrin/metalloprotease ADAM 10 is essential for Notch signalling but not for alpha-secretase activity in fibroblasts. Human molecular genetics 11:2615-2624.

Hayashida K, Bartlett AH, Chen Y, Park PW (2010) Molecular and cellular mechanisms of ectodomain shedding. Anatomical record 293:925-937.

He Y, Chipman PR, Howitt J, Bator CM, Whitt MA, Baker TS, Kuhn RJ, Anderson CW, Freimuth P, Rossmann MG (2001) Interaction of coxsackievirus B3 with the full length coxsackievirus-adenovirus receptor. Nature structural biology 8:874-878.

Hemming ML, Elias JE, Gygi SP, Selkoe DJ (2008) Proteomic profiling of gamma-secretase substrates and mapping of substrate requirements. PLoS biology 6:e257.

Herreman A, Hartmann D, Annaert W, Saftig P, Craessaerts K, Serneels L, Umans L, Schrijvers V, Checler F, Vanderstichele H, Baekelandt V, Dressel R, Cupers P, Huylebroeck D, Zwijsen A, Van Leuven F, De Strooper B (1999) Presenilin 2 deficiency causes a mild pulmonary phenotype and no changes in amyloid precursor protein processing but enhances the embryonic lethal phenotype of presenilin 1 deficiency. Proc Natl Acad Sci U S A 96:11872-11877.

Herreman A, Van Gassen G, Bentahir M, Nyabi O, Craessaerts K, Mueller U, Annaert W, De Strooper B (2003) gamma-Secretase activity requires the presenilin-dependent trafficking of nicastrin through the Golgi apparatus but not its complex glycosylation. Journal of cell science 116:1127-1136.

Hinkle CL, Diestel S, Lieberman J, Maness PF (2006) Metalloprotease-induced ectodomain shedding of neural cell adhesion molecule (NCAM). Journal of neurobiology 66:1378-1395.

Hinkle CL, Mohan MJ, Lin P, Yeung N, Rasmussen F, Milla ME, Moss ML (2003) Multiple metalloproteinases process protransforming growth factor-alpha (proTGF-alpha). Biochemistry 42:2127-2136.

Honda T, Saitoh H, Masuko M, Katagiri-Abe T, Tominaga K, Kozakai I, Kobayashi K, Kumanishi T, Watanabe YG, Odani S, Kuwano R (2000) The coxsackievirus-adenovirus receptor protein as a cell adhesion molecule in the developing mouse brain. Brain research 77:19-28.

Horiuchi K, Kimura T, Miyamoto T, Miyamoto K, Akiyama H, Takaishi H, Morioka H, Nakamura T, Okada Y, Blobel CP, Toyama Y (2009) Conditional inactivation of TACE by a Sox9 promoter leads to osteoporosis and increased granulopoiesis via dysregulation of IL-17 and G-CSF. Journal of immunology 182:2093-2101.

Horiuchi K, Le Gall S, Schulte M, Yamaguchi T, Reiss K, Murphy G, Toyama Y, Hartmann D, Saftig P, Blobel CP (2007) Substrate selectivity of epidermal growth factor-receptor ligand sheddases and their regulation by phorbol esters and calcium influx. Mol Biol Cell 18:176-188.

Horiuchi K, Weskamp G, Lum L, Hammes HP, Cai H, Brodie TA, Ludwig T, Chiusaroli R, Baron R, Preissner KT, Manova K, Blobel CP (2003) Potential role for ADAM15 in pathological neovascularization in mice. Molecular and cellular biology 23:5614-5624.

Hotta Y, Honda T, Naito M, Kuwano R (2003) Developmental distribution of coxsackie virus and adenovirus receptor localized in the nervous system. Brain research Developmental brain research 143:1-13.

Huang J, Bridges LC, White JM (2005a) Selective modulation of integrinmediated cell migration by distinct ADAM family members. Mol Biol Cell 16:4982-4991. Huang K-C (2008) The secret life of a novel cell adhesion molecule CAR: the Coxsackie and Adenovirus Receptor in neuronal development. p 242 leaves.

Huang KC, Altinoz M, Wosik K, Larochelle N, Koty Z, Zhu L, Holland PC, Nalbantoglu J (2005b) Impact of the coxsackie and adenovirus receptor (CAR) on glioma cell growth and invasion: requirement for the C-terminal domain. International journal of cancer 113:738-745.

Huang KC, Yasruel Z, Guerin C, Holland PC, Nalbantoglu J (2007) Interaction of the Coxsackie and adenovirus receptor (CAR) with the cytoskeleton: binding to actin. FEBS Lett 581:2702-2708.

Hubschmann MV, Skladchikova G, Bock E, Berezin V (2005) Neural cell adhesion molecule function is regulated by metalloproteinase-mediated ectodomain release. Journal of neuroscience research 80:826-837.

Huovila AP, Turner AJ, Pelto-Huikko M, Karkkainen I, Ortiz RM (2005) Shedding light on ADAM metalloproteinases. Trends in biochemical sciences 30:413-422.

Iba K, Albrechtsen R, Gilpin B, Frohlich C, Loechel F, Zolkiewska A, Ishiguro K, Kojima T, Liu W, Langford JK, Sanderson RD, Brakebusch C, Fassler R, Wewer UM (2000) The cysteine-rich domain of human ADAM 12 supports cell adhesion through syndecans and triggers signaling events that lead to beta1 integrindependent cell spreading. The Journal of cell biology 149:1143-1156.

Inoue E, Deguchi-Tawarada M, Togawa A, Matsui C, Arita K, Katahira-Tayama S, Sato T, Yamauchi E, Oda Y, Takai Y (2009) Synaptic activity prompts gamma-secretase-mediated cleavage of EphA4 and dendritic spine formation. The Journal of cell biology 185:551-564.

Ito M, Kodama M, Masuko M, Yamaura M, Fuse K, Uesugi Y, Hirono S, Okura Y, Kato K, Hotta Y, Honda T, Kuwano R, Aizawa Y (2000) Expression of coxsackievirus and adenovirus receptor in hearts of rats with experimental autoimmune myocarditis. Circ Res 86:275-280.

Iwanaga T, Tsutsumi R, Noritake J, Fukata Y, Fukata M (2009) Dynamic protein palmitoylation in cellular signaling. Progress in lipid research 48:117-127.

Jiang S, Caffrey M (2007) Solution structure of the coxsackievirus and adenovirus receptor domain 2. Protein science: a publication of the Protein Society 16:539-542.

Jorissen E, De Strooper B (2010) Gamma-secretase and the intramembrane proteolysis of Notch. Current topics in developmental biology 92:201-230.

Jorissen E, Prox J, Bernreuther C, Weber S, Schwanbeck R, Serneels L, Snellinx A, Craessaerts K, Thathiah A, Tesseur I, Bartsch U, Weskamp G, Blobel CP, Glatzel M, De Strooper B, Saftig P (2010) The disintegrin/metalloproteinase ADAM10 is essential for the establishment of the brain cortex. J Neurosci 30:4833-4844.

Kajita M, Itoh Y, Chiba T, Mori H, Okada A, Kinoh H, Seiki M (2001) Membrane-type 1 matrix metalloproteinase cleaves CD44 and promotes cell migration. The Journal of cell biology 153:893-904.

Kakidani H, Ptashne M (1988) GAL4 activates gene expression in mammalian cells. Cell 52:161-167.

Kalus I, Bormann U, Mzoughi M, Schachner M, Kleene R (2006) Proteolytic cleavage of the neural cell adhesion molecule by ADAM17/TACE is involved in neurite outgrowth. J Neurochem 98:78-88.

Kang Q, Cao Y, Zolkiewska A (2000) Metalloprotease-disintegrin ADAM 12 binds to the SH3 domain of Src and activates Src tyrosine kinase in C2C12 cells. The Biochemical journal 352 Pt 3:883-892.

Kang Q, Cao Y, Zolkiewska A (2001) Direct interaction between the cytoplasmic tail of ADAM 12 and the Src homology 3 domain of p85alpha activates phosphatidylinositol 3-kinase in C2C12 cells. The Journal of biological chemistry 276:24466-24472.

Kashimura T, Kodama M, Hotta Y, Hosoya J, Yoshida K, Ozawa T, Watanabe R, Okura Y, Kato K, Hanawa H, Kuwano R, Aizawa Y (2004) Spatiotemporal changes of coxsackievirus and adenovirus receptor in rat hearts during postnatal development and in cultured cardiomyocytes of neonatal rat. Virchows Archiv: an international journal of pathology 444:283-292.

Kasuga K, Kaneko H, Nishizawa M, Onodera O, Ikeuchi T (2007) Generation of intracellular domain of insulin receptor tyrosine kinase by gamma-secretase. Biochem Biophys Res Commun 360:90-96.

Kataoka H (2009) EGFR ligands and their signaling scissors, ADAMs, as new molecular targets for anticancer treatments. Journal of dermatological science 56:148-153.

Kirby I, Davison E, Beavil AJ, Soh CP, Wickham TJ, Roelvink PW, Kovesdi I, Sutton BJ, Santis G (2000) Identification of contact residues and definition of the CAR-binding site of adenovirus type 5 fiber protein. Journal of virology 74:2804-2813.

Kiryushko D, Berezin V, Bock E (2004) Regulators of neurite outgrowth: role of cell adhesion molecules. Annals of the New York Academy of Sciences 1014:140-154.

Kleino I, Ortiz RM, Yritys M, Huovila AP, Saksela K (2009) Alternative splicing of ADAM15 regulates its interactions with cellular SH3 proteins. Journal of cellular biochemistry 108:877-885.

Kohutek ZA, diPierro CG, Redpath GT, Hussaini IM (2009) ADAM-10-mediated N-cadherin cleavage is protein kinase C-alpha dependent and promotes glioblastoma cell migration. J Neurosci 29:4605-4615.

Kolawole AO, Sharma P, Yan R, Lewis KJ, Xu Z, Hostetler HA, Ashbourne Excoffon KJ (2012) The PDZ1 and PDZ3 domains of MAGI-1 regulate the eight-exon isoform of the coxsackievirus and adenovirus receptor. Journal of virology 86:9244-9254.

Konietzko U, Goodger ZV, Meyer M, Kohli BM, Bosset J, Lahiri DK, Nitsch RM (2010) Co-localization of the amyloid precursor protein and Notch intracellular domains in nuclear transcription factories. Neurobiology of aging 31:58-73.

Kopan R (2012) Notch signaling. Cold Spring Harbor perspectives in biology 4.

Kopan R, Ilagan MX (2004) Gamma-secretase: proteasome of the membrane? Nature reviews Molecular cell biology 5:499-504.

Kopan R, Ilagan MX (2009) The canonical Notch signaling pathway: unfolding the activation mechanism. Cell 137:216-233.

Kopan R, Nye JS, Weintraub H (1994) The intracellular domain of mouse Notch: a constitutively activated repressor of myogenesis directed at the basic helix-loophelix region of MyoD. Development 120:2385-2396.

Korn WM, Macal M, Christian C, Lacher MD, McMillan A, Rauen KA, Warren RS, Ferrell L (2006) Expression of the coxsackievirus- and adenovirus receptor in gastrointestinal cancer correlates with tumor differentiation. Cancer gene therapy 13:792-797.

Kosugi S, Hasebe M, Tomita M, Yanagawa H (2009) Systematic identification of cell cycle-dependent yeast nucleocytoplasmic shuttling proteins by prediction of composite motifs. Proc Natl Acad Sci U S A 106:10171-10176.

Kuhn PH, Wang H, Dislich B, Colombo A, Zeitschel U, Ellwart JW, Kremmer E, Rossner S, Lichtenthaler SF (2010) ADAM10 is the physiologically relevant, constitutive alpha-secretase of the amyloid precursor protein in primary neurons. The EMBO journal 29:3020-3032.

Kurohara K, Komatsu K, Kurisaki T, Masuda A, Irie N, Asano M, Sudo K, Nabeshima Y, Iwakura Y, Sehara-Fujisawa A (2004) Essential roles of Meltrin beta (ADAM19) in heart development. Developmental biology 267:14-28.

Kurooka H, Kuroda K, Honjo T (1998) Roles of the ankyrin repeats and C-terminal region of the mouse notch1 intracellular region. Nucleic acids research 26:5448-5455.

Kuster K, Koschel A, Rohwer N, Fischer A, Wiedenmann B, Anders M (2010) Downregulation of the coxsackie and adenovirus receptor in cancer cells by hypoxia depends on HIF-1alpha. Cancer gene therapy 17:141-146.

Larsson C (2006) Protein kinase C and the regulation of the actin cytoskeleton. Cellular signalling 18:276-284.

Le Gall SM, Bobe P, Reiss K, Horiuchi K, Niu XD, Lundell D, Gibb DR, Conrad D, Saftig P, Blobel CP (2009) ADAMs 10 and 17 represent differentially regulated components of a general shedding machinery for membrane proteins

such as transforming growth factor alpha, L-selectin, and tumor necrosis factor alpha. Mol Biol Cell 20:1785-1794.

Lemieux GA, Blumenkron F, Yeung N, Zhou P, Williams J, Grammer AC, Petrovich R, Lipsky PE, Moss ML, Werb Z (2007) The low affinity IgE receptor (CD23) is cleaved by the metalloproteinase ADAM10. The Journal of biological chemistry 282:14836-14844.

Leon RP, Hedlund T, Meech SJ, Li S, Schaack J, Hunger SP, Duke RC, DeGregori J (1998) Adenoviral-mediated gene transfer in lymphocytes. Proc Natl Acad Sci U S A 95:13159-13164.

Li N, Boyd K, Dempsey PJ, Vignali DA (2007a) Non-cell autonomous expression of TNF-alpha-converting enzyme ADAM17 is required for normal lymphocyte development. Journal of immunology 178:4214-4221.

Li X, Perez L, Pan Z, Fan H (2007b) The transmembrane domain of TACE regulates protein ectodomain shedding. Cell research 17:985-998.

Li Y, Pong RC, Bergelson JM, Hall MC, Sagalowsky AI, Tseng CP, Wang Z, Hsieh JT (1999) Loss of adenoviral receptor expression in human bladder cancer cells: a potential impact on the efficacy of gene therapy. Cancer research 59:325-330.

Li YM, Xu M, Lai MT, Huang Q, Castro JL, DiMuzio-Mower J, Harrison T, Lellis C, Nadin A, Neduvelil JG, Register RB, Sardana MK, Shearman MS, Smith AL, Shi XP, Yin KC, Shafer JA, Gardell SJ (2000) Photoactivated gammasecretase inhibitors directed to the active site covalently label presenilin 1. Nature 405:689-694.

Lichtenthaler SF, Haass C, Steiner H (2011) Regulated intramembrane proteolysis--lessons from amyloid precursor protein processing. J Neurochem 117:779-796.

Lie PP, Cheng CY, Mruk DD (2010) Crosstalk between desmoglein-2/desmocollin-2/Src kinase and coxsackie and adenovirus receptor/ZO-1 protein complexes, regulates blood-testis barrier dynamics. The international journal of biochemistry & cell biology 42:975-986.

Lim BK, Xiong D, Dorner A, Youn TJ, Yung A, Liu TI, Gu Y, Dalton ND, Wright AT, Evans SM, Chen J, Peterson KL, McCulloch AD, Yajima T, Knowlton KU (2008) Coxsackievirus and adenovirus receptor (CAR) mediates atrioventricular-node function and connexin 45 localization in the murine heart. J Clin Invest 118:2758-2770.

Lisewski U, Shi Y, Wrackmeyer U, Fischer R, Chen C, Schirdewan A, Juttner R, Rathjen F, Poller W, Radke MH, Gotthardt M (2008) The tight junction protein CAR regulates cardiac conduction and cell-cell communication. J Exp Med 205:2369-2379.

Loechel F, Fox JW, Murphy G, Albrechtsen R, Wewer UM (2000) ADAM 12-S cleaves IGFBP-3 and IGFBP-5 and is inhibited by TIMP-3. Biochem Biophys Res Commun 278:511-515.

Logeat F, Bessia C, Brou C, LeBail O, Jarriault S, Seidah NG, Israel A (1998) The Notch1 receptor is cleaved constitutively by a furin-like convertase. Proc Natl Acad Sci U S A 95:8108-8112.

Lonberg-Holm K, Crowell RL, Philipson L (1976) Unrelated animal viruses share receptors. Nature 259:679-681.

Lorenzen I, Trad A, Grotzinger J (2011) Multimerisation of A disintegrin and metalloprotease protein-17 (ADAM17) is mediated by its EGF-like domain. Biochem Biophys Res Commun 415:330-336.

Lortat-Jacob H, Chouin E, Cusack S, van Raaij MJ (2001) Kinetic analysis of adenovirus fiber binding to its receptor reveals an avidity mechanism for trimeric receptor-ligand interactions. The Journal of biological chemistry 276:9009-9015.

Ludwig A, Hundhausen C, Lambert MH, Broadway N, Andrews RC, Bickett DM, Leesnitzer MA, Becherer JD (2005) Metalloproteinase inhibitors for the disintegrin-like metalloproteinases ADAM10 and ADAM17 that differentially block constitutive and phorbol ester-inducible shedding of cell surface molecules. Combinatorial chemistry & high throughput screening 8:161-171.

Luo WJ, Wang H, Li H, Kim BS, Shah S, Lee HJ, Thinakaran G, Kim TW, Yu G, Xu H (2003) PEN-2 and APH-1 coordinately regulate proteolytic processing of presenilin 1. The Journal of biological chemistry 278:7850-7854.

Lynch JP, 3rd, Fishbein M, Echavarria M (2011) Adenovirus. Seminars in respiratory and critical care medicine 32:494-511.

Macleod AS, Havran WL (2011) Functions of skin-resident gammadelta T cells. Cellular and molecular life sciences: CMLS 68:2399-2408.

Maetzel D, Denzel S, Mack B, Canis M, Went P, Benk M, Kieu C, Papior P, Baeuerle PA, Munz M, Gires O (2009) Nuclear signalling by tumour-associated antigen EpCAM. Nature cell biology 11:162-171.

Marambaud P, Wen PH, Dutt A, Shioi J, Takashima A, Siman R, Robakis NK (2003) A CBP binding transcriptional repressor produced by the PS1/epsilon-cleavage of N-cadherin is inhibited by PS1 FAD mutations. Cell 114:635-645.

Marcello E, Gardoni F, Mauceri D, Romorini S, Jeromin A, Epis R, Borroni B, Cattabeni F, Sala C, Padovani A, Di Luca M (2007) Synapse-associated protein-97 mediates alpha-secretase ADAM10 trafficking and promotes its activity. J Neurosci 27:1682-1691.

Maretzky T, Reiss K, Ludwig A, Buchholz J, Scholz F, Proksch E, de Strooper B, Hartmann D, Saftig P (2005a) ADAM10 mediates E-cadherin shedding and regulates epithelial cell-cell adhesion, migration, and beta-catenin translocation. Proc Natl Acad Sci U S A 102:9182-9187.

Maretzky T, Schulte M, Ludwig A, Rose-John S, Blobel C, Hartmann D, Altevogt P, Saftig P, Reiss K (2005b) L1 is sequentially processed by two differently activated metalloproteases and presenilin/gamma-secretase and regulates neural cell adhesion, cell migration, and neurite outgrowth. Molecular and cellular biology 25:9040-9053.

Martin TA, Watkins G, Jiang WG (2005) The Coxsackie-adenovirus receptor has elevated expression in human breast cancer. Clinical and experimental medicine 5:122-128.

Martino TA, Petric M, Weingartl H, Bergelson JM, Opavsky MA, Richardson CD, Modlin JF, Finberg RW, Kain KC, Willis N, Gauntt CJ, Liu PP (2000) The coxsackie-adenovirus receptor (CAR) is used by reference strains and clinical isolates representing all six serotypes of coxsackievirus group B and by swine vesicular disease virus. Virology 271:99-108.

Matsumoto K, Shariat SF, Ayala GE, Rauen KA, Lerner SP (2005) Loss of coxsackie and adenovirus receptor expression is associated with features of aggressive bladder cancer. Urology 66:441-446.

McCarthy JV, Twomey C, Wujek P (2009) Presenilin-dependent regulated intramembrane proteolysis and gamma-secretase activity. Cellular and molecular life sciences: CMLS 66:1534-1555.

Mechtersheimer S, Gutwein P, Agmon-Levin N, Stoeck A, Oleszewski M, Riedle S, Postina R, Fahrenholz F, Fogel M, Lemmon V, Altevogt P (2001) Ectodomain shedding of L1 adhesion molecule promotes cell migration by autocrine binding to integrins. The Journal of cell biology 155:661-673.

Mentlein R, Hattermann K, Held-Feindt J (2012) Lost in disruption: role of proteases in glioma invasion and progression. Biochimica et biophysica acta 1825:178-185.

Mirza M, Hreinsson J, Strand ML, Hovatta O, Soder O, Philipson L, Pettersson RF, Sollerbrant K (2006) Coxsackievirus and adenovirus receptor (CAR) is expressed in male germ cells and forms a complex with the differentiation factor JAM-C in mouse testis. Experimental cell research 312:817-830.

Mirza M, Pang MF, Zaini MA, Haiko P, Tammela T, Alitalo K, Philipson L, Fuxe J, Sollerbrant K (2012) Essential role of the coxsackie- and adenovirus receptor (CAR) in development of the lymphatic system in mice. PLoS One 7:e37523.

Mirza M, Petersen C, Nordqvist K, Sollerbrant K (2007) Coxsackievirus and adenovirus receptor is up-regulated in migratory germ cells during passage of the blood-testis barrier. Endocrinology 148:5459-5469.

Mirza M, Raschperger E, Philipson L, Pettersson RF, Sollerbrant K (2005) The cell surface protein coxsackie- and adenovirus receptor (CAR) directly associates with the Ligand-of-Numb Protein-X2 (LNX2). Experimental cell research 309:110-120.

Mohanan V, Temburni MK, Kappes JC, Galileo DS (2013) L1CAM stimulates glioma cell motility and proliferation through the fibroblast growth factor receptor. Clinical & experimental metastasis 30:507-520.

Monteith GR, Davis FM, Roberts-Thomson SJ (2012) Calcium channels and pumps in cancer: changes and consequences. The Journal of biological chemistry 287:31666-31673.

Mori T, Arakawa H, Tokino T, Mineura K, Nakamura Y (1999) Significant increase of adenovirus infectivity in glioma cell lines by extracellular domain of hCAR. Oncology research 11:513-521.

Moss ML, Bomar M, Liu Q, Sage H, Dempsey P, Lenhart PM, Gillispie PA, Stoeck A, Wildeboer D, Bartsch JW, Palmisano R, Zhou P (2007) The ADAM10 prodomain is a specific inhibitor of ADAM10 proteolytic activity and inhibits cellular shedding events. The Journal of biological chemistry 282:35712-35721.

Moss ML, Jin SL, Milla ME, Bickett DM, Burkhart W, Carter HL, Chen WJ, Clay WC, Didsbury JR, Hassler D, Hoffman CR, Kost TA, Lambert MH, Leesnitzer MA, McCauley P, McGeehan G, Mitchell J, Moyer M, Pahel G, Rocque W, Overton LK, Schoenen F, Seaton T, Su JL, Becherer JD, et al. (1997) Cloning of a disintegrin metalloproteinase that processes precursor tumournecrosis factor-alpha. Nature 385:733-736.

Moss ML, Sklair-Tavron L, Nudelman R (2008) Drug insight: tumor necrosis factor-converting enzyme as a pharmaceutical target for rheumatoid arthritis. Nature clinical practice Rheumatology 4:300-309.

Muckelbauer JK, Kremer M, Minor I, Diana G, Dutko FJ, Groarke J, Pevear DC, Rossmann MG (1995) The structure of coxsackievirus B3 at 3.5 A resolution. Structure 3:653-667.

Mueller BK (1999) Growth cone guidance: first steps towards a deeper understanding. Annual review of neuroscience 22:351-388.

Mumm JS, Kopan R (2000) Notch signaling: from the outside in. Developmental biology 228:151-165.

Mumm JS, Schroeter EH, Saxena MT, Griesemer A, Tian X, Pan DJ, Ray WJ, Kopan R (2000) A ligand-induced extracellular cleavage regulates gamma-secretase-like proteolytic activation of Notch1. Molecular cell 5:197-206.

Murphy G (2009) Regulation of the proteolytic disintegrin metalloproteinases, the 'Sheddases'. Semin Cell Dev Biol 20:138-145.

Murphy G (2010) Fell-Muir Lecture: Metalloproteinases: from demolition squad to master regulators. International journal of experimental pathology 91:303-313.

Na HW, Shin WS, Ludwig A, Lee ST (2012) The cytosolic domain of protein-tyrosine kinase 7 (PTK7), generated from sequential cleavage by a disintegrin and metalloprotease 17 (ADAM17) and gamma-secretase, enhances cell proliferation and migration in colon cancer cells. The Journal of biological chemistry 287:25001-25009.

Nagano O, Murakami D, Hartmann D, De Strooper B, Saftig P, Iwatsubo T, Nakajima M, Shinohara M, Saya H (2004) Cell-matrix interaction via CD44 is independently regulated by different metalloproteinases activated in response to extracellular Ca(2+) influx and PKC activation. The Journal of cell biology 165:893-902.

Najy AJ, Day KC, Day ML (2008a) ADAM15 supports prostate cancer metastasis by modulating tumor cell-endothelial cell interaction. Cancer research 68:1092-1099.

Najy AJ, Day KC, Day ML (2008b) The ectodomain shedding of E-cadherin by ADAM15 supports ErbB receptor activation. The Journal of biological chemistry 283:18393-18401.

Nalbantoglu J, Pari G, Karpati G, Holland PC (1999) Expression of the primary coxsackie and adenovirus receptor is downregulated during skeletal muscle maturation and limits the efficacy of adenovirus-mediated gene delivery to muscle cells. Hum Gene Ther 10:1009-1019.

Nath D, Slocombe PM, Stephens PE, Warn A, Hutchinson GR, Yamada KM, Docherty AJ, Murphy G (1999) Interaction of metargidin (ADAM-15) with alphavbeta3 and alpha5beta1 integrins on different haemopoietic cells. Journal of cell science 112 (Pt 4):579-587.

Naus S, Richter M, Wildeboer D, Moss M, Schachner M, Bartsch JW (2004) Ectodomain shedding of the neural recognition molecule CHL1 by the metalloprotease-disintegrin ADAM8 promotes neurite outgrowth and suppresses neuronal cell death. The Journal of biological chemistry 279:16083-16090.

Niimura M, Isoo N, Takasugi N, Tsuruoka M, Ui-Tei K, Saigo K, Morohashi Y, Tomita T, Iwatsubo T (2005) Aph-1 contributes to the stabilization and trafficking of the gamma-secretase complex through mechanisms involving intermolecular

and intramolecular interactions. The Journal of biological chemistry 280:12967-12975.

Niwa M, Sidrauski C, Kaufman RJ, Walter P (1999) A role for presenilin-1 in nuclear accumulation of Ire1 fragments and induction of the mammalian unfolded protein response. Cell 99:691-702.

Noutsias M, Fechner H, de Jonge H, Wang X, Dekkers D, Houtsmuller AB, Pauschinger M, Bergelson J, Warraich R, Yacoub M, Hetzer R, Lamers J, Schultheiss HP, Poller W (2001) Human coxsackie-adenovirus receptor is colocalized with integrins alpha(v)beta(3) and alpha(v)beta(5) on the cardiomyocyte sarcolemma and upregulated in dilated cardiomyopathy: implications for cardiotropic viral infections. Circulation 104:275-280.

Ohtsu H, Dempsey PJ, Eguchi S (2006) ADAMs as mediators of EGF receptor transactivation by G protein-coupled receptors. American journal of physiology Cell physiology 291:C1-10.

Okamoto I, Tsuiki H, Kenyon LC, Godwin AK, Emlet DR, Holgado-Madruga M, Lanham IS, Joynes CJ, Vo KT, Guha A, Matsumoto M, Ushio Y, Saya H, Wong AJ (2002) Proteolytic cleavage of the CD44 adhesion molecule in multiple human tumors. The American journal of pathology 160:441-447.

Okegawa T, Li Y, Pong RC, Bergelson JM, Zhou J, Hsieh JT (2000) The dual impact of coxsackie and adenovirus receptor expression on human prostate cancer gene therapy. Cancer research 60:5031-5036.

Okegawa T, Li Y, Pong RC, Hsieh JT (2002) Cell adhesion proteins as tumor suppressors. The Journal of urology 167:1836-1843.

Okegawa T, Pong RC, Li Y, Bergelson JM, Sagalowsky AI, Hsieh JT (2001) The mechanism of the growth-inhibitory effect of coxsackie and adenovirus receptor (CAR) on human bladder cancer: a functional analysis of car protein structure. Cancer research 61:6592-6600.

Ortiz RM, Karkkainen I, Huovila AP (2004) Aberrant alternative exon use and increased copy number of human metalloprotease-disintegrin ADAM15 gene in breast cancer cells. Genes, chromosomes & cancer 41:366-378.

Pan D, Rubin GM (1997) Kuzbanian controls proteolytic processing of Notch and mediates lateral inhibition during Drosophila and vertebrate neurogenesis. Cell 90:271-280.

Pardossi-Piquard R, Checler F (2012) The physiology of the beta-amyloid precursor protein intracellular domain AICD. J Neurochem 120 Suppl 1:109-124.

Patzke C, Max KE, Behlke J, Schreiber J, Schmidt H, Dorner AA, Kroger S, Henning M, Otto A, Heinemann U, Rathjen FG (2010) The coxsackievirus-adenovirus receptor reveals complex homophilic and heterophilic interactions on neural cells. J Neurosci 30:2897-2910.

Pazirandeh A, Sultana T, Mirza M, Rozell B, Hultenby K, Wallis K, Vennstrom B, Davis B, Arner A, Heuchel R, Lohr M, Philipson L, Sollerbrant K (2011) Multiple phenotypes in adult mice following inactivation of the Coxsackievirus and Adenovirus Receptor (Car) gene. PLoS One 6:e20203.

Persson A, Fan X, Widegren B, Englund E (2006) Cell type- and region-dependent coxsackie adenovirus receptor expression in the central nervous system. Journal of neuro-oncology 78:1-6.

Peschon JJ, Slack JL, Reddy P, Stocking KL, Sunnarborg SW, Lee DC, Russell WE, Castner BJ, Johnson RS, Fitzner JN, Boyce RW, Nelson N, Kozlosky CJ, Wolfson MF, Rauch CT, Cerretti DP, Paxton RJ, March CJ, Black RA (1998) An essential role for ectodomain shedding in mammalian development. Science 282:1281-1284.

Petrella J, Cohen CJ, Gaetz J, Bergelson JM (2002) A zebrafish coxsackievirus and adenovirus receptor homologue interacts with coxsackie B virus and adenovirus. Journal of virology 76:10503-10506.

Philipson L, Lonberg-Holm K, Pettersson U (1968) Virus-receptor interaction in an adenovirus system. Journal of virology 2:1064-1075.

Pickles RJ, Fahrner JA, Petrella JM, Boucher RC, Bergelson JM (2000) Retargeting the coxsackievirus and adenovirus receptor to the apical surface of polarized epithelial cells reveals the glycocalyx as a barrier to adenovirus-mediated gene transfer. Journal of virology 74:6050-6057.

Poller W, Fechner H, Noutsias M, Tschoepe C, Schultheiss HP (2002) Highly variable expression of virus receptors in the human cardiovascular system. Implications for cardiotropic viral infections and gene therapy. Zeitschrift für Kardiologie 91:978-991.

Ponten J, Westermark B (1978) Properties of human malignant glioma cells in vitro. Medical biology 56:184-193.

Postina R, Schroeder A, Dewachter I, Bohl J, Schmitt U, Kojro E, Prinzen C, Endres K, Hiemke C, Blessing M, Flamez P, Dequenne A, Godaux E, van Leuven F, Fahrenholz F (2004) A disintegrin-metalloproteinase prevents amyloid plaque formation and hippocampal defects in an Alzheimer disease mouse model. J Clin Invest 113:1456-1464.

Potter CJ, Tasic B, Russler EV, Liang L, Luo L (2010) The Q system: a repressible binary system for transgene expression, lineage tracing, and mosaic analysis. Cell 141:536-548.

Pruessmeyer J, Ludwig A (2009) The good, the bad and the ugly substrates for ADAM10 and ADAM17 in brain pathology, inflammation and cancer. Semin Cell Dev Biol 20:164-174.

Qin M, Escuadro B, Dohadwala M, Sharma S, Batra RK (2004) A novel role for the coxsackie adenovirus receptor in mediating tumor formation by lung cancer cells. Cancer research 64:6377-6380.

Raschperger E, Thyberg J, Pettersson S, Philipson L, Fuxe J, Pettersson RF (2006) The coxsackie- and adenovirus receptor (CAR) is an in vivo marker for epithelial tight junctions, with a potential role in regulating permeability and tissue homeostasis. Experimental cell research 312:1566-1580.

Reiland J, Ott VL, Lebakken CS, Yeaman C, McCarthy J, Rapraeger AC (1996) Pervanadate activation of intracellular kinases leads to tyrosine phosphorylation and shedding of syndecan-1. The Biochemical journal 319 (Pt 1):39-47.

Reiss K, Ludwig A, Saftig P (2006a) Breaking up the tie: disintegrin-like metalloproteinases as regulators of cell migration in inflammation and invasion. Pharmacology & therapeutics 111:985-1006.

Reiss K, Maretzky T, Haas IG, Schulte M, Ludwig A, Frank M, Saftig P (2006b) Regulated ADAM10-dependent ectodomain shedding of gamma-protocadherin C3 modulates cell-cell adhesion. The Journal of biological chemistry 281:21735-21744.

Reiss K, Maretzky T, Ludwig A, Tousseyn T, de Strooper B, Hartmann D, Saftig P (2005) ADAM10 cleavage of N-cadherin and regulation of cell-cell adhesion and beta-catenin nuclear signalling. The EMBO journal 24:742-752.

Reiss K, Saftig P (2009) The "A Disintegrin And Metalloprotease" (ADAM) family of sheddases: Physiological and cellular functions. Semin Cell Dev Biol 20:126-137.

Riedle S, Kiefel H, Gast D, Bondong S, Wolterink S, Gutwein P, Altevogt P (2009) Nuclear translocation and signalling of L1-CAM in human carcinoma cells requires ADAM10 and presenilin/gamma-secretase activity. The Biochemical journal 420:391-402.

Roelvink PW, Lizonova A, Lee JG, Li Y, Bergelson JM, Finberg RW, Brough DE, Kovesdi I, Wickham TJ (1998) The coxsackievirus-adenovirus receptor protein can function as a cellular attachment protein for adenovirus serotypes from subgroups A, C, D, E, and F. Journal of virology 72:7909-7915.

Rosse C, Linch M, Kermorgant S, Cameron AJ, Boeckeler K, Parker PJ (2010) PKC and the control of localized signal dynamics. Nature reviews Molecular cell biology 11:103-112.

Roy R, Wewer UM, Zurakowski D, Pories SE, Moses MA (2004) ADAM 12 cleaves extracellular matrix proteins and correlates with cancer status and stage. The Journal of biological chemistry 279:51323-51330.

Sachs MD, Rauen KA, Ramamurthy M, Dodson JL, De Marzo AM, Putzi MJ, Schoenberg MP, Rodriguez R (2002) Integrin alpha(v) and coxsackie adenovirus receptor expression in clinical bladder cancer. Urology 60:531-536.

Saftig P, Reiss K (2011) The "A Disintegrin And Metalloproteases" ADAM10 and ADAM17: novel drug targets with therapeutic potential? European journal of cell biology 90:527-535.

Sagane K, Hayakawa K, Kai J, Hirohashi T, Takahashi E, Miyamoto N, Ino M, Oki T, Yamazaki K, Nagasu T (2005) Ataxia and peripheral nerve hypomyelination in ADAM22-deficient mice. BMC neuroscience 6:33.

Sahin U, Weskamp G, Kelly K, Zhou HM, Higashiyama S, Peschon J, Hartmann D, Saftig P, Blobel CP (2004) Distinct roles for ADAM10 and ADAM17 in ectodomain shedding of six EGFR ligands. The Journal of cell biology 164:769-779.

Saito K, Sakaguchi M, Iioka H, Matsui M, Nakanishi H, Huh NH, Kondo E (2013) Coxsackie and adenovirus receptor is a critical regulator for the survival and growth of oral squamous carcinoma cells. Oncogene.

Salaun C, Greaves J, Chamberlain LH (2010) The intracellular dynamic of protein palmitoylation. The Journal of cell biology 191:1229-1238.

Sanchez-Irizarry C, Carpenter AC, Weng AP, Pear WS, Aster JC, Blacklow SC (2004) Notch subunit heterodimerization and prevention of ligand-independent proteolytic activation depend, respectively, on a novel domain and the LNR repeats. Molecular and cellular biology 24:9265-9273.

Saxena MT, Schroeter EH, Mumm JS, Kopan R (2001) Murine notch homologs (N1-4) undergo presenilin-dependent proteolysis. The Journal of biological chemistry 276:40268-40273.

Schachtner S, Buck C, Bergelson J, Baldwin H (1999) Temporally regulated expression patterns following in utero adenovirus-mediated gene transfer. Gene therapy 6:1249-1257.

Scheinfeld MH, Ghersi E, Laky K, Fowlkes BJ, D'Adamio L (2002) Processing of beta-amyloid precursor-like protein-1 and -2 by gamma-secretase regulates transcription. The Journal of biological chemistry 277:44195-44201.

Scheller J, Chalaris A, Garbers C, Rose-John S (2011) ADAM17: a molecular switch to control inflammation and tissue regeneration. Trends in immunology 32:380-387.

Schroeter EH, Kisslinger JA, Kopan R (1998) Notch-1 signalling requires ligand-induced proteolytic release of intracellular domain. Nature 393:382-386.

Schulz B, Pruessmeyer J, Maretzky T, Ludwig A, Blobel CP, Saftig P, Reiss K (2008) ADAM10 regulates endothelial permeability and T-Cell transmigration by proteolysis of vascular endothelial cadherin. Circ Res 102:1192-1201.

Schulz JG, Annaert W, Vandekerckhove J, Zimmermann P, De Strooper B, David G (2003) Syndecan 3 intramembrane proteolysis is presenilin/gamma-secretase-dependent and modulates cytosolic signaling. The Journal of biological chemistry 278:48651-48657.

Seki M, Watanabe A, Enomoto S, Kawamura T, Ito H, Kodama T, Hamakubo T, Aburatani H (2010) Human ROBO1 is cleaved by metalloproteinases and gamma-secretase and migrates to the nucleus in cancer cells. FEBS Lett 584:2909-2915.

Selinka HC, Wolde A, Sauter M, Kandolf R, Klingel K (2004) Virus-receptor interactions of coxsackie B viruses and their putative influence on cardiotropism. Medical microbiology and immunology 193:127-131.

Selkoe DJ (2001) Alzheimer's disease: genes, proteins, and therapy. Physiological reviews 81:741-766.

Shah S, Lee SF, Tabuchi K, Hao YH, Yu C, LaPlant Q, Ball H, Dann CE, 3rd, Sudhof T, Yu G (2005) Nicastrin functions as a gamma-secretase-substrate receptor. Cell 122:435-447.

Sharma A, Li X, Bangari DS, Mittal SK (2009) Adenovirus receptors and their implications in gene delivery. Virus research 143:184-194.

Sharma P, Kolawole AO, Core SB, Kajon AE, Excoffon KJ (2012) Sidestream smoke exposure increases the susceptibility of airway epithelia to adenoviral infection. PLoS One 7:e49930.

Shaw CA, Holland PC, Sinnreich M, Allen C, Sollerbrant K, Karpati G, Nalbantoglu J (2004) Isoform-specific expression of the Coxsackie and adenovirus receptor (CAR) in neuromuscular junction and cardiac intercalated discs. BMC cell biology 5:42.

Shi W, Chen H, Sun J, Buckley S, Zhao J, Anderson KD, Williams RG, Warburton D (2003) TACE is required for fetal murine cardiac development and modeling. Developmental biology 261:371-380.

Shi Z, Xu W, Loechel F, Wewer UM, Murphy LJ (2000) ADAM 12, a disintegrin metalloprotease, interacts with insulin-like growth factor-binding protein-3. The Journal of biological chemistry 275:18574-18580.

Shieh JT, Bergelson JM (2002) Interaction with decay-accelerating factor facilitates coxsackievirus B infection of polarized epithelial cells. Journal of virology 76:9474-9480.

Shuman Moss LA, Jensen-Taubman S, Stetler-Stevenson WG (2012) Matrix metalloproteinases: changing roles in tumor progression and metastasis. The American journal of pathology 181:1895-1899.

Sinnreich M, Shaw CA, Pari G, Nalbantoglu J, Holland PC, Karpati G (2005) Localization of coxsackie virus and adenovirus receptor (CAR) in normal and regenerating human muscle. Neuromuscular disorders: NMD 15:541-548.

Sollerbrant K, Raschperger E, Mirza M, Engstrom U, Philipson L, Ljungdahl PO, Pettersson RF (2003) The Coxsackievirus and adenovirus receptor (CAR) forms a complex with the PDZ domain-containing protein ligand-of-numb protein-X (LNX). The Journal of biological chemistry 278:7439-7444.

Sotillos S, Roch F, Campuzano S (1997) The metalloprotease-disintegrin Kuzbanian participates in Notch activation during growth and patterning of Drosophila imaginal discs. Development 124:4769-4779.

Stecker K, Koschel A, Wiedenmann B, Anders M (2009) Loss of Coxsackie and adenovirus receptor downregulates alpha-catenin expression. British journal of cancer 101:1574-1579.

Stecker K, Vieth M, Koschel A, Wiedenmann B, Rocken C, Anders M (2011) Impact of the coxsackievirus and adenovirus receptor on the adenoma-carcinoma sequence of colon cancer. British journal of cancer 104:1426-1433.

Sterchi EE, Stocker W, Bond JS (2008) Meprins, membrane-bound and secreted astacin metalloproteinases. Molecular aspects of medicine 29:309-328.

Stevenson BR, Keon BH (1998) The tight junction: morphology to molecules. Annual review of cell and developmental biology 14:89-109.

Stoeck A, Shang L, Dempsey PJ (2010) Sequential and gamma-secretase-dependent processing of the betacellulin precursor generates a palmitoylated intracellular-domain fragment that inhibits cell growth. Journal of cell science 123:2319-2331.

Struhl G, Adachi A (1998) Nuclear access and action of notch in vivo. Cell 93:649-660.

Struhl G, Greenwald I (1999) Presenilin is required for activity and nuclear access of Notch in Drosophila. Nature 398:522-525.

Su L, Mruk DD, Cheng CY (2012) Regulation of the blood-testis barrier by coxsackievirus and adenovirus receptor. American journal of physiology Cell physiology 303:C843-853.

Subramanian SV, Fitzgerald ML, Bernfield M (1997) Regulated shedding of syndecan-1 and -4 ectodomains by thrombin and growth factor receptor activation. The Journal of biological chemistry 272:14713-14720.

Tagami S, Okochi M, Yanagida K, Ikuta A, Fukumori A, Matsumoto N, Ishizuka-Katsura Y, Nakayama T, Itoh N, Jiang J, Nishitomi K, Kamino K, Morihara T, Hashimoto R, Tanaka T, Kudo T, Chiba S, Takeda M (2008) Regulation of Notch signaling by dynamic changes in the precision of S3 cleavage of Notch-1. Molecular and cellular biology 28:165-176.

Tallone T, Malin S, Samuelsson A, Wilbertz J, Miyahara M, Okamoto K, Poellinger L, Philipson L, Pettersson S (2001) A mouse model for adenovirus gene delivery. Proc Natl Acad Sci U S A 98:7910-7915.

Tanaka T, Kuroki M, Hamada H, Kato K, Kinugasa T, Shibaguchi H, Zhao J, Kuroki M (2007) Cancer-targeting gene therapy using tropism-modified adenovirus. Anticancer research 27:3679-3684.

Taniguchi Y, Kim SH, Sisodia SS (2003) Presenilin-dependent "gamma-secretase" processing of deleted in colorectal cancer (DCC). The Journal of biological chemistry 278:30425-30428.

Tape CJ, Willems SH, Dombernowsky SL, Stanley PL, Fogarasi M, Ouwehand W, McCafferty J, Murphy G (2011) Cross-domain inhibition of TACE ectodomain. Proc Natl Acad Sci U S A 108:5578-5583.

Thodeti CK, Albrechtsen R, Grauslund M, Asmar M, Larsson C, Takada Y, Mercurio AM, Couchman JR, Wewer UM (2003) ADAM12/syndecan-4 signaling promotes beta 1 integrin-dependent cell spreading through protein kinase Calpha and RhoA. The Journal of biological chemistry 278:9576-9584.

Thoelen I, Magnusson C, Tagerud S, Polacek C, Lindberg M, Van Ranst M (2001) Identification of alternative splice products encoded by the human coxsackie-adenovirus receptor gene. Biochem Biophys Res Commun 287:216-222.

Tomko RP, Johansson CB, Totrov M, Abagyan R, Frisen J, Philipson L (2000) Expression of the adenovirus receptor and its interaction with the fiber knob. Experimental cell research 255:47-55.

Tomko RP, Xu R, Philipson L (1997) HCAR and MCAR: the human and mouse cellular receptors for subgroup C adenoviruses and group B coxsackieviruses. Proc Natl Acad Sci U S A 94:3352-3356.

Tousseyn T, Jorissen E, Reiss K, Hartmann D (2006) (Make) stick and cut loose-disintegrin metalloproteases in development and disease. Birth defects research Part C, Embryo today: reviews 78:24-46.

Tousseyn T, Thathiah A, Jorissen E, Raemaekers T, Konietzko U, Reiss K, Maes E, Snellinx A, Serneels L, Nyabi O, Annaert W, Saftig P, Hartmann D, De Strooper B (2009) ADAM10, the rate-limiting protease of regulated intramembrane proteolysis of Notch and other proteins, is processed by ADAMS-9, ADAMS-15, and the gamma-secretase. The Journal of biological chemistry 284:11738-11747.

Uemura K, Kihara T, Kuzuya A, Okawa K, Nishimoto T, Ninomiya H, Sugimoto H, Kinoshita A, Shimohama S (2006) Characterization of sequential N-cadherin cleavage by ADAM10 and PS1. Neuroscience letters 402:278-283.

van't Hof W, Crystal RG (2001) Manipulation of the cytoplasmic and transmembrane domains alters cell surface levels of the coxsackie-adenovirus receptor and changes the efficiency of adenovirus infection. Hum Gene Ther 12:25-34.

van't Hof W, Crystal RG (2002) Fatty acid modification of the coxsackievirus and adenovirus receptor. Journal of virology 76:6382-6386.

van Raaij MJ, Chouin E, van der Zandt H, Bergelson JM, Cusack S (2000) Dimeric structure of the coxsackievirus and adenovirus receptor D1 domain at 1.7 A resolution. Structure 8:1147-1155.

van Tetering G, van Diest P, Verlaan I, van der Wall E, Kopan R, Vooijs M (2009) Metalloprotease ADAM10 is required for Notch1 site 2 cleavage. The Journal of biological chemistry 284:31018-31027.

Varshavsky A (1997) The N-end rule pathway of protein degradation. Genes to cells: devoted to molecular & cellular mechanisms 2:13-28.

Vassar R, Bennett BD, Babu-Khan S, Kahn S, Mendiaz EA, Denis P, Teplow DB, Ross S, Amarante P, Loeloff R, Luo Y, Fisher S, Fuller J, Edenson S, Lile J, Jarosinski MA, Biere AL, Curran E, Burgess T, Louis JC, Collins F, Treanor J, Rogers G, Citron M (1999) Beta-secretase cleavage of Alzheimer's amyloid precursor protein by the transmembrane aspartic protease BACE. Science 286:735-741.

Veena MS, Qin M, Andersson A, Sharma S, Batra RK (2009) CAR mediates efficient tumor engraftment of mesenchymal type lung cancer cells. Laboratory investigation; a journal of technical methods and pathology 89:875-886.

Verdino P, Witherden DA, Havran WL, Wilson IA (2010) The molecular interaction of CAR and JAML recruits the central cell signal transducer PI3K. Science 329:1210-1214.

Vigl B, Zgraggen C, Rehman N, Banziger-Tobler NE, Detmar M, Halin C (2009) Coxsackie- and adenovirus receptor (CAR) is expressed in lymphatic vessels in human skin and affects lymphatic endothelial cell function in vitro. Experimental cell research 315:336-347.

Vincent T, Neve EP, Johnson JR, Kukalev A, Rojo F, Albanell J, Pietras K, Virtanen I, Philipson L, Leopold PL, Crystal RG, de Herreros AG, Moustakas A, Pettersson RF, Fuxe J (2009) A SNAIL1-SMAD3/4 transcriptional repressor complex promotes TGF-beta mediated epithelial-mesenchymal transition. Nature cell biology 11:943-950.

Vindrieux D, Le Corre L, Hsieh JT, Metivier R, Escobar P, Caicedo A, Brigitte M, Lazennec G (2011) Coxsackie and adenovirus receptor is a target and a mediator of estrogen action in breast cancer. Endocrine-related cancer 18:311-321.

Vingtdeux V, Marambaud P (2012) Identification and biology of alpha-secretase. J Neurochem 120 Suppl 1:34-45.

Walsh DM, Fadeeva JV, LaVoie MJ, Paliga K, Eggert S, Kimberly WT, Wasco W, Selkoe DJ (2003) gamma-Secretase cleavage and binding to FE65 regulate the nuclear translocation of the intracellular C-terminal domain (ICD) of the APP family of proteins. Biochemistry 42:6664-6673.

Walsh FS, Doherty P (1997) Neural cell adhesion molecules of the immunoglobulin superfamily: role in axon growth and guidance. Annual review of cell and developmental biology 13:425-456.

Walters RW, Freimuth P, Moninger TO, Ganske I, Zabner J, Welsh MJ (2002) Adenovirus fiber disrupts CAR-mediated intercellular adhesion allowing virus escape. Cell 110:789-799.

Walters RW, Grunst T, Bergelson JM, Finberg RW, Welsh MJ, Zabner J (1999) Basolateral localization of fiber receptors limits adenovirus infection from the apical surface of airway epithelia. The Journal of biological chemistry 274:10219-10226.

Walters RW, van't Hof W, Yi SM, Schroth MK, Zabner J, Crystal RG, Welsh MJ (2001) Apical localization of the coxsackie-adenovirus receptor by glycosylphosphatidylinositol modification is sufficient for adenovirus-mediated gene transfer through the apical surface of human airway epithelia. Journal of virology 75:7703-7711.

Wang X, Bergelson JM (1999) Coxsackievirus and adenovirus receptor cytoplasmic and transmembrane domains are not essential for coxsackievirus and adenovirus infection. Journal of virology 73:2559-2562.

Wang X, Mizushima H, Adachi S, Ohishi M, Iwamoto R, Mekada E (2006) Cytoplasmic domain phosphorylation of heparin-binding EGF-like growth factor. Cell structure and function 31:15-27.

Wang Y, Jiang T (2013) Understanding high grade glioma: molecular mechanism, therapy and comprehensive management. Cancer letters 331:139-146.

Webber CA, Hocking JC, Yong VW, Stange CL, McFarlane S (2002) Metalloproteases and guidance of retinal axons in the developing visual system. J Neurosci 22:8091-8100.

Weber S, Niessen MT, Prox J, Lullmann-Rauch R, Schmitz A, Schwanbeck R, Blobel CP, Jorissen E, de Strooper B, Niessen CM, Saftig P (2011) The disintegrin/metalloproteinase Adam10 is essential for epidermal integrity and Notch-mediated signaling. Development 138:495-505.

Webster N, Jin JR, Green S, Hollis M, Chambon P (1988) The yeast UASG is a transcriptional enhancer in human HeLa cells in the presence of the GAL4 transactivator. Cell 52:169-178.

Werb Z, Yan Y (1998) A cellular striptease act. Science 282:1279-1280.

Wickham TJ, Mathias P, Cheresh DA, Nemerow GR (1993) Integrins alpha v beta 3 and alpha v beta 5 promote adenovirus internalization but not virus attachment. Cell 73:309-319.

Wild-Bode C, Fellerer K, Kugler J, Haass C, Capell A (2006) A basolateral sorting signal directs ADAM10 to adherens junctions and is required for its function in cell migration. The Journal of biological chemistry 281:23824-23829.

Witherden DA, Verdino P, Rieder SE, Garijo O, Mills RE, Teyton L, Fischer WH, Wilson IA, Havran WL (2010) The junctional adhesion molecule JAML is a costimulatory receptor for epithelial gammadelta T cell activation. Science 329:1205-1210.

Woodruff JF (1980) Viral myocarditis. A review. The American journal of pathology 101:425-484.

Xu D, Farmer A, Chook YM (2010) Recognition of nuclear targeting signals by Karyopherin-beta proteins. Current opinion in structural biology 20:782-790.

Xu R, Crowell RL (1996) Expression and distribution of the receptors for coxsackievirus B3 during fetal development of the Balb/c mouse and of their brain cells in culture. Virus research 46:157-170.

Yamashita M, Ino A, Kawabata K, Sakurai F, Mizuguchi H (2007) Expression of coxsackie and adenovirus receptor reduces the lung metastatic potential of murine tumor cells. International journal of cancer 121:1690-1696.

Yanagawa B, Spiller OB, Proctor DG, Choy J, Luo H, Zhang HM, Suarez A, Yang D, McManus BM (2004) Soluble recombinant coxsackievirus and adenovirus receptor abrogates coxsackievirus b3-mediated pancreatitis and myocarditis in mice. The Journal of infectious diseases 189:1431-1439.

Yang M, Li Y, Chilukuri K, Brady OA, Boulos MI, Kappes JC, Galileo DS (2011) L1 stimulation of human glioma cell motility correlates with FAK activation. Journal of neuro-oncology 105:27-44.

Yang P, Baker KA, Hagg T (2006) The ADAMs family: coordinators of nervous system development, plasticity and repair. Progress in neurobiology 79:73-94.

Yee NS, Langen H, Besmer P (1993) Mechanism of kit ligand, phorbol ester, and calcium-induced down-regulation of c-kit receptors in mast cells. The Journal of biological chemistry 268:14189-14201.

Zabner J, Freimuth P, Puga A, Fabrega A, Welsh MJ (1997) Lack of high affinity fiber receptor activity explains the resistance of ciliated airway epithelia to adenovirus infection. J Clin Invest 100:1144-1149.

Zen K, Liu Y, McCall IC, Wu T, Lee W, Babbin BA, Nusrat A, Parkos CA (2005) Neutrophil migration across tight junctions is mediated by adhesive interactions between epithelial coxsackie and adenovirus receptor and a junctional adhesion molecule-like protein on neutrophils. Mol Biol Cell 16:2694-2703.

Zhang X, Fang B, Mohan R, Chang JY (2012) Coxsackie-adenovirus receptor as a novel marker of stem cells in treatment-resistant non-small cell lung cancer. Radiotherapy and oncology: journal of the European Society for Therapeutic Radiology and Oncology 105:250-257.

Zhao G, Cui MZ, Mao G, Dong Y, Tan J, Sun L, Xu X (2005) gamma-Cleavage is dependent on zeta-cleavage during the proteolytic processing of amyloid precursor protein within its transmembrane domain. The Journal of biological chemistry 280:37689-37697.

Zhao J, Chen H, Peschon JJ, Shi W, Zhang Y, Frank SJ, Warburton D (2001) Pulmonary hypoplasia in mice lacking tumor necrosis factor-alpha converting enzyme indicates an indispensable role for cell surface protein shedding during embryonic lung branching morphogenesis. Developmental biology 232:204-218.

Zhou HM, Weskamp G, Chesneau V, Sahin U, Vortkamp A, Horiuchi K, Chiusaroli R, Hahn R, Wilkes D, Fisher P, Baron R, Manova K, Basson CT, Hempstead B, Blobel CP (2004) Essential role for ADAM19 in cardiovascular morphogenesis. Molecular and cellular biology 24:96-104.

Zolkiewska A (1999) Disintegrin-like/cysteine-rich region of ADAM 12 is an active cell adhesion domain. Experimental cell research 252:423-431.